

Applicants : BERMUDEZ, et al.
U.S. Serial No.: 10/790,586
Filed : March 1, 2004
Page : 10

Remarks

Applicants amended lines 24-33 on page 42 of the specification to add "Strain 72 is synonymous with Clone 72 in WO 96/40238, where Clone 72 is listed as a strain in tables 20B, 20C and 20E." Support for the amendment can be found on Table 20(B), line 11, page 113; Table 20(C), line 27, page 114; and Table 20(D), line 30, page 115 of WO 96/40238, which has been incorporated by reference into this Application. Accordingly, there is no issue of new matter.

Claims 1-9 and 11-18 are pending in this Application. By this Amendment, Applicants have canceled claims 1-9 and 11-18 and submitted new claims 25-43. Enablement and support for new claims 25-43 can be found in the pages and line numbers of the specification indicated below. Therefore, there is no issue of new matter, and Applicants respectfully request the entry of this Amendment. Upon entry of this Amendment, claims 25-43 will be pending and under examination.

Claims 25-26: Addition of the F' into Salmonella capable of targeting tumors by intravenous administration is on page 41, lines 23-34 of WO 0114579. A copy of WO 0114579 is attached herein as **Exhibit A**. Also see page 45, lines 1-2, of the specification. An example of targeting tumors by one of these strains is on pages 42-44 of the specification. Salmonella "strain 72" on page 41 is synonymous with "clone

BEST AVAILABLE COPY

Applicants : **BERMUDES, et al.**
U.S. Serial No.: **10/790,586**
Filed : **March 1, 2004**
Page : **11**

72" in WO 0114579. Strain 8.7 is address on page 10, lines 19-21 of the Specification.

Claims 27-28 and 31-32: Salmonella "strain 72" on page 41, line 23, of the specification is attenuated. Strains VNP20009 and YS1456 on page 41, line 33 are attenuated. Section 6.4 on page 43-44 of the specification is directed towards attenuated Salmonella.

Claims 33 and 35: Strains VNP20009 and YS1456 on page 41, line 33 of the specification are attenuated by msbB⁻ mutation. Section 6.4 on page 43-44 of the specification is directed towards attenuated Salmonella 8.7, which is attenuated by msbB⁻ mutation.

Claims 34 and 36: Salmonella "strain 72" on page 41 line 23 of the specification is attenuated by pur⁻ mutation. Strain VNP20009 and YS1456 on page 41, line 33 of the specification are attenuated by purI⁻.

Claim 37: Section 6.3 page 42-43 of the specification is directed towards delivery of phage to tumors.

Claim 38: Combined data from page 41 to 46 of the specification demonstrate the components necessary to construct a kit.

Claim 39: The composition of the kit is discussed on page 40, lines 19-32 of the specification. Combined data from page 41 to 46 of the specification demonstrate utility of

Applicants : BERMUDEZ, et al.
U.S. Serial No.: 10/790,586
Filed : March 1, 2004
Page : 12

the components necessary to construct a kit. Use of CMV promoter is discussed in Section 6.1 on page 41, line 9-11 of the specification. The plasmid pEGFP-N1 on page 47, line 3 contains the CMV promoter.

Claim 40-41: Amount of phage delivered to tumor cells by Salmonella is shown on page 44, Table 1, lines 1-19.

Claim 42-43: Amount of phage delivered to tumor cells by attenuated Salmonella is shown on page 45, Table 2, lines 7-24.

Specification

The disclosure is objected to by the Examiner because the page numbers on the Table of Contents pages of the specification (i-ii) do not correspond to the page numbering of the rest of the specification.

Upon review of the Table of Contents pages of the specification (i-ii), Applicants are unable to identify the error in the page numbering. Therefore, Applicants respectfully request the Examiner to clarify the error(s) that the Examiner would like Applicants to correct.

Claims Objections

The Examiner stated that the Markush group language should be perfected in claim 6 to read "the group consisting of a".

Without conceding the correctness of the Examiner's position and to expedite the prosecution of this

Applicants : BERMUDEZ, et al.
U.S. Serial No.: 10/790,586
Filed : March 1, 2004
Page : 13

Application, Applicants have canceled claim 6, thereby rendering the above objection moot.

Claims Rejections - 35 U.S.C. § 112, first paragraph

The Examiner rejected claims 1-9 and 11-18 under 35 U.S.C. § 112, first paragraph, as failing to comply with the enablement requirement. The Examiner stated that "the claim(s) contains subject matter which was not described in the specification in such a way as to enable one skilled in the art to which it pertains, or with which it is most nearly connected, to make and/or use the invention."

1. The Examiner alleged that the present claims are very broad in that "the bacterium may be any Gram-negative bacterium, the gene product of interest can be virtually anything, the composition can be administered by any route, and the method can be used for treatment of any tumor-based disease."

Without conceding the correctness of the Examiner's position and to expedite the prosecution of this Application, Applicants have canceled claims 1-9 and 11-18. New claims 25-43 recite "Salmonella strain expressing F' pilus and capable of producing a filamentous bacteriophage directly wherein the Salmonella is capable of targeting tumors by intravenous administration..." which do not contain the above mentioned issues, thereby rendering the above ground(s) of rejection moot.

Applicants : BERMUDEZ, et al.
U.S. Serial No.: 10/790,586
Filed : March 1, 2004
Page : 14

2. The Examiner stated that "the only disclosed use for the pharmaceutical composition is gene therapy." Applicants respectfully maintain that this invention offers several utilities, such as a method and composition for delivering phage to tumors. One utility is directed toward gene therapy. Another utility is in the discovery of tumor-specific peptide ligands, as disclosed by Pasqualini et al., 1997. A copy of Pasqualini et al. is attached herein as **Exhibit B**. Another utility of delivering phage to tumors is as a delivery agent for an MHC class I antigen, such as a LLO 91-99 peptide is described on pp 46-47.

3. The Examiner alleged that "an analysis of the prior art as of the effective filing date of the present application show a complete lack of documented success for gene therapy." See page 5, paragraph 1, of the September 8, 2004 Office Action ("OA").

Without conceding the correctness of the Examiner's position and to expedite the prosecution of this Application, Applicants have canceled claims 1-9 and 11-18 . New claims 25-43 recite "Salmonella strain expressing F' pilus and capable of producing a filamentous bacteriophage directly wherein the Salmonella is capable of targeting tumors by intravenous administration..." which do not contain the above mentioned issues, thereby rendering the above ground(s) of rejection moot.

Applicants : BERMUDEZ, et al.
U.S. Serial No.: 10/790,586
Filed : March 1, 2004
Page : 15

The Examiner further stated that:

- (a) No form of gene therapy can yet be considered a success, and the major problem still lies in delivery mechanism. (page 5, line 9-10, of OA)

Without conceding the correctness of the Examiner's position and to expedite the prosecution of this Application, Applicants have canceled claims 1-9 and 11-18. New claims 25-43 recite "Salmonella strain expressing F' pilus and capable of producing a filamentous bacteriophage directly wherein the Salmonella is capable of targeting tumors by intravenous administration..." and **is directed toward a mechanism to effectively deliver a bacteriophage agent**. Accordingly, new claims 25-43 do not contain the above mentioned issues, thereby rendering the above ground(s) of rejection moot.

- (b) Only a few cells, if any, may be transformed with DNA carried by a bacterial vehicle... It would appear that use of bacteria as DNA delivery vehicles is not very efficient in other cell lines. (page 6, line 2-4 and 11-12, of OA)

Applicants respectfully maintain that methods using Salmonella to deliver antitumor agents or genes encoding antitumor agents or molecules are not complex and are not limited to specific cell types because Salmonella targeting to tumors is very broad. Lee et al., 2004 Cancer Gene

Applicants : BERMUDEZ, et al.
U.S. Serial No.: 10/790,586
Filed : March 1, 2004
Page : 16

Therapy, and other investigators have shown that a tumor targeted Salmonella, simply transformed with a plasmid containing a CMV promoter driven antiangiogenic factor thrombospondin, were effective in treating murine tumors. A copy of Lee et al. is attached herein as **Exhibit C**.

- (c) Expression of a heterologous nucleotide sequence is not stable over time. (page 6, line 18-19, of OA)

Applicants respectfully maintain that stability may improve efficacy, but it is not required, e.g., (Lee et al., 2004 Cancer Gene Therapy).

- (d) There is ample evidence in the prior art that the delivery of heterologous genes to eukaryotic cells via bacterial vectors is unpredictable and far from routine. (page 7, line 5-6, of OA)

Without conceding the correctness of the Examiner's position and to expedite the prosecution of this Application, Applicants have canceled claims 1-9 and 11-18. New claims 25-43 recite "Salmonella strain expressing F' pilus and capable of producing a filamentous bacteriophage directly wherein the Salmonella is capable of targeting tumors by intravenous administration..." which do not contain the above mentioned issues, thereby rendering the above ground(s) of rejection moot.

- (e) It is not routine in the art to administer the bacteria by any route. There is unpredictability

Applicants : BERMUDEZ, et al.
U.S. Serial No.: 10/790,586
Filed : March 1, 2004
Page : 17

regarding antigen stability and antigen expressing
when administering attenuated bacteria orally. (page
7, line 9-12, of OA)

Without conceding the correctness of the Examiner's
position and to expedite the prosecution of this
Application, Applicants have canceled claims 1-9 and 11-18 .
New claims 25-43 recite "Salmonella strain expressing F'
pilus and capable of producing a filamentous bacteriophage
directly wherein the Salmonella is capable of targeting
tumors by intravenous administration..." which do not contain
the above mentioned issues, thereby rendering the above
ground(s) of rejection moot.

In regard to the status of "gene therapy", Applicants
respectfully disagree with the examiner. Gene therapy
methods also provide useful research tools necessary for
pharmaceutical industry basic research. Filamentous phage
has documented use in cancer diagnostic and therapeutic
discovery. See Pasqualini et al., 1997, and Figini et al.,
1998, attached herein as **Exhibit D**. It has also been
shown that filamentous phage have utility in transformation
of mammalian cells with ex-vivo application. See Larocca
et al., 1999, attached herein as **Exhibit E**, and Poul and
Marks, 1999, attached herein as **Exhibit F**. In vivo
application is absent due to insufficient delivery to
tumors in vivo. However, none of the prior art provides
methodology for delivery of filamentous phage directly to
tumors in high numbers by intravenous administration. For
example, Pasqualini et al., (1997) demonstrated

Applicants : BERMUDEZ, et al.
U.S. Serial No.: 10/790,586
Filed : March 1, 2004
Page : 18

approximately $2 \times 10^3/\text{mg}$ or $2 \times 10^6/\text{g}$ (Figure 1) phage within tumors; only a two-fold increase compared to brain or kidney (based on total phage in those organs). In the instant application on pages 42 to 44, it is demonstrated that in several cases, greater than 2×10^9 p.f.u./g (phage/gram of tumor) were present; and corrected values were as high as 4.6×10^{11} . Therefore, **bacterial delivery to tumors by intravenous administration was 1000 to 100,000 times greater than intravenous administration of the phage.**

Delivery directly to tumors by intravenously administered attenuated, tumor-targeted *Salmonella* is a novel composition and method for delivering phage to tumors in high numbers.

Furthermore, genetically engineered *Salmonella* have been demonstrated to be capable of tumor targeting, possess anti-tumor activity and are useful in delivering effector genes such as the herpes simplex thymidine kinase (HSV TK) to solid tumors. See page 3, lines 26-29, of specification and Pawelek et al., WO96/40238.

4. The Examiner alleged that the "effectiveness of a potential new delivery system, such as tumor-targeted bacteria containing a bacteriophage encoding a gene of interest, cannot be predicted in the absence of in vivo testing for a therapeutic effect." (page 8, line 13-15, of OA)

Applicants : **BERMUDES, et al.**
U.S. Serial No.: **10/790,586**
Filed : **March 1, 2004**
Page : **19**

Without conceding the correctness of the Examiner's position and to expedite the prosecution of this Application, Applicants have canceled claims 1-9 and 11-18. New claims 25-43 do not recite a "tumor-targeted bacteria containing a bacteriophage encoding a gene of interest." Moreover, Examples 6.3 and 6.4 clearly demonstrated that tumor-targeting Salmonella strain can deliver phage to tumors, thereby rendering the above ground(s) of rejection moot.

5. The Examiner alleged that the present specification provides little direction or guidance because "no direction is provided on how to generate tumor target bacterium in Gram-negative species other than Salmonella..., and the basis for the tumor targeting in the Salmonella used is not disclosed." (page 8, line 19-22, of OA)

In response, Applicants have submitted new claims 25-43 for the Examiner's consideration. The new claims recite a Salmonella strain expressing F' pilus and a filamentous bacteriophage. In addition, the "basis for the tumor targeting in the Salmonella used" is disclosed in the specification on page 44, lines 27-35 and page 45, lines 26-27, thereby rendering the above ground(s) of rejection moot.

6. The Examiner alleged that (a) the working examples do not demonstrate gene expression or therapeutic effect due to expression of a gene of interest. The

Applicants : BERMUDEZ, et al.
U.S. Serial No.: 10/790,586
Filed : March 1, 2004
Page : 20

Examiner further alleged that (b) "it is highly questionable whether a mouse model provides a basis for predictability of results in higher order mammals, specifically humans. (page 9, line 14-17, of OA)

Applicants respectfully traverse the Examiner's above ground of rejection. Applicants maintain that mouse models are key to the study of many human pathologies, and that numerous mouse tumor models resembling human cancers have been developed or are available. These models have been widely used for anticancer drug testing and with high reliability and predictability. For example, see Monosov et al., U.S. Patent Nos. 5,491,284, issued February 13, 1996, and 5,569,812, filed October 29, 1996, attached herein as **Exhibit G**. Monosov et al., U.S. Patent No. 5,491,284, discloses and claims a nude mouse model for human neoplastic disease which mimic the progression of neoplastic disease in the human donor (col 3, lines 1-7 and col. 11, lines 19-29).

In response, applicants' new claims recite a composition comprising a Salmonella strain expressing the F' pilus and a filamentous bacteriophage wherein the Salmonella is capable of targeting tumors by intravenous administration, i.e., page 43, lines 20-34, page 44, and page 45, lines 1-27. New claims 25-43 do not contain the above issues raised by the Examiner, thereby rendering the above ground(s) of reject moot.

Applicants : BERMUDEZ, et al.
U.S. Serial No.: 10/790,586
Filed : March 1, 2004
Page : 21

7. The Examiner alleged that the quantity of experimentation necessary to carry out the invention is high because one of skill in the art would have to determine (a) if a gene of interest encoded by a bacteriophage and delivered by a bacteria is delivered efficiently and preferentially to the targeted tumor type; (b) if the gene of interest is expressed efficiently; (c) if such expression provides any therapeutic effect; and (d) if the bacterial composition would survive and bacteria would reach the targeted tumors efficiently and in sufficient number to achieve a therapeutic effect

Without conceding the correctness of the Examiner's position and to expedite the prosecution of this Application, Applicants have canceled claims 1-9 and 11-18. New claims 25-43 do not recite "a gene of interest encoded by a bacteriophage," thereby rendering the above ground(s) of rejection moot.

Claims Rejections - 35 U.S.C. § 112, second paragraph

The Examiner rejected claims 1-9 and 11-18 under 35 U.S.C. § 112, second paragraph, as being indefinite for failing to particularly point out and distinctly claim the subject matter which applicant regards as the invention.

Without conceding the correctness of the Examiner's position and to expedite the prosecution of this Application, Applicants have canceled claims 1-9 and 11-18

Applicants : **BERMUDES, et al.**
U.S. Serial No.: **10/790,586**
Filed : **March 1, 2004**
Page : **22**

and added new claims 25-44, which do not contain the above mentioned issues, thereby rendering the above rejection(s) moot.

Applicants : BERMUDEZ, et al.
U.S. Serial No.: 10/790,586
Filed : March 1, 2004
Page : 23

CONCLUSION

Applicants believe that all grounds of objections and rejections raised in the outstanding Office Action have been fully addressed. Accordingly, Applicants respectfully request the reconsideration and withdrawal of these grounds of objections and rejections, and respectfully request favorable action to be rendered by the Examiner.

If a telephone interview would be of assistance in advancing prosecution of the subject application, Applicants' undersigned attorney invites the Examiner to telephone him at the number provided below.

No fee is deemed necessary in connection with the filing of this Communication. However, if any fee is required, authorization is hereby given to charge the amount of any such fee to Deposit Account No. 50-1891.

Respectfully submitted,

Albert Wai Kit Chan

Albert Wai-Kit Chan
Registration No. 36,479
Attorney for Applicants
Law Offices of
Albert Wai-Kit Chan, LLC
World Plaza, Suite 604
141-07 20th Avenue
Whitestone, New York 11357
Tel: (718) 357-8836
Fax: (718) 357-8615
e-mail: kitchanlaw@aol.com

I hereby certify that this paper is being deposited this date with the U.S. Postal Service with sufficient postage for first class mail in an envelope addressed to:

Commissioner for Patents
P.O. Box 1450
Alexandria, VA 22313-1450

Albert Wai Kit Chan 12/8/04
Albert Wai-Kit Chan Date
Reg. No. 36,479

α_v Integrins as receptors for tumor targeting by circulating ligands

Renata Pasqualini*, Erkki Koivunen¹, and Erkki Ruoslahti*

La Jolla Cancer Research Center, The Burnham Institute, La Jolla, CA, and ¹Department of Biosciences, Division of Biochemistry, University of Helsinki, Finland
*Corresponding authors: (e-mail: rarap@ljcrf.edu [RP]; ruoslahti@ljcrf.edu [ER])

Received 14 January 1997; accepted 3 April 1997

Phage displaying an Arg-Gly-Asp (RGD)-containing peptide with a high affinity for α_v integrins homed to tumors when injected intravenously into tumor-bearing mice. A substantially higher amount of α_v -directed RGD phage than control phage was recovered from malignant melanomas and breast carcinoma. Antibodies detected the α_v -directed RGD phage in tumor blood vessels, but not in several normal tissues. These results show that the α_v integrins present in tumor blood vessels can bind circulating ligands and that RGD peptides selective for these integrins may be suitable tools in tumor targeting for diagnostic and therapeutic purposes.

Keywords: phage display, tumor targeting, RGD, angiogenesis, integrins

Endothelial cells in different parts of the vasculature are not alike; various organs and tissues express specific endothelial surface markers, while a separate set of surface molecules marks the endothelium at sites of inflammation¹⁻⁶.

Tumor vasculature undergoes continuous angiogenesis and expresses molecular markers that characterize these vessels. The markers in angiogenic endothelium include certain receptors for vascular growth factors, such as various VEGF receptors⁷⁻¹³, and the $\alpha_v\beta_3$ integrin¹⁴. Preventing the $\alpha_v\beta_3$ integrin, and in some cases $\alpha_v\beta_5$, from binding to their ligands causes apoptosis in the endothelial cells of newly formed blood vessels^{15,16}. Peptides that mimic ligands of these integrins and anti-integrin antibodies capable of inhibiting their ligand-binding have antitumor effects^{16,17}. Blockers of α_v integrins also show promise as inhibitors of pathological angiogenesis in other situations, such as in retinopathy¹⁸.

An immunohistochemical study indicates that various integrins, including $\alpha_v\beta_3$, can be expressed on the apical surface of blood vessels¹⁹. We asked whether $\alpha_v\beta_3$ integrins are active and available for binding of circulating ligands and whether the expression levels of this integrin in tumor and normal vasculature are sufficiently different to permit tumor targeting.

We recently developed an *in vivo* targeting system that uses peptides expressed on the surface of bacteriophage to study organ-specific targeting⁶. Peptides in as many as 10^9 permutations are expressed on the surface of phage where the peptide is fused to one of the phage surface proteins²⁰; in the *in vivo* procedure, phage capable of homing into certain organs or tissues following an intravenous injection are selected from such a peptide library. The ability of individual peptides to target a tissue can also be analyzed by this method⁶.

We use phage-displayed peptides to target tumors, focusing on targeting of α_v integrins in tumor blood vessels with a selected peptide. Many integrins, the α_v integrins in particular, recognize an Arg-Gly-Asp (RGD) sequence as the critical determinant in their ligands. Peptides containing the RGD sequence are commonly employed as specific probes for the various integrins²¹. We

used a nine-amino acid peptide that contains an RGD sequence in a cyclic conformation with two disulfide bonds, which is highly selective for the α_v integrins²². We have found that phage bearing this cyclic nonapeptide, CDCRGDCFC, become selectively concentrated in tumors, suggesting that α_v -directed peptides can be useful in diagnostic and therapeutic tumor targeting.

Results

Targeting of CDCRGDCFC-phage into tumors. We studied the distribution of phage carrying the CDCRGDCFC peptide (RGD-4C phage) and various control phage after intravenous injection into tumor-bearing nude mice. MD-MBA-435 human breast cancer tumor (diameter 1–1.5 cm) grown in the mammary fat pad was used as the initial target. The phage was rescued from the tissues 4 min after the injection, and the number of phage per gram of tissue was quantitated. The control phage mixture shows no appreciable enrichment in any organ without multiple rounds of selection, allowing comparison of the RGD-4C phage distribution with that of unselected control phage. The control phage mixture (and several individual phage used as additional controls, see below) were found in about 20-fold higher levels in the two normal tissues studied, the brain and the kidney, than in the tumors (Fig. 1A); the difference probably reflects greater blood flow into these normal organs than into tumor tissue. In contrast, twofold to threefold more of the RGD-4C phage was rescued from the tumors than from the control tissues, and less of this phage was found in the control tissues than of the control phage.

We have also quantitated the RGD-4C phage in tumor and brain tissues obtained after the mice were perfused through the heart, and have found that 20-fold more RGD-4C phage can be recovered from the tumor (not shown). This observation is in agreement with the immunostaining data detailed below (performed under the same conditions), which also show that the majority of phage in the normal tissues is not bound to the tissues, and it is likely to represent background.

The difference in the amount of the RGD-4C phage relative to the control unselected phage mixture was, on average, tenfold

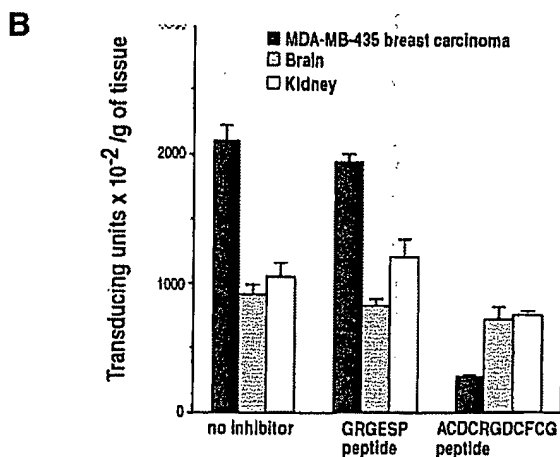
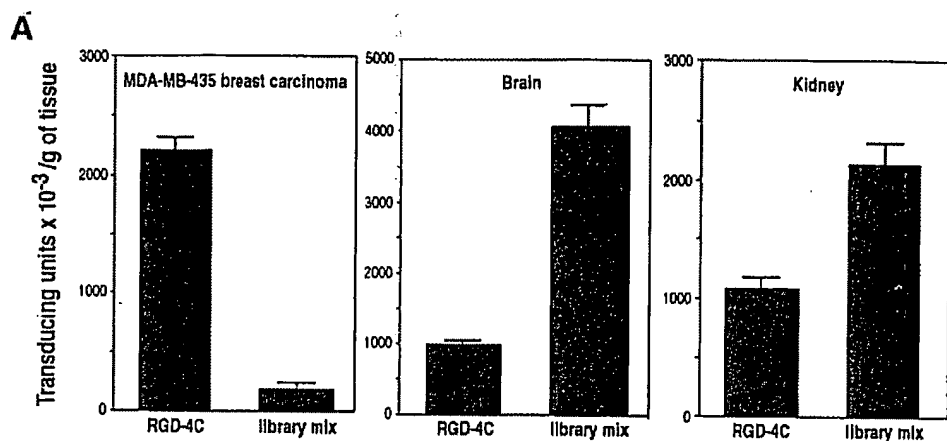
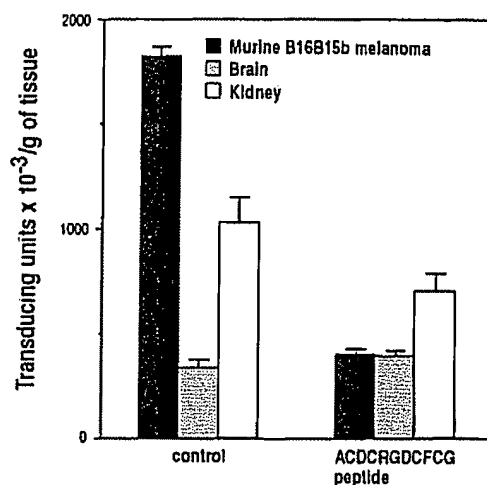


Figure 1. Intravenously injected phage carrying an α_v -directed RGD peptide are preferentially recovered from MDA-MB-435 derived breast carcinoma tumors. (A) Recovery of α_v -directed CDCRGDCFC-phage from tissues. Phage carrying the peptide, or pooled phage (CX5-7C libraries), were injected in the tail vein of mice bearing MDA-MB-435 breast carcinoma size-matched tumors (about 1.2 cm in diameter). The number of phage recovered and standard error of the mean (S.E.M.) from triplicate platings are shown. All differences are statistically significant ($p < 0.001$). (B) Inhibition of CDCRGDCFC-phage targeting by the corresponding soluble peptide. Phage carrying the peptide (10^6 transducing units) were injected in the tail vein of mice carrying MB-MDA-435 breast carcinoma tumors that were about 1.2 cm in diameter. The amounts of phage recovered from various tissues without inhibition and in the presence of a soluble peptide similar to the sequence displayed by the phage (ACDCRGDCFCG) or a control peptide (GRGESP) are shown. S.E.M. from triplicate platings is shown. All differences are statistically significant ($p < 0.001$).

Figure 2. Targeting of the CDCRGDCFC-phage into B16B15b murine melanoma tumors. Phage carrying the peptide (10^6 transducing units) were injected in the tail vein of mice bearing tumors that were about 1 cm in diameter. The phage was coinjected with 500 μ g of either the corresponding soluble peptide, ACDCRGDCFCG, or a control peptide (GRGESP). The number of phage recovered is shown. S.E.M. from triplicate platings is shown; all differences are statistically significant ($p < 0.001$).



(10 independent experiments). Taking into account this difference and also the lower background of the RGD-4C phage in the control organs, the overall tumor selectivity of the RGD-4C phage is estimated to be in the range of 40-fold to 80-fold. In addition, the specificity of the RGD-4C localization into the tumors was further demonstrated by a substantial reduction in the tumor accumulation upon coinjection of the cognate RGD peptide, ACDCRGDCFCG, (Fig. 1B). Coinjection of a control peptide, which has no appreciable affinity for integrins (GRGESP), had no effect; similar results were obtained in six experiments. In contrast to what was seen in the tumors, the RGD-4C peptide reduced only slightly, or did not affect at all, the amount of RGD-4C phage recovered from brain and kidneys, supporting the con-

clusion that the phage was nonspecifically trapped in these organs. Another RGD phage, which carries a peptide selective for the $\alpha_5\beta_1$ integrin, CRGDGWC (ref. 22), was also tested. It was found to be similar to the control phage mixture, showing no preferential accumulation into the MDA-MB-435-derived tumors (data not shown).

The RGD-4C phage also accumulated preferentially into subcutaneous murine B16B15b melanoma (Fig. 2) and human C8161 melanoma tumors (data not shown). The tumor homing was, in each case, greatly reduced by coinjection of the cognate peptide, but not by the GRGESP control peptide (Fig. 2). We also observed that when the C8161-derived and MDA-MB-435-derived tumors were smaller than 0.5 cm, less specific targeting was seen than with

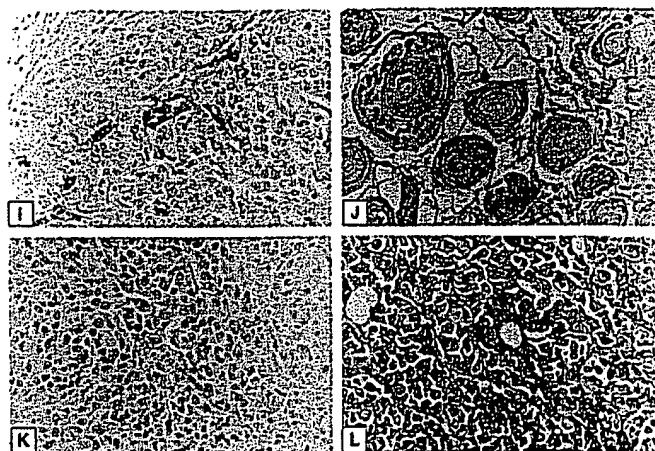
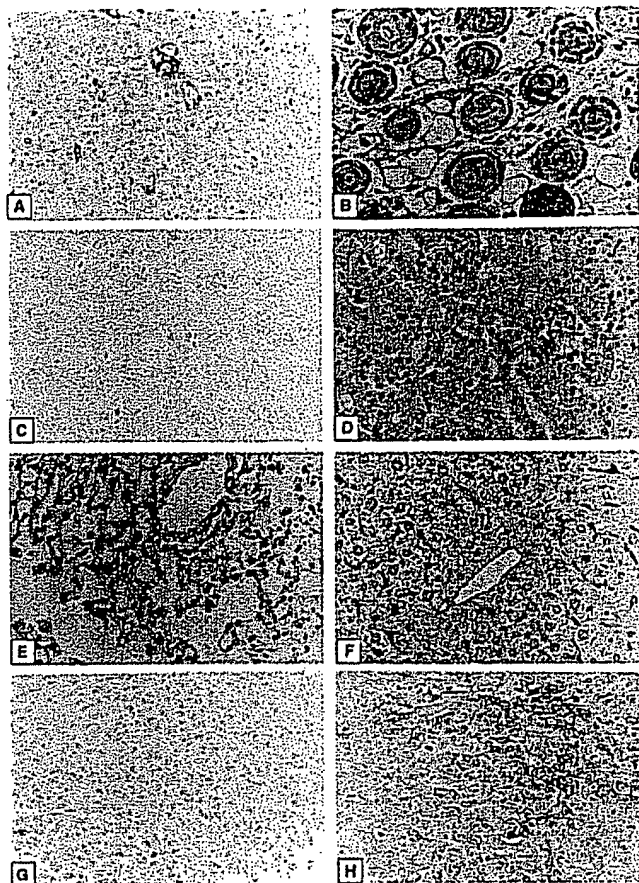


Figure 3. Immunohistochemical staining of phage in tumors and tissues of tumor-bearing mice. Phage carrying the α v-directed peptide CDCRGDCFC or insertless control phage were injected intravenously into mice. An antibody against M13 phage and a polyclonal anti- α v β 3 were used for staining. (A through F) Mice that received the phage carrying the α v-directed peptide CDCRGDCFC. (A) MDA-MB-435 breast carcinoma tumor tissue. (B) Skin adjacent to the tumor. (C) Brain. (D) Kidney. (E) Lung. (F) Liver. (G) Phage staining of MDA-MB-435 tumor tissue from a mouse that received insertless phage. (H) MDA-MB-435 tumor tissue stained with anti- α v β 3 antiserum. (I through L) Mice bearing B16B15b-derived melanoma. (I and J) Mice injected with the phage carrying the α v-directed peptide CDCRGDCFC. (I) Tumor. (J) Skin adjacent to the tumor. (K) Phage in tumor tissue from mice that received the insertless phage. (L) Tumor tissue stained with the anti- α v β 3 antiserum. Magnification = 400x.

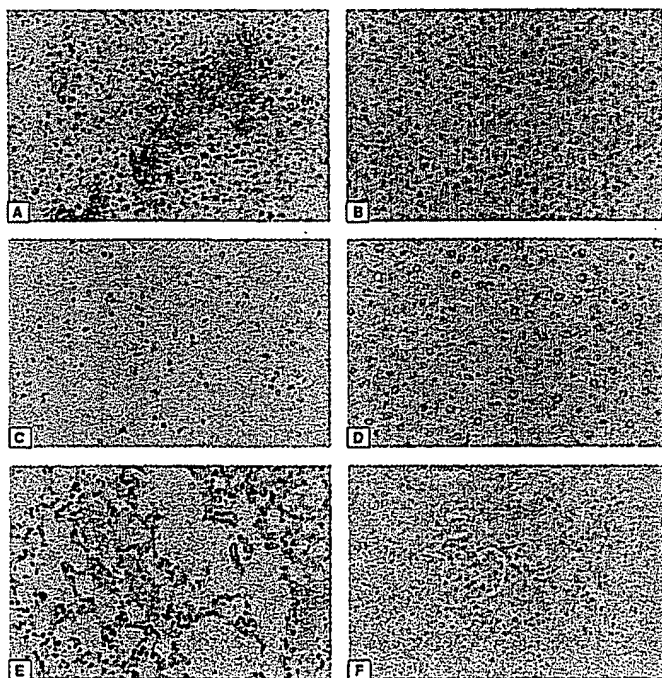


Figure 4. Detection of phage antigens in tissues 24 h after intravenous injection. Phage carrying the α v-directed peptide CDCRGDCFC or insertless control phage were injected intravenously into mice. (A, C, E, F) Mice that received the phage carrying the α v-directed peptide CDCRGDCFC. (A) MDA-MB-435 breast carcinoma tumor tissue. (C) Brain. (E) Lung. (F) Kidney. (B) Phage staining of MDA-MB-435 tumor tissue from a mouse that received insertless phage. (D) Brain tissue from an animal injected with a brain-selective phage (CSSRLDAC-phage⁹). Magnification = 100x.

larger tumors. This is likely due to the lower degree of vascularization in the smaller tumors, which we observed by staining for von Willebrand factor as a marker of blood vessels.

Immunohistochemical staining of phage in tumors and tissues of tumor-bearing mice. The phage experiments described above were performed by quantitating the phage in tissue extracts after a short circulation time. This experimental arrangement was chosen to avoid having the specifically bound phage be taken up by the cells and inactivated. However, we did note that perfusion of the mice through the heart reduced the background phage counts in the nontumor tissues. As any phage inactivation was not likely to be critical in immunostaining experiments, the mice were perfused prior to processing the tissues for staining. Marked staining for the phage was seen in an MDA-MB-435-derived breast carcinoma tumor from an animal injected with the RGD-4C phage (Fig. 3A), whereas injection of the control phage mixture or an insertless control phage (Fig. 3G) gave no staining in size-matched tumors. The staining observed in the tumors followed the small blood vessels and appeared to localize to the endothelial lining. Control tissues (skin adjacent to the tumor, brain, kidney, and lung) from animals injected with the RGD-4C phage showed no staining (Figs. 3B to E).

In keeping with the previously observed capture of circulating phage into tissues containing a reticuloendothelial system (RES) component⁴, both the RGD-4C and control phage caused staining in the liver (Fig. 3F). Phage quantitation experiments have shown that the liver uptake of the phage can be prevented by coinjecting the mice with an excess of noninfective fuse 5 phage (not shown). This and the fact that the liver localization was independent of the peptide carried by the phage clearly indicate that the liver uptake is a property of the phage, not of the peptide.

Immunostaining also localized the RGD-4C phage to blood

vessels within the melanoma tumors (Fig. 3I). The skin adjacent to the tumor was not stained (Fig. 3J) and control phage gave no staining in the tumor (Fig. 3K).

The MDA-MB-435 carcinoma and the B16B15b melanoma cells express the $\alpha v\beta 3$ integrin, as determined by FACS analysis (data not shown). Immunostaining of tumor sections with a polyclonal anti- $\alpha v\beta 3$ antibody revealed staining of both the tumor tissue and the blood vessels in it (Figs. 3H and L).

To mimic more closely a clinically relevant tumor-targeting situation, we have also conducted a series of experiments in which the $\alpha v\beta 3$ -directed RGD phage was allowed to circulate for 24 h prior to harvesting of the tissues for immunostaining. At the 24 h time point, about 90% of the phage had been eliminated from the circulation. Immunostaining revealed phage proteins in and around the small blood vessels within the tumor (Fig. 4A), but all other organs studied (with the exception of the liver and the spleen) were negative (Fig. 4B, C, E, and F). A phage carrying a brain-homing peptide stays inside the blood vessels, even after 24 h (Fig. 4D).

Discussion

We have shown that an RGD peptide selective for αv integrins can direct phage displaying such a peptide to home into tumors. Blood vessels appear to be the structural component targeted by the phage displaying the αv -directed peptide.

We used peptides displayed on phage as a probe in our tumor targeting experiments. While phage as a carrier has some limitations, such as being taken up by the RES^{6,23}, it can serve to illustrate the potential of peptides to target materials into selected tissues. In this regard, the phage mimics the targeting of particles, such as liposomes, as well as the viruses used in gene therapy. The phage can readily be detected in tissues both by counting infectious phage particles and by employing immunohistochemistry. Moreover, the specificity of the RGD-4C phage can be assessed by inhibiting the localization with free peptide and by using control phage that carry another peptide or no peptide at all.

Several observations attested to the specificity of the tumor targeting by the αv -directed RGD-4C phage and the peptide displayed by it. First, only the phage carrying the RGD-4C peptide accumulated in tumors, whereas phage carrying another RGD peptide with a different integrin specificity or phage with unrelated inserts did not (except those we have specifically selected for tumor homing after multiple rounds, data not shown). Secondly, the difference between the tumor accumulation of the RGD-4C phage and various control phage was substantial, an average of tenfold. Taking into account the lower background of the RGD-4C phage in nontumor tissues, the estimated tumor selectivity of this phage is even more impressive. Thirdly, the cognate peptide inhibited the tumor homing of the RGD-4C phage. This latter result shows that the phage homing is dependent on the peptide displayed by the phage, and is not caused by some other coincidental property of the phage. Another control, lack of any effect by a control peptide on the tumor homing of the RGD-4C phage, further substantiates the specificity.

The large difference in the tumor homing of the RGD-4C phage relative to control phage reflects the potential of the system in tumor targeting. We did recover significant quantities of the RGD-4C phage from various control organs in the experiments that used phage counting as the read-out. However, at least a majority, if not all, of this phage recovery represents nonspecific background, because it was not reduced upon coinjection of the cognate peptide. Moreover, perfusion of the mice greatly improved the tumor tissue/normal tissue ratio. Examination of histological sections of the tumors revealed fewer blood vessels in the tumors than, for example, in the brain (Fig. 3), suggesting that the back-

ground phage level in a given tissue may reflect the number of blood vessels in that tissue.

The liver and spleen, unlike the other normal tissues we analyzed, contained phage detectable by immunostaining even after perfusion, which tends to minimize or eliminate background in other organs. The RES is known to capture circulating particles, including phage²³, and this appears to be the reason for the presence of phage in liver and spleen. Administration of noninfective phage prevents the capture by the RES of phage from a coinjected peptide library (data not shown), making it possible to reduce or eliminate this limitation of the phage targeting system. As the liver uptake is property of the phage, and not related to the peptide carried by the phage, it is not likely to limit the tumor-targeting potential of the RGD-4C peptide. This potential is illustrated by the high overall tumor selectivity; the expectation is that other materials coupled to the same peptide would display similar preference for tumors.

Even though both the endothelia and the tumors themselves expressed the αv integrin(s) targeted by the RGD-4C peptide, our observations indicate that the RGD-4C phage binds to the blood vessels within the tumors. Endothelial binding of the phage was strongly suggested by the staining results, which showed that the phage is confined to the tumor blood vessels. Our earlier results with phage targeting into the brain and kidney also showed exclusive blood vessel localization of the phage⁶. The endothelium is a likely—and the tumor cells an unlikely—target for the RGD-4C phage (and targeting using phage-displayed peptides in general). The large size of the phage (900 nm in length) makes it unlikely that the phage would exit the circulation and penetrate into tissues²⁴, particularly within the few minutes we allowed the phage to circulate. Moreover, the vasculature is a likely common denominator for the three tumors we targeted with the RGD-4C phage, because the tumors came from two different species (murine and human) and represented two distinct tumor types (melanoma and carcinoma). As blood vessels in tumors are known to be "leaky"²¹⁻²², it may be that *in vivo* screening will also yield phage capable of binding to receptor molecules in the parenchyma of tumors.

RGD peptides are generally accepted as probes for integrin functions *in vitro* and *in vivo*. Moreover, drugs are being developed based on peptides and their mimetics that specifically block individual integrins²¹. Blocking ligand binding by the $\alpha v\beta 3$ (or $\alpha v\beta 5$) integrin with RGD peptides or antibodies shows promise as an antiangiogenic therapy. Such treatment causes apoptosis in those endothelial cells that are in the process of forming new blood vessels, while not harming established blood vessels¹⁴⁻¹⁸. These results imply that αv integrin(s), while accessible to soluble peptides and antibodies in neovasculature, are engaged in endothelial cell interactions with the underlying extracellular matrix. However, in agreement with immunohistochemical studies showing $\alpha v\beta 3$ on the apical surface of blood vessels¹⁹, our results show that sufficient amounts of these integrins are accessible to a particulate ligand from the circulation, and that the available integrin is concentrated in tumor vasculature.

The experimental paradigm in which RGD-C-phage was allowed to circulate for 24 h parallels an actual drug targeting into a tumor in a clinical setting. Under these conditions the tumor contained substantial phage staining, whereas less than 10% of the injected phage was left in the circulation, and all normal tissues examined, except the RES, were devoid of phage staining. The breast carcinoma cells used in these experiments express the $\alpha v\beta 3$ integrin as do many human tumors¹⁴, and binding of the phage to the tumor cells may have contributed to the staining outside the blood vessels in the 24-h experiments. These results suggest that it may be possible to use αv -directed reagents, either peptides or antibodies, to carry drugs, radionuclides, genes, and other thera-

peutic substances and devices into tumor vasculature, and from there, into tumor parenchyma. Peptides may have advantages in this regard, because they are smaller, more likely to diffuse efficiently within the tumor, and less likely to be immunogenic

Experimental protocol

Animals. Female 2-month old nude mice (Harlan Sprague Dawley, San Diego, CA) were used in this study. The animals were cared for according to the Institute's animal facility guidelines. Avertin (0.015 ml/g) was used as anesthetic.

Cell lines and tumors. The human tumor cells used in this study were: human MDA-MB-435 breast carcinoma²⁸, murine B16B15b melanoma²⁹, and C8161 human melanoma³⁰. Cells were cultured in DMEM, 10% FCS (Irvine Scientific, Irvine, CA) with sodium pyruvate, L-glutamine, and penicillin/streptomycin (Gibco BRL, Bethesda, MD). Culture medium was changed 12 h before the cells were injected into mice. Cells were detached from monolayers at 80% confluence with PBS containing 2.5 mM EDTA, washed three times with DMEM, counted, and resuspended in DMEM. Tumor cells were injected in the mammary fat pad (10⁵ per site); tumor growth was monitored daily. Between 20 to 40 days postinjection, when the tumors were 0.4 to 1.5 cm in diameter, animals bearing tumors of similar sizes were selected and used for targeting experiments and histological analysis.

Tumor targeting. Phage (10⁸ transducing units) were injected intravenously into mice carrying tumors, and the phage that had accumulated in the tumor and in various tissues were quantitated as described⁴, with minor modifications. In brief, 2 to 4 min after the injection, the mice were snap frozen in liquid nitrogen while under deep anesthesia. To recover the bound phage, the carcasses were partially thawed at room temperature, and organs and tumors were removed, weighed, and ground in 1 ml of DMEM-PI (DMEM containing the protease inhibitors phenyl methyl sulfonyl fluoride (1 mM), aprotinin (20 µg/ml), and leupeptin (1 µg/ml)). Tissue and tumor samples were washed three times with ice-cold DMEM-PI containing 1% BSA and incubated with 1 ml of competent K91-kan bacteria for 20 min at room temperature. Ten milliliters of NZY medium containing 0.2 µg/ml tetracycline were added, the mixture was incubated at room temperature for 20 min, and 5 to 50 µl aliquots diluted in 100 µl of TBS/1% gelatin were plated in agar plates in the presence of 40 µg/ml of tetracycline. After 12 h, the colonies were counted. In peptide inhibition experiments, phage were coinjected with 500 µg of ACDCRGDCFCG or GRGESP. The peptides, ACDCRGDCFCG and GRGESP, were synthesized by Immunodynamics Inc. (San Diego, CA) and purified to homogeneity by HPLC. The ACDCRGDCFCG peptide (RGD-4C) is a cyclic peptide that reproduces the sequence of the insert in a phage isolated from a peptide-display library and includes two amino acids from the phage sequence as flanking exocyclic residues at each end³¹. As the present experiments were carried out in mice, we confirmed that the RGD-4C peptide binds specifically to αv integrins in mouse endothelial cells (Bend 3)³¹ by showing that the attachment of these cells to vitronectin (an αv integrin function) could be inhibited without affecting their attachment to fibronectin or laminin, which are $\beta 1$ integrin functions (results not shown). Control experiments also showed that none of the peptides used in this work affected the ability of the phage to infect bacteria. The selectivity of the RGD-4C towards tumors was calculated based on multiple parameters; (1) the overall number of RGD-4C phage recovered from the tumors, brain, and kidney; (2) the background counts found in tumors, brain, and kidney for unselected phage mixtures (which is high in brain and kidney); and (3) the lower background of the RGD-4C phage in the control organs. A mixture of phage was used as a control in most of the experiments to eliminate the bias that the use of a single control phage might introduce in an experiment. We have, however, also used individual phage as controls.

Immunohistochemical staining of phage in tumor blood vessels. Tissue sections were prepared from mice injected with phage as described above; the anesthetized mice were then perfused through the heart with DMEM. In some experiments, the phage were allowed to circulate for 24 h. The organs and tumors were fixed in Bouin's solution; an antibody against M13 (Pharmacia, Piscataway, NJ) was used for the staining, followed by a peroxidase-conjugated secondary antibody (Sigma, St. Louis, MO), as described⁴. Tumor sections were also stained with a rabbit polyclonal antibody against $\alpha v \beta 3$ ³².

Acknowledgments

We thank Wadiah Arap, Eva Engvall, and Kathryn Ely for comments on the manuscript, the Institute's Animal Facility staff for their assistance, and Garth

Nicolson (University of Texas, M.D. Anderson Cancer Center) for the B16B15b melanoma cell line. This work was supported by grants CA 28896 and Cancer Center Support Grant CA 30199 from the National Cancer Institute. EK is supported by the Academy of Finland; RP was supported by the Arthritis Foundation and the Susan G. Komen Breast Cancer Foundation.

1. Pauli, B.U., Augustin-Voss, H.G., El-Sabban, M.E., Johnson, R.C., and Hammer, D.A. 1990. Organ-preference of metastasis: The role of endothelial cell adhesion molecules. *Cancer Metastasis Rev.* 9:175-189.
2. Zetter, B.R. 1990. The cellular basis of site-specific tumor metastasis. *N Engl J Med.* 322:605-612.
3. Springer, T.A. 1994. Traffic signals for lymphocyte recirculation and leukocyte emigration: the multistep paradigm. *Cell* 76:301-314.
4. Butcher, E.C., and Picker, L.J. 1996. Lymphocyte homing and homeostasis. *Science* 272:60-66.
5. Goetz, D.J., El-Sabban, M.E., Hammer, D.A., and Pauli, B.U. 1996. Lu-ECAM-1-mediated adhesion of melanoma cells to endothelium under conditions of flow. *Int J. Cancer* 65:192-199.
6. Pasqualini, R., and Ruoslahti, E. 1996. Organ targeting in vivo using phage display peptide libraries. *Nature* 380:364-366.
7. Baillie, C.T., Winslet, M.C., and Bradley, N.J. 1995. Tumour vasculature—a potential therapeutic target. *Br. J. Cancer* 72:257-267.
8. Burrows, F.J., and Thorpe, P.E. 1994. Vascular targeting—a new approach to the therapy of solid tumors. *Pharmacol Ther.* 64:155-174.
9. Buckle, R. 1994. Vascular targeting and the inhibition of angiogenesis. *Ann Oncol.* 4(suppl.):45-50.
10. Mustonen, T., and Alitalo, K. 1995. Endothelial receptor tyrosine kinases involved in angiogenesis. *J. Cell Biol.* 129:895-898.
11. Lappi, D.A. 1995. Tumor targeting through fibroblast growth factor receptors. *Semin. Cancer Biol.* 6:279-288.
12. Martiny-Baron, G., and Marme, D. 1995. VEGF-mediated tumor angiogenesis: a new target for cancer therapy. *Curr. Opin. Biotechnol.* 6:675-680.
13. Rettig, W.J., Garin-Chesa, P., Healey, J.H., Su, S.L., Jaffe, E.A., and Old, L.J. 1992. Identification of endosialin, a cell surface glycoprotein of vascular endothelial cells in human cancer. *Proc. Natl. Acad. Sci. USA* 89:10832-10836.
14. Brooks, P.C., Clark, R.A., and Cheresch, D.A. 1994. Requirement of vascular integrin $\alpha v \beta 3$ for angiogenesis. *Science* 264:569-571.
15. Friedlander, M., Brooks, P.C., Shaffer, R.W., Kincaid, C.M., Varnier, J.A., and Cheresch, D.A. 1995. Definition of two angiogenic pathways by distinct αv integrins. *Science* 270:1500-1502.
16. Brooks, P.C., Montgomery, A.M., Rosenfeld, M., Reisfeld, R.A., Hu, T., Klier, G., et al. 1994. Integrin $\alpha v \beta 3$ antagonists promote tumor regression by inducing apoptosis of angiogenic blood vessels. *Cell* 79:1157-1164.
17. Brooks, P.C., Stromblad, S., Klein, R., Visscher, D., Sarkar, F.H., and Cheresch, D.A. 1995. Anti-integrin $\alpha v \beta 3$ blocks human breast cancer growth and angiogenesis in human skin. *J. Clin. Invest.* 96:1815-1822.
18. Hammes, H.-P., Brownlee, M., Jonczyk, A., Sutter, A., and Preissner, K.T. 1996. Subcutaneous injection of a cyclic peptide antagonist of vitronectin receptor-type I integrins inhibits retinal neovascularization. *Nature Med.* 5:529-533.
19. Conforti, G., Dominguez-Jimenez, C., Zanetti, A., Gimbrone, M.A., Cremona, O., Marchisio, P.C., et al. 1992. Human endothelial cells express integrin receptors on the luminal aspect of their membrane. *Blood* 80:437-446.
20. Smith, G.P., and Scott, J.K. 1993. Libraries of peptides and proteins displayed in filamentous phage. *Methods Enzymol.* 212:228-257.
21. Ruoslahti, E. 1996. RGD and other recognition sequences for integrins. *Annu Rev. Cell Dev. Biol.* 12:697-715.
22. Kolvinen, E., Wang, B., and Ruoslahti, E. 1995. Phage libraries displaying cyclic peptides with different ring sizes: ligand specificities of the RGD-directed integrins. *Bio/Technology* 13:265-270.
23. Geter, M.R., Trigg, M.E., and Merrill, C.R. 1973. Fate of bacteriophage lambda in non-immune germ-free mice. *Nature* 246:221-223.
24. Shockley, T.R., Lin, K., Nagy, J.A., Tompkins, R.G., Dvorak, H.F., and Yarmush, M.L. 1991. Penetration of tumor tissue by antibodies and other immunoproteins. *Ann. N.Y. Acad. Sci.* 618:367-382.
25. Dvorak, H.F., Nagy, J.A., and Dvorak, A.M. 1991. Structure of solid tumors and their vasculature: implications for therapy with monoclonal antibodies. *Cancer Cells* 3:77-85.
26. Folkman, J. 1995. Angiogenesis in cancer, vascular, rheumatoid and other disease. *Nature Med.* 1:27-31.
27. Hanahan, D., and Folkman, J. 1996. Patterns and emerging mechanisms of the angiogenic switch during tumorigenesis. *Cell* 86:353-364.
28. Rak, J.W., St. Croix, B.D., and Kerbel, R.S. 1995. Consequences of angiogenesis for tumor progression, metastasis and cancer. *Anticancer Drugs* 6:3-18.
29. Price, J.E., Polyzos, A., Zhang, R.D., and Daniels, L.M. 1990. Tumorigenicity and metastasis of human breast carcinoma cell lines in nude mice. *Cancer Res.* 50:717-721.
30. Nicolson, G.L., Inoue, T., Van Pelt, C.S., and Cavanaugh, P.G. 1990. Differential expression of a Mr approximately 90,000 cell surface transferin receptor-related glycoprotein on murine B16 metastatic melanoma sublines selected for enhanced brain or ovary colonization. *Cancer Res.* 50:515-520.
31. Welch, D.R., Bisl, J.E., Miller, B.E., Conaway, D., Sefter, E.A., Yohem, K.H., et al. 1991. Characterization of a highly invasive and spontaneously metastatic human malignant melanoma cell line. *Int. J. Cancer* 47:227-237.
32. Montesano, R., Pepper, M.S., Mühle-Steinlein, U., Risau, W., Wagner, E.F., and Orci, L. 1990. Increased proteolytic activity is responsible for the aberrant morphogenetic behavior of endothelial cells expressing the middle T oncogene. *Cell* 62:435-445.

Systemic administration of attenuated *Salmonella choleraesuis* carrying thrombospondin-1 gene leads to tumor-specific transgene expression, delayed tumor growth and prolonged survival in the murine melanoma model

Che-Hsin Lee,¹ Chao-Liang Wu,^{1,2} and Ai-Li Shiau^{1,3}

¹Institute of Basic Medical Sciences, National Cheng Kung University Medical College, Tainan, Taiwan;

²Department of Biochemistry, National Cheng Kung University Medical College, Tainan, Taiwan; and

³Department of Microbiology and Immunology, National Cheng Kung University Medical College, Tainan, Taiwan.

Some anaerobic and facultative anaerobic bacteria have been used experimentally as anticancer agents because of their selective growth in the hypoxia regions of solid tumors after systemic administration. We have previously shown the feasibility of using attenuated *Salmonella choleraesuis* as a gene delivery vector. In this study, we exploited *S. choleraesuis* carrying thrombospondin-1 (TSP-1) gene for treating primary melanoma and experimental pulmonary metastasis in the syngeneic murine B16F10 melanoma model. Systemic administration of *S. choleraesuis* allowed targeted gene delivery to tumors. The bacteria accumulated preferentially in tumors over livers and spleens at ratios ranging from 1000:1 to 10,000:1. The level of transgene expression via *S. choleraesuis*-mediated gene transfer in tumors could reach more than 1800-fold higher than in livers and spleens. Notably, bacterial accumulation was also observed in the lungs with metastatic nodules, but not in healthy lungs. When administered into mice bearing subcutaneous or pulmonary metastatic melanomas, *S. choleraesuis* carrying TSP-1 gene significantly inhibited tumor growth and enhanced survival of the mice. Immunohistochemical studies in the tumors from these mice displayed decreased intratumoral microvessel density. Taken together, these findings suggest that TSP-1 gene therapy delivered by *S. choleraesuis* may be effective for the treatment of primary as well as metastatic melanomas.

Cancer Gene Therapy advance online publication, 17 September 2004; doi:10.1038/sj.cgt.7700777

Keywords: *Salmonella choleraesuis*; thrombospondin-1; tumor-targeted; antiangiogenesis

The use of preferentially replicating bacteria as an oncolytic agent is one of the innovative approaches for the treatment of cancer. This is based on the observation that some obligate or facultative anaerobic bacteria are capable of multiplying selectively in tumors and inhibiting their growth.^{1–3} Genetically modified, nonpathogenic bacteria have been tested as potential antitumor agents, either to provide direct tumoricidal effects or to deliver tumoricidal molecules. Apart from obligate anaerobes that target hypoxic/necrotic areas of solid tumors,^{4–8} *Salmonella typhimurium*, a facultative anaerobe capable of growing under both aerobic and anaerobic conditions, has also been exploited as a potential oncolytic agent.^{1,9} In addition, these tumor-targeted bacteria can be used to deliver genes encoding

prodrug-converting enzymes,^{5,10} angiogenic inhibitors,⁸ or cytokines,¹¹ aiming to enhance bacteriolytic effects.

A hypoxic microenvironment is characteristic of many solid tumors. Hypoxia is also associated with a more malignant phenotype, affecting genomic stability, apoptosis, angiogenesis, and metastasis.¹² Induction of angiogenesis plays an important role in the development and progression of most human tumors, including melanoma.¹³ Currently available therapies for malignant melanoma produce low response rates in patients. Therefore, more effective treatment modalities are needed. Therapeutic targeting of angiogenesis has recently been explored to inhibit malignant melanoma growth and metastasis.¹⁴ Thrombospondin-1 (TSP-1), an endogenous angiogenic inhibitor, has been shown to inhibit melanoma growth and metastasis in the B16F10 melanoma model.^{15,16}

As hypoxia is a common characteristic of human tumors, which adversely affects the prognosis of cancer patients, targeting hypoxia may be an effective means of improving cancer treatment. We have used a vaccine strain of *Salmonella choleraesuis* as a live vector for

Received February 19, 2004.

Address correspondence and reprint requests to: Dr Ai-Li Shiau, PhD, Department of Microbiology and Immunology, National Cheng Kung University Medical College, 1 Dashiue Road, Tainan 701, Taiwan. E-mail: alshiau@mail.ncku.edu.tw

carrying DNA vaccines.¹⁷ Recently, we have demonstrated its tumor-targeted potential in various primary tumor models.¹⁸ In this study, we exploited *S. choleraesuis* carrying a eukaryotic expression vector encoding TSP-1 as a tumor-targeted anticancer agent for primary and metastatic tumors of B16F10 melanoma, a highly aggressive and poorly immunogenic murine tumor. Our results suggest that by the dual effect of tumoricidal and antiangiogenic activities, *S. choleraesuis* carrying TSP-1 gene may have therapeutic potential for the treatment of primary as well as metastatic melanomas.

Materials and methods

Plasmids and bacteria

The TSP-1 expression vector pTCYTSP-1, under the control of the rat β -actin promoter, was constructed by cloning the 3.7-kb cDNA fragment of mouse TSP-1 into the *HindIII*/*SmaI* sites of pTCY.¹⁷ The coding region of luciferase was excised from the plasmid pGL3 (Promega, Madison, WI) by digestion with *HindIII* and *XbaI*, and cloned into the *HindIII*/*XbaI* sites of pTCY to generate pTCYLuc. Attenuated *S. choleraesuis*, which was used previously as an oral DNA vaccine vector,¹⁷ was transformed individually with pTCY, pTCYLacZ,¹⁷ pTCYLuc, and pTCYTSP-1 by electroporation, resulting in S.C./VO carrying the empty vector, S.C./LacZ encoding β -galactosidase (β -gal), S.C./Luc encoding luciferase, and S.C./TSP-1 encoding TSP-1, respectively.

Cell lines and mice

Murine B16F10 melanoma and human A549 lung adenocarcinoma cells were cultured in Dulbecco's modified Eagle's medium (DMEM) supplemented with 50 μ g/ml gentamicin, 2 mM L-glutamine, and 10% heat-inactivated fetal bovine serum (FBS) at 37°C in 5% CO₂. Human HMEC-1 microvascular endothelial cells¹⁹ were cultured in EGM endothelial growth medium containing 30 mg/ml bovine brain extract, 10 ng/ml human EGF, 1 μ g/ml hydrocortisone, 2% FBS, 50 μ g/ml gentamicin, and amphotericin B (Cambrex, East Rutherford, NJ). B16F10 cells cultured in six-well plates were transfected with 2 μ g of pTCYLacZ, and clonal derivatives were isolated by G418 (400 μ g/ml) selection and expanded to independent B16F10-LacZ clones. Male C57BL/6 mice (6–8 weeks old) were obtained from the Laboratory Animal Center of the National Cheng Kung University. The animals were maintained in specific pathogen-free animal care facility under isothermal conditions with regular photoperiods. The experimental protocol adhered to the rules of the Animal Protection Act of Taiwan and was approved by the Laboratory Animal Care and Use Committee of the National Cheng Kung University.

Assay of tumor targeting and gene transfer in vivo

B16F10 cells (10^6) were inoculated subcutaneously (s.c.) into the flank of C57BL/6 mice at day 0. At day 8, when tumor nodules ranging from 50 to 100 mm³ developed, the

mice were injected intraperitoneally (i.p.) with 2×10^6 colony-forming units (CFU) of S.C./Luc. At various time points after bacterial inoculation, groups of 7–8 mice were killed, and their tumors, livers, spleens, and whole blood were collected, weighed, and homogenized in 2 ml ice-cold, sterile PBS. Bacterial counts were performed after plating these homogenates or blood onto LB agar plate containing kanamycin (50 μ g/ml). Alternatively, tissue homogenates were lysed and examined for luciferase activities by a luciferase assay kit (Tropix, Bedford, MA) using a luminometer. The protein content in each sample was determined by the bicinchoninic acid (BCA) protein assay (Pierce, Rockford, IL). The final firefly luciferase activity is expressed in relative light units per microgram protein. In the experimental murine model for pulmonary metastatic melanoma, eight mice were injected with B16F10 cells (5×10^4) via the tail vein at day 0. At day 15, these mice were inoculated i.p. with S.C./LacZ (2×10^6 CFU) or PBS, and their lungs, livers, and spleens were collected at day 20 for quantification of S.C./LacZ numbers. Some of the lungs were snap frozen for determination of β -gal expression. Cryostat sections (4 μ m) were prepared, incubated with X-gal solution containing 100 mM K₃Fe(CN)₆, 100 mM K₄Fe(CN)₆, 1 M MgCl₂, and 1 mg/ml X-gal for 24 h, and then counterstained with eosin.

Assay of endothelial cell proliferation

A549 cells that have been seeded in 6-well plates at 10^5 cells/well and cultured overnight were infected with 2×10^6 CFU of S.C./TSP-1 or S.C./VO, or were mock-infected in antibiotic-free medium for 8 hours. The bacteria-containing medium was then removed, and the cells were carefully washed with PBS followed by replenishment with fresh DMEM supplemented with 2% FBS and 50 μ g/ml gentamicin. After 48 hours, the conditioned medium was collected, filtered through a 0.22- μ m filter, and analyzed for its activity to inhibit endothelial cell proliferation. HMEC-1 cells were seeded in hexaplicate at 2×10^3 cells/well in 96-well plates and cultured overnight. The medium was replaced with 50 μ l of EGM medium and 50 μ l of A549 conditioned medium. After 48 hours, cell proliferation was assessed by the colorimetric WST-1 assay according to the manufacturer's instructions.

Immunohistochemistry

A549 cells that had been infected with S.C./VO or S.C./TSP-1, or mock-infected as described above were fixed in 3.7% formaldehyde, treated with cold acetone, and quenched in 3.7% H₂O₂ for detection of TSP-1 expression by immunohistochemical staining using goat anti-mouse TSP-1 antibody (C-20, Santa Cruz, Santa Cruz, CA). To analyze microvessel density in tumors, groups of eight mice that had been inoculated s.c. with 10^6 of B16F10 cells at day 0 were injected i.p. with 2×10^6 CFU of S.C./TSP-1 or S.C./VO, or with PBS at day 8, and the tumors were excised and snap frozen at day 15. Cryostat sections (4 μ m) were prepared, fixed, and incubated with rabbit

antibody against factor VIII-related antigen (DAKO, Carpinteria, CA). After sequential incubation with appropriate peroxidase-labeled secondary antibody and aminoethyl carbazole (AEC) as substrate chromogen, the slides were counterstained with hematoxylin. Vessel density was determined by averaging the number of vessels in three areas of highest vessel density at $\times 400$ magnification in each section.²⁰

Treatment of primary melanoma and experimental pulmonary metastasis with S. choleraesuis carrying TSP-1 gene

In the primary melanoma model, groups of 7–8 C57BL/6 mice that had been inoculated s.c. with B16F10 cells (10^6) at day 0 were injected i.p. with 2×10^6 CFU of S.C./TSP-1 or S.C./VO, or with PBS at day 8. Palpable tumors were measured every 3 days in two perpendicular axes with a tissue caliper and the tumor volume was calculated as: (length of tumor) \times (width of tumor)² $\times 0.45$. The mean tumor volumes were calculated while all of the mice were still alive. The survival of the mice was also recorded daily.

In the experimental metastatic model, groups of 7–8 C57BL/6 mice that had been injected with B16F10 cells (5×10^4) via the tail vein at day 0 were injected i.p. with 2×10^6 CFU of S.C./TSP-1 or S.C./VO, or with PBS at day 15. The survival of the mice was monitored daily. To enhance the ability to quantify tumor burden in the lungs, pulmonary metastasis was also induced using B16F10-LacZ cells for evaluating the antimetastatic effect of S.C./TSP-1. The wet lung weight and β -gal activity of the lungs from these mice were measured at day 20. Lung homogenates were lysed and examined for β -gal activities by the β -gal assay kit (Tropix, Bedford, MA).

Statistical analysis

Tumor volumes were compared at a given time point using the unpaired, two-tailed Student's *t*-test. The survival analysis was performed using the Kaplan–Meier survival curve and log-rank test. Any *P*-value less than .05 is regarded as statistically significant.

Results

Preferential accumulation of S. choleraesuis and expression of transgene in melanomas via S. choleraesuis-mediated luciferase gene transfer

We monitored the kinetics of bacterial distribution in B16F10 tumor-bearing mice after injection with 2×10^6 CFU of S.C./Luc (Fig 1a). The bacterial amount was much higher in tumors than in livers and spleens at all the time points examined. Their amounts in the tumors reached a peak level at days 4–7 after bacterial inoculation, which were approximately three to four orders of magnitude higher than that found in livers or spleens. At day 12, a considerable amount of S.C./Luc was still found in the tumors, whereas S.C./Luc was detected to a much lesser extent in the spleens or livers. On the contrary, as

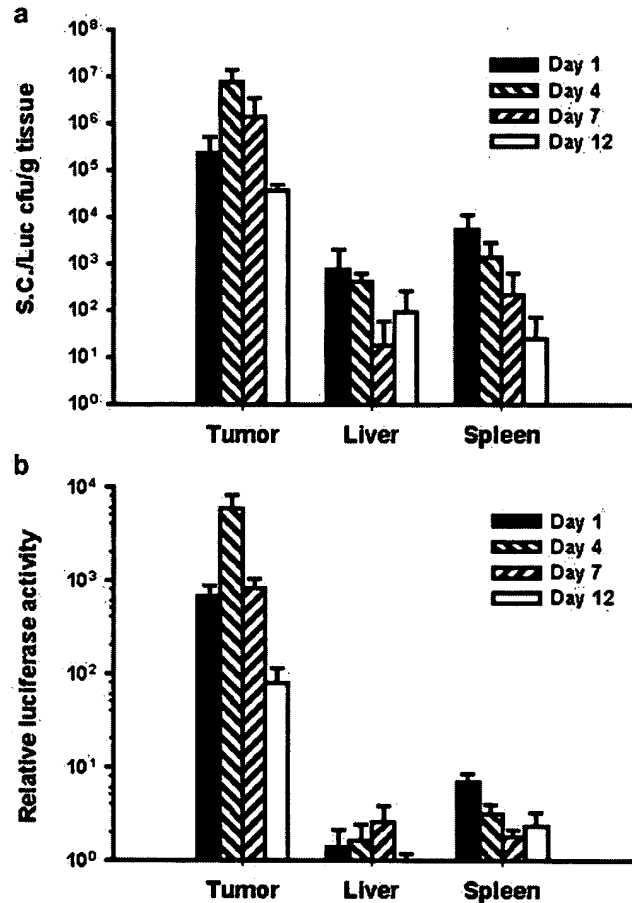


Figure 1 Preferential accumulation of *S. choleraesuis* and expression of luciferase in the tumors of mice administered systemically with S.C./Luc. C57BL/6 mice bearing subcutaneous B16F10 tumors of 50 to 100 mm³ received 2×10^6 CFU of S.C./Luc. (a) The amounts of accumulated S.C./Luc in the tumors, livers, and spleens were determined at 1, 4, 7, and 12 days postinfection. Each value represents mean \pm SD ($n=7-8$). (b) Luciferase activities in the tumors, livers, and spleens were determined at 1, 4, 7, and 12 days postinfection. Each column shows relative luciferase activity (mean \pm SD, $n=7-8$) to that for liver at day 12.

early as day 7, S.C./Luc was undetectable in the blood from all the mice tested (data not shown). After systemic administration of S.C./Luc to melanoma-bearing mice, luciferase activities over time were determined. As shown in Figure 1b, luciferase activity was detected for at least 12 days in the tumors but negligible in the livers and spleens from melanoma-bearing mice. At the peak at day 4, luciferase activity in the tumors was increased 1860-fold compared with that in the spleens, the next highest organ ($P=.016$). At day 12, luciferase activity in the tumor was still 33-fold higher than that in normal organs. Taken together, these results show that S.C./Luc, when injected i.p. to mice bearing established melanoma, preferentially accumulated and retained in large amounts in the tumors for at least 12 days, where luciferase expression, although gradually declined after day 4, persisted for at least 12 days.

Expression of bioactive TSP-1 in tumor cells via *S. choleraesuis*-mediated gene transfer

To test the feasibility of exploiting *S. choleraesuis* carrying TSP-1 gene for delivery and expression of the TSP-1 gene in tumor cells, S.C./TSP-1 and S.C./VO-infected A549 cells, as well as mock-infected cells were examined for TSP-1 expression. TSP-1 expression was clearly detectable in S.C./TSP-1-infected cells, but not in S.C./VO- or mock-infected counterparts (Fig 2a). The conditioned media of A549 cells infected with the bacteria were tested for their ability to inhibit endothelial cell proliferation *in vitro*. As shown in Figure 2b, the proliferation of HMEC-1 cells was significantly decreased upon addition of the conditioned medium from S.C./TSP-1-infected A549 cells compared with that from S.C./VO-infected ($P = .0000009$) or mock-infected cells ($P = .0000003$). Nevertheless, the conditioned medium from S.C./VO-infected A549 cells also slightly inhibited the proliferation of HMEC-1 cells as compared with that from the control cells ($P = .0153$). Collectively, these results indicate that *S. choleraesuis*-mediated gene transfer of TSP-1 gene allowed production of biologically active TSP-1 released from the infected cells.

Inhibition of subcutaneous melanoma growth by *S. choleraesuis* carrying TSP-1 gene

The *in vivo* antitumor effect of S.C./TSP-1 was evaluated in terms of tumor growth and survival in mice bearing subcutaneous B16F10 melanoma. Figure 3a shows that melanoma-bearing mice treated i.p. with S.C./TSP-1 at day 8 resulted in significant retardation of the tumor growth compared with those treated with S.C./VO ($P = .0438$) or PBS ($P = .0012$) at day 17 after tumor inoculation. The mean tumor volume in S.C./TSP-1-treated group was lowered by 45 and 61% compared with that in S.C./VO-treated and PBS-treated groups, respectively. Furthermore, as shown in Figure 3b, S.C./TSP-1 administration significantly prolonged the survival time of mice bearing subcutaneous melanoma compared with S.C./VO ($P = .0286$) or PBS ($P = .0272$) treatment. Taken together, a single systemic administration of *S. choleraesuis* carrying TSP-1 gene was effective in retarding tumor growth and enhancing survival in mice bearing subcutaneous melanoma.

Inhibition of tumor angiogenesis by *S. choleraesuis* carrying TSP-1 gene

At 7 days after systemic treatment of mice bearing day 8 subcutaneous melanoma with S.C./TSP-1, S.C./VO, or PBS, microvessel density within the tumors was analyzed by immunohistochemistry. Tumors from S.C./TSP-1-treated mice appeared much less vascularized than their S.C./VO- or PBS-treated counterparts, whereas no difference was found between S.C./VO- and PBS-treated groups (Fig 4a). As shown in Figure 4b, the number of factor VIII-positive intratumoral microvessels in

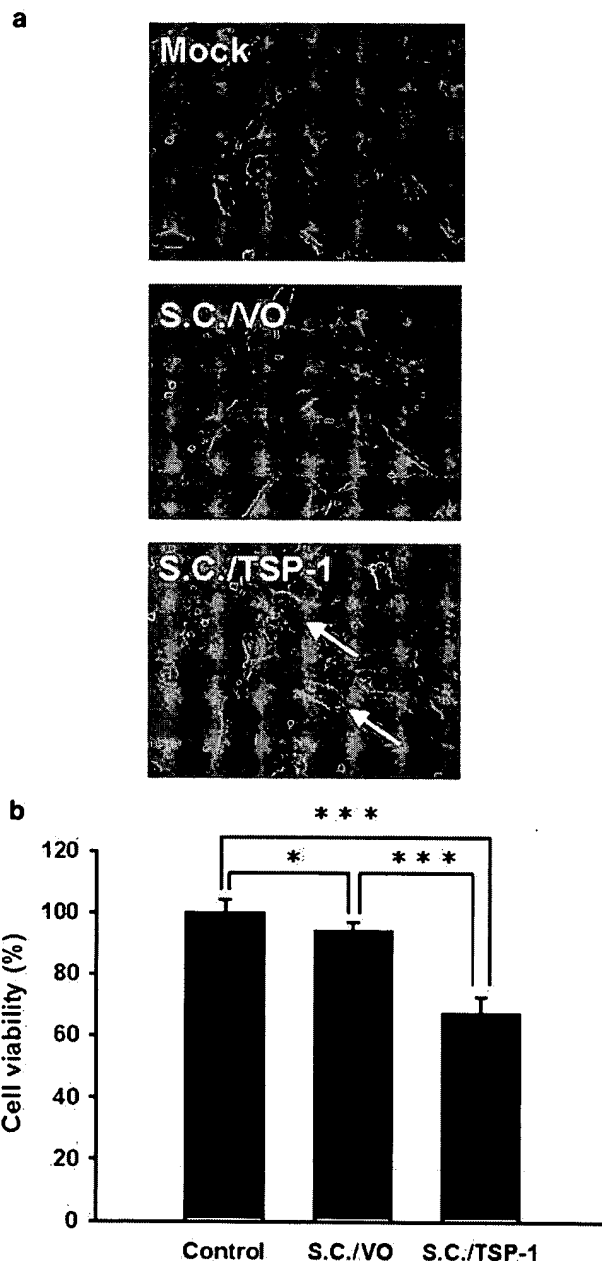


Figure 2 Expression of bioactive TSP-1 in A549 cells via *S. choleraesuis*-mediated gene transfer. (a) Detection of TSP-1 expression in A549 cells treated with S.C./TSP-1. A549 cells were infected with 2×10^6 CFU of S.C./TSP-1 or S.C./VO, or mock-infected for 8 hours, replenished with gentamicin-containing fresh medium, and further cultured for 48 hours. Expression of TSP-1 by the cells was detected by immunohistochemical staining with goat anti-mouse TSP-1 antibody. Arrows indicate the location of TSP-1-expressing cells. (b) Inhibition of endothelial cell proliferation by the conditioned medium from S.C./TSP-1-infected A549 cells. The 48-hour conditioned medium derived from A549 cells treated with S.C./TSP-1, S.C./VO, or PBS was diluted in EGM medium at 1:1 and used to treat HMEC-1 cells for 48 hours. Cell viability was then assessed by the WST-1 assay. The percentage of surviving cells (mean \pm SD, $n = 6$) was calculated by comparing surviving cells of the conditioned medium-treated cells to PBS-treated cells. * $P < .05$; *** $P < .001$.

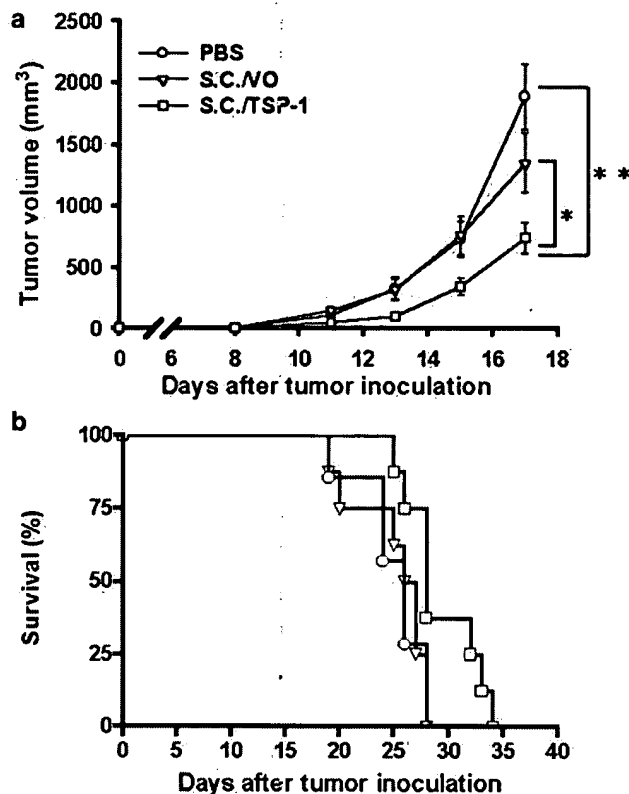


Figure 3 Antitumor effects of *S. choleraesuis* carrying TSP-1 gene on mice bearing subcutaneous melanoma. C57BL/6 mice that had been inoculated s.c. with B16F10 cells (10^6) at day 0 were injected i.p. with 2×10^6 CFU of S.C./TSP-1 or S.C./VO, or with PBS at day 8. (a) Tumor volumes (mean \pm SEM, $n=7-8$) among different treatment groups were compared at day 17. * $P < .05$; ** $P < .01$. (b) Kaplan-Meier survival curves of melanoma-bearing mice with various treatments are shown ($P < .05$ for S.C./TSP-1 versus S.C./VO or PBS).

S.C./TSP-1-treated mice was reduced by approximately 50% compared with that in mice treated with S.C./VO ($P = .0219$) or PBS ($P = .0113$).

Accumulation of *S. choleraesuis* and expression of exogenous β -gal in the lung bearing metastatic melanoma after systemic administration of *S. choleraesuis* carrying LacZ gene

To test whether *S. choleraesuis* was capable of targeting to metastatic pulmonary nodules, and hence may have therapeutic potential for inhibiting metastasis, mice bearing pulmonary metastatic melanoma ($n=8$) and normal healthy mice ($n=8$) were inoculated i.p. with S.C./LacZ, and the amounts of S.C./LacZ in the lungs, livers, and spleens were determined, and β -gal expression in the lungs were assessed 5 days after bacterial inoculation. As shown in Figure 5a, although there was no significant difference in the amount of S.C./LacZ in the livers or spleens, where no tumors were found, between melanoma-bearing and normal healthy mice, the bacterial numbers per gram tissue in the lungs with metastatic melanoma were much higher than those in the lungs from normal healthy mice ($P = .0000002$). Furthermore, β -gal expression was detected in the pulmonary

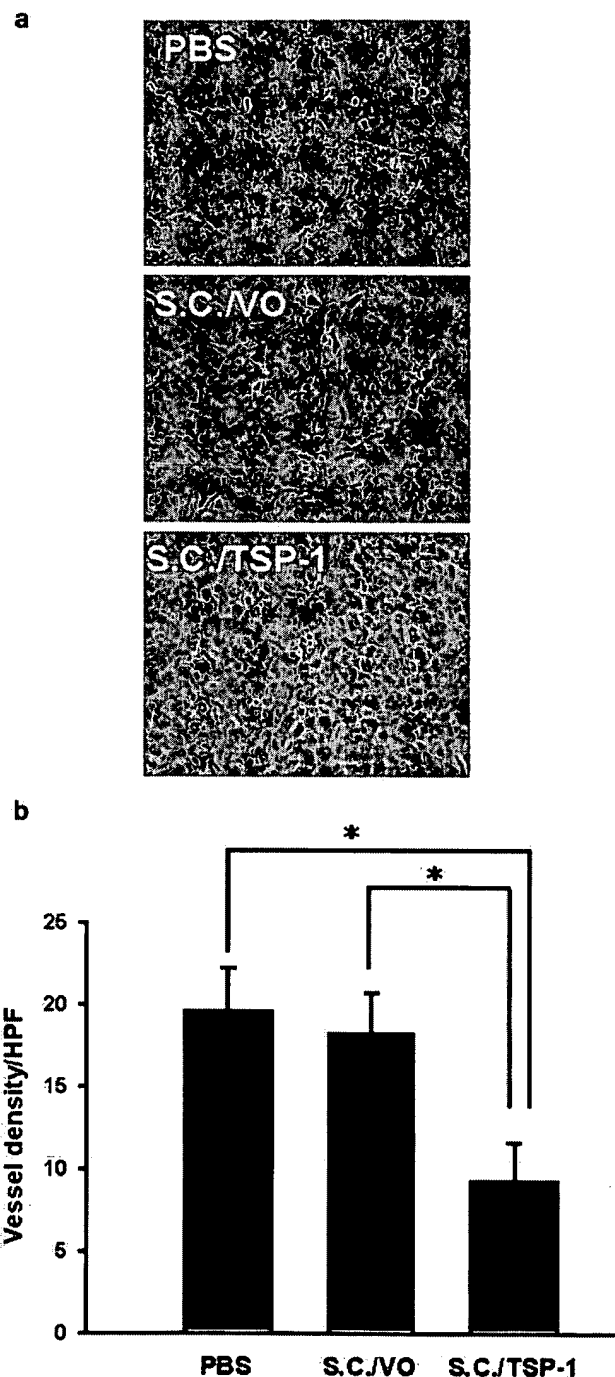


Figure 4 (a) Inhibition of angiogenesis in B16F10 melanomas by *S. choleraesuis* carrying TSP-1 gene. C57BL/6 mice that had been inoculated s.c. with 10^6 of B16F10 cells at day 0 were injected i.p. with 2×10^6 CFU of S.C./TSP-1 or S.C./VO, or with PBS at day 8. Tumors were excised at day 15, snap frozen and immunostained with rabbit antibody against factor VIII-related antigen ($\times 400$). (b) Intratumoral microvessel density was determined by averaging the number of vessels in three areas of highest vessel density at $\times 400$ magnification in each section. Each value represents mean \pm SEM from eight mice. * $P < .05$.

metastatic tumors of mice treated with S.C./LacZ, but not in those treated with PBS (Fig 5b). Taken together, *S. choleraesuis* not only accumulated in subcutaneous

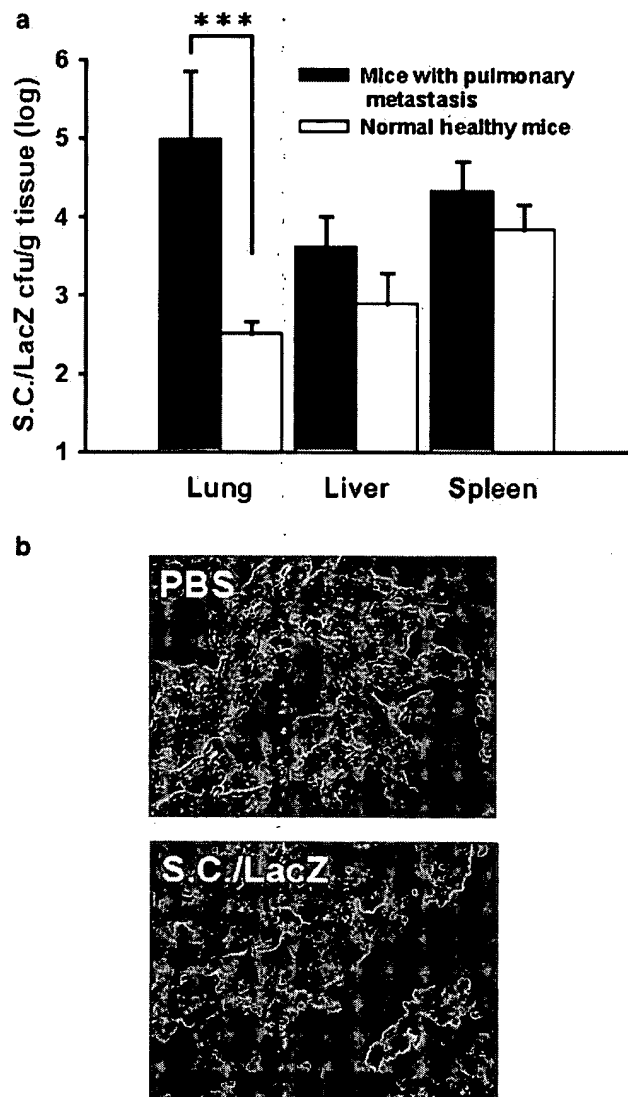


Figure 5 Accumulation of *S. choleraesuis* and β -gal expression in the lungs with melanoma metastatic nodules via *S. choleraesuis*-mediated LacZ gene transfer. C57BL/6 mice that had been injected with B16F10 cells (5×10^4) via the tail vein at day 0 were inoculated i.p. with S.C./LacZ (2×10^6 CFU) at day 15. A parallel experiment was performed using normal healthy mice inoculated with S.C./LacZ. (a) The amounts of S.C./LacZ (mean \pm SD, $n = 8$) accumulated in the lungs, livers, and spleens from metastatic melanoma-bearing mice and normal healthy mice were determined after 5 days. *** $P < .001$. (b) β -gal expression was detected in the lungs with metastatic nodules from tumor-bearing mice treated with S.C./LacZ, but not in those treated with PBS.

melanomas but also in metastatic pulmonary nodules after systemic administration, thus providing impetus to explore its use for inhibiting metastatic tumor growth.

Reduced metastatic nodules and prolonged survival in mice bearing experimental pulmonary metastatic melanoma by systemic delivery of S. choleraesuis carrying TSP-1 gene

Because inhibition of metastatic tumor growth is still a major challenge for melanoma treatment, we next

investigated whether S.C./TSP-1 inhibited established pulmonary tumor nodules. As we treated mice with the bacteria 15 days after establishment of pulmonary nodules and monitored tumor nodules 5 days later, at this stage black nodules of various sizes were disseminated and overlapping, making the quantification of tumor nodules problematic. To facilitate quantification of the metastatic tumor burden in the lungs, pulmonary metastases were induced by using B16F10-LacZ melanoma cells expressing β -gal. Mice were injected with B16F10-LacZ cells via the tail vein at day 0, treated i.p. with S.C./TSP-1, S.C./VO, or PBS at day 15, and killed at day 20. A majority of lungs from mice treated with S.C./VO or PBS possessed numerous confluent pulmonary nodules, whereas lungs from mice treated with S.C./TSP-1 exhibited smaller and fewer tumor nodules. To further quantify tumor burden, wet lung weights and β -gal activities were measured. Figure 6a shows that the wet lung weights from mice treated with S.C./TSP-1 were decreased by more than 50% compared with those treated with S.C./VO ($P = .0063$) or PBS ($P = .0095$). When β -gal gene expression in the lungs was quantified, a similar pattern was observed. More than 47% reduction in β -gal expression was found in the lungs from S.C./TSP-1-treated mice compared with those from S.C./VO-treated ($P = .0006$) or PBS-treated ($P = .00008$) mice (Fig 6b). S.C./TSP-1 treatment also prolonged the survival of mice with pulmonary metastases as compared with S.C./VO-treated ($P = .0157$) or PBS-treated ($P = .0070$) counterparts (Fig 6c). No significant differences were found in the lung weight, β -gal gene expression, and survival between S.C./VO-treated and PBS-treated groups (Figs 6a–c). Collectively, these results indicate that intraperitoneal delivery of S.C./TSP-1 decreased tumor burden in the lungs and prolonged survival in mice bearing pulmonary metastatic melanoma.

Discussion

In the work described here, we show that *S. choleraesuis* is capable of targeting and multiplying in primary and metastatic melanomas via systemic administration. *S. choleraesuis* preferentially targets tumors for growth, with numbers in tumors far exceeding those in the liver, which is the normal site of *Salmonella* replication in nontumor-bearing mice. Moreover, tumor-specific transgene expression can be achieved via *S. choleraesuis*-mediated gene transfer. TSP-1 expression in the tumors, which leads to decreased intratumoral microvessel density, may contribute, in part, to the antitumor effect of *S. choleraesuis* carrying TSP-1 gene on melanoma. The propensity of *S. choleraesuis* to target melanoma cells, either primary tumors or metastatic nodules, may also contribute to inhibiting melanoma growth and metastasis, as well as prolonging the survival of melanoma-bearing mice. Recently, we have also shown that *S. choleraesuis* carrying endostatin gene inhibited tumor growth in murine models of melanoma, bladder cancer, and hepatoma.¹⁸ Therefore,

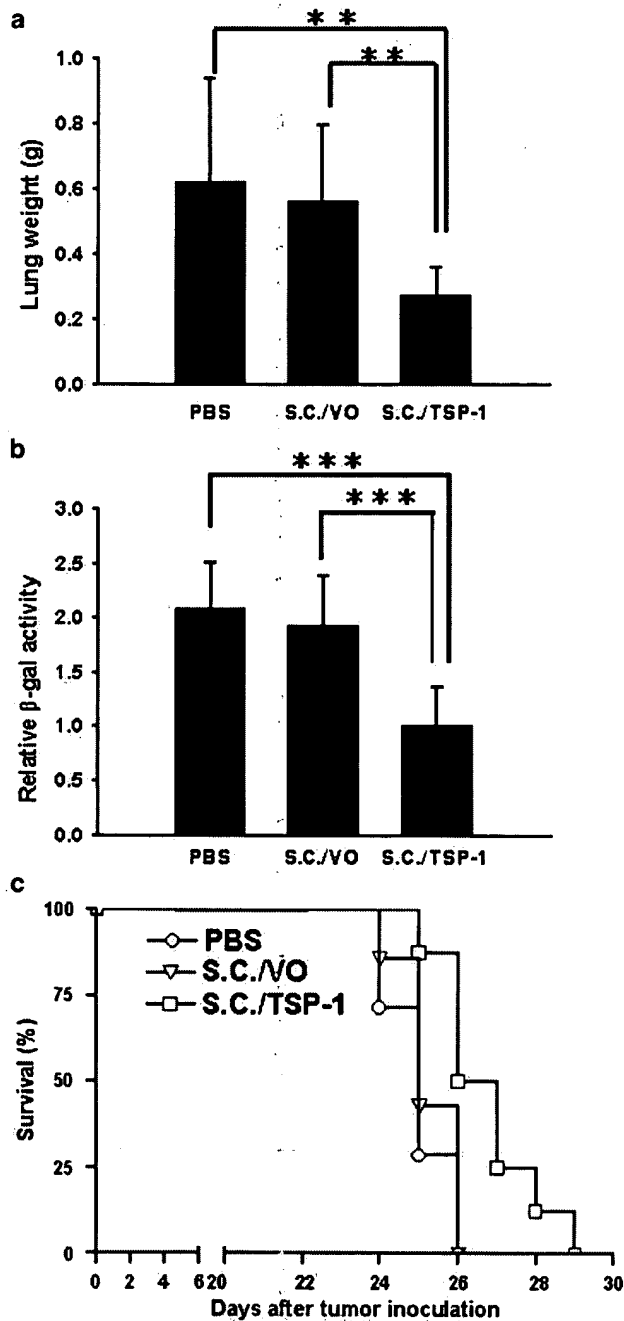


Figure 6 Antitumor effects of *S. choleraesuis* carrying TSP-1 gene on mice bearing pulmonary metastatic melanoma. Groups of 8 C57BL/6 mice that had been injected with B16F10-LacZ cells (5×10^4) via the tail vein at day 0 were treated i.p. with 2×10^6 CFU of S.C./TSP-1 or S.C./VO, or with PBS at day 15. (a) The wet lung weight and (b) β -gal activity of lungs from these mice were measured at day 20. Each value represents mean \pm SD ($n=8$). $**P<.01$; $***P<.001$. (c) Prolongation of survival in mice bearing pulmonary metastatic melanoma treated with *S. choleraesuis* carrying TSP-1 gene compared with those treated with S.C./VO or PBS. Groups of 7–8 C57BL/6 mice that had been injected with B16F10 cells (5×10^4) via the tail vein at day 0 were treated i.p. with 2×10^6 CFU of S.C./TSP-1 or S.C./VO, or with PBS at day 15. The survival time of the mice was recorded. Kaplan–Meier survival curves were shown ($P<.05$ for S.C./TSP-1 versus S.C./VO and $P<.01$ for S.C./TSP-1 versus PBS).

combining our previous data with those found here, we suggest that *S. choleraesuis* carrying TSP-1 gene or other antiangiogenic genes, such as endostatin gene, may be further explored as an anticancer agent for primary and metastatic melanomas, as well as other solid tumors.

Salmonella has been exploited to transfer eukaryotic expression plasmids to mammalian cells *in vitro* and *in vivo*.²¹ However, bacteria at high multiplicity of infection (MOI) may be toxic to mammalian cells.^{22,23} In the present study, because A549 cells were more resistant to *S. choleraesuis*-induced cytotoxicity than B16F10 cells, and thereby less prone to detachment from culture plates after bacterial infection, we used them to demonstrate *S. choleraesuis*-mediated gene transfer *in vitro*. After an 8-hour incubation with *S. choleraesuis* at the initial inoculum level of approximately 10 MOIs, most, if not all, of the A549 cells remained intact. The cells were then carefully washed and refilled with gentamicin-containing fresh culture medium in order to kill any residual extracellular bacteria. Expression of TSP-1 by S.C./TSP-1-infected cells was observed 48 hours later. We also demonstrate that the 48-hour conditioned medium collected from the infected cells inhibited the proliferation of HMEC-1 endothelial cells, suggesting that TSP-1 expressed by S.C./TSP-1 infected cells was biologically active. Nevertheless, the conditioned medium from A549 cells infected with *S. choleraesuis* carrying the empty vector also slightly inhibited the proliferation of HMEC-1 cells as compared with that from the control cells. Lipopolysaccharide (LPS), which resides in the outer membrane of Gram-negative bacteria, has been shown to induce apoptosis in endothelial cells.²⁴ Therefore, the *Salmonella* components, such as LPS, or other unidentified factor(s) produced from *Salmonella*-infected A549 cells and secreted into the culture medium may also inhibit, albeit to a much lesser extent than TSP-1, the proliferation of endothelial cells or exert cytotoxic effect on endothelial cells.

In this study, we demonstrate that a single intraperitoneal administration of attenuated *S. choleraesuis* carrying TSP-1 gene into melanoma-bearing mice inhibited the growth of subcutaneous melanoma and experimental lung metastasis by more than 40% compared with injection of *S. choleraesuis* carrying the empty vector. Furthermore, tumor inhibition was associated with approximately 50% reduction in intratumoral microvessel numbers. However, complete tumor regression was not observed in the treated mice, and they eventually died despite significant improvement of survival. The lack of complete tumor regression in S.C./TSP-1-treated mice may have been attributable, in part, to the rapidly progressive nature of B16F10 melanoma. Different tumors may respond differently to the same dose of angiogenic inhibitors.^{25,26} Notably, more-slowly growing tumors are more effectively suppressed by the same dose of endostatin than fast-growing tumors.²⁷ To this end, Bergers et al²⁸ showed that various angiogenic inhibitors, such as endostatin and angiostatin, have distinct efficacy profiles, which depend on the stage of tumor development and probably the kinetics of cell growth. On the other

hand, in the present study multiple injections of the bacteria may be necessary to increase and prolong TSP-1 production, and hence to increase antitumor activity. Alternatively, combination with other therapeutic strategies, such as chemotherapy and radiotherapy, may be further explored.

Induction of angiogenesis is a critical point in the development of melanoma. Transition from the radial to vertical growth phase, which is considered to be the critical switch in melanoma progression, depends on the formation of new capillary.^{29,30} In addition, the density of microvessels in primary melanomas gradually increases along with the simultaneous presence of local and distant metastases, indicating that angiogenesis is also crucial in the process of melanoma metastasis.¹³ Although the regulators of angiogenesis biologically relevant for melanoma remain unclear, several hypoxia-inducible angiogenic factors, such as basic fibroblast growth factor, vascular endothelial growth factor, interleukin-8, and angiogenin, show enhanced expression in melanoma metastases *in vivo* and in highly metastatic cell lines.^{12,14,31,32} Therefore, antiangiogenic strategy targeting tumor vasculature may hold promise for the treatment of primary and metastatic melanomas. Clinical trials of antiangiogenic therapy for patients with advanced malignant melanoma are currently under investigation.¹⁴ As malignant melanoma cells secrete a number of different proangiogenic factors, a combination of different antiangiogenic factors or combination of antiangiogenic therapy with other therapeutic strategies may be needed to enhance therapeutic efficacy against melanoma.

Bacteria have been investigated as gene delivery vectors over many years.^{1,3} They have several desirable attributes that make them potentially suitable as gene delivery vectors. Furthermore, they can be motile and grow in hypoxic areas of tumors. Although replication-selective oncolytic viruses represent a promising cancer treatment platform, intratumoral spread appears to be a substantial hurdle for viral agents. In this regard, live bacteria as antitumor agents may hold great promise. As *Salmonellae* survive and replicate in both oxygenated and hypoxic conditions, they would be expected to colonize small metastatic lesions as well as larger tumors. In this study, we demonstrate that *S. choleraesuis* not only accumulated in subcutaneous melanomas but also in metastatic pulmonary nodules after systemic administration, resulting in decreasing more than 47% tumor burden in the lungs and prolonging survival in mice bearing experimental lung metastatic melanoma. With regard to growth characteristics of bacteria used as anticancer agents, *Salmonellae* have advantages over obligate anaerobes. Obligate anaerobic bacteria may only target large, well-established tumors, but not small metastatic tumors that lack apparent hypoxic regions. In fact, metastatic cancer is the major cause of death in most cancers. In many patients, microscopic or clinically evident metastasis has already occurred by the time the primary tumor is diagnosed. As a result, complete treatment of widely spread metastases in distant organs by surgery, radiation,

or chemotherapy is nearly impossible. Effective chemotherapeutic treatment, for example, is hindered by the fact that metastatic tumors are generally less sensitive to chemotherapy when compared with their corresponding primary tumors. To this end, our results show that *S. choleraesuis* could colonize and transfer therapeutic genes not only to primary tumors, but also to small metastatic tumors, resulting in inhibiting tumor growth and prolonging survival in melanoma-bearing mice.

Live attenuated *S. choleraesuis* triggers innate and adoptive immune responses in the host. The persistence of high levels of *Salmonella* in tumors may induce inflammatory responses, which may lead to the recruitment of immune cells, such as macrophages, neutrophils, and lymphocytes to the tumor site. Moreover, LPS, which has been shown to induce apoptosis in endothelial cells, may contribute, in part, to the antiangiogenic and antitumor activities of S.C./TSP-1.²⁴ Another point of interest is that TSP-1 production via *S. choleraesuis*-mediated gene transfer may considerably enhance bacterial accumulation in tumors. Presumably, vascular collapse may further reduce the oxygen tension to induce tumor cell apoptosis, as well as enhance *S. choleraesuis* growth and increase immune cell infiltration in the tumor site. Indeed, it has been demonstrated that vascular collapsing agents increase the germination of bacterial spores in tumors.³³ Dolastatin, a vascular collapsing agent, has been shown to enhance the ability of *Clostridium novyi* spores to lyse tumors.⁶

Several activities of TSP-1 may contribute to its antitumor effect. These include the activities to inhibit angiogenesis,^{16,34,35} activate transforming growth factor- β (TGF- β),^{15,36} and regulate extracellular proteases.³⁷⁻³⁹ Previous reports are consistent with the observation that overexpression of TSP-1 in tumor cells decreases the capillary density in tumors. Furthermore, B16F10 experimental tumors grown in TSP-1-deficient mice display increased capillary density.⁴⁰ Miao et al¹⁵ have shown that the ability of TSP-1 to inhibit B16F10 tumor growth appears to be attributed, in part, to the activation of TGF- β . TGF- β induces apoptosis of several tumor cell lines.^{15,41} Local injection of TGF- β around experimental A549 human lung carcinomas inhibits tumor growth in athymic mice.⁴² Furthermore, TSP-1 regulates enzyme activity of metalloproteinase (MMP)-2 and MMP-9 by inhibiting conversion of the MMP zymogen to the activated form.³⁷ Regulations of MMP activity by TSP-1 probably contribute to the antiangiogenic activity of TSP-1. Our results obtained here are consistent with previous reports showing the antitumor activity of TSP-1 against primary and metastatic tumors.

In conclusion, we have demonstrated that tumor-targeted TSP-1 gene delivery can be achieved by systemic administration of attenuated *S. choleraesuis* carrying a eukaryotic expression vector encoding murine TSP-1, resulting in inhibiting tumor growth and enhancing survival in established murine melanoma models, including primary and metastatic tumors. By taking advantages of the tumor-targeted and oncolytic effects of *Salmonella* and the antiangiogenic activity of TSP-1, *S. choleraesuis*

carrying TSP-1 gene appears to hold promise for the treatment of melanoma or other solid tumors.

Acknowledgments

This work was supported by Grants (NSC 91-3112-B-006-013 and NSC 92-3112-B-006-007) from the National Science Council, Taiwan.

References

- Pawelek JM, Low KB, Bermudes D. Tumor-targeted *Salmonella* as a novel anticancer vector. *Cancer Res.* 1997;57:4537–4544.
- Sznol M, Lin SL, Bermudes D, et al. Use of preferentially replicating bacteria for the treatment of cancer. *J Clin Invest.* 2000;105:1027–1030.
- Pawelek JM, Low KB, Bermudes D. Bacteria as tumour-targeting vectors. *Lancet Oncol.* 2003;4:548–556.
- Lemmon MJ, van Zijl P, Fox ME, et al. Anaerobic bacteria as a gene delivery system that is controlled by the tumor microenvironment. *Gene Therapy.* 1997;4:791–796.
- Theys J, Landuyt W, Nuyts S, et al. Specific targeting of cytosine deaminase to solid tumors by engineered *Clostridium acetobutylicum*. *Cancer Gene Ther.* 2001;8:294–297.
- Dang LH, Bettegowda C, Huso DL, et al. Combination bacteriolytic therapy for the treatment of experimental tumors. *Proc Natl Acad Sci USA.* 2001;98:15155–15160.
- Yazawa K, Fujimori M, Amano J, et al. *Bifidobacterium longum* as a delivery system for cancer gene therapy: selective localization and growth in hypoxic tumors. *Cancer Gene Ther.* 2000;7:269–274.
- Li X, Fu GF, Fan YR, et al. *Bifidobacterium adolescentis* as a delivery system of endostatin for cancer gene therapy: selective inhibitor of angiogenesis and hypoxic tumor growth. *Cancer Gene Ther.* 2003;10:105–111.
- Low KB, Ittensohn M, Le T, et al. Lipid A mutant *Salmonella* with suppressed virulence and TNF- α induction retain tumor-targeting *in vivo*. *Nat Biotechnol.* 1999;17:37–41.
- King I, Bermudes D, Lin S, et al. Tumor-targeted *Salmonella* expressing cytosine deaminase as an anticancer agent. *Hum Gene Ther.* 2002;13:1225–1233.
- Nuyts S, Van Mellaert L, Theys J, et al. Radio-responsive-*recA* promoter significantly increases TNF- α production in recombinant clostridia after 2 Gy irradiation. *Gene Therapy.* 2001;8:1197–1201.
- Hartmann A, Kunz M, Kostlin S, et al. Hypoxia-induced up-regulation of angiogenin in human malignant melanoma. *Cancer Res.* 1999;59:1578–1583.
- Neitzel LT, Neitzel CD, Magee KL, Malafa MP. Angiogenesis correlates with metastasis in melanoma. *Ann Surg Oncol.* 1999;6:70–74.
- Streit M, Detmar M. Angiogenesis, lymphangiogenesis, and melanoma metastasis. *Oncogene.* 2003;22:3172–3179.
- Miao WM, Seng WL, Duquette M, Lawler P, Laus C, Lawler J. Thrombospondin-1 type 1 repeat recombinant proteins inhibit tumor growth through transforming growth factor- β -dependent and -independent mechanisms. *Cancer Res.* 2001;61:7830–7839.
- Volpert OV, Lawler J, Bouck NP. A human fibrosarcoma inhibits systemic angiogenesis and the growth of experimental metastases via thrombospondin-1. *Proc Natl Acad Sci USA.* 1998;95:6343–6348.
- Shiau AL, Chen YL, Liao CY, Huang YS, Wu CL. Prothymosin α enhances protective immune responses induced by oral DNA vaccination against pseudorabies delivered by *Salmonella choleraesuis*. *Vaccine.* 2001;19:3947–3956.
- Lee CH, Wu CL, Shiau AL. Endostatin gene therapy delivered by *Salmonella choleraesuis* in murine tumor models. *J Gene Med.* in press.
- Ades EW, Candal FJ, Swerlick RA, et al. HMEC-1: establishment of an immortalized human microvascular endothelial cell line. *J Invest Dermatol.* 1992;99:683–690.
- Weidner N, Semple JP, Welch WR, Folkman J. Tumor angiogenesis and metastasis—correlation in invasive breast carcinoma. *N Engl J Med.* 1991;324:1–8.
- Weiss S, Chakraborty T. Transfer of eukaryotic expression plasmids to mammalian host cells by bacterial carriers. *Curr Opin Biotechnol.* 2001;12:467–472.
- Critchley RJ, Jezzard S, Radford KJ, et al. Potential therapeutic applications of recombinant, invasive *E. coli*. *Gene Therapy.* 2004;11:1224–1233.
- Grillot-Courvalin C, Goussard S, Courvalin P. Wild-type intracellular bacteria deliver DNA into mammalian cells. *Cell Microbiol.* 2002;4:177–186.
- Bannerman DD, Tupper JC, Ricketts WA, Bennett CF, Winn RK, Harlan JM. A constitutive cytoprotective pathway protects endothelial cells from lipopolysaccharide-induced apoptosis. *J Biol Chem.* 2001;276:14924–14932.
- Dkhissi F, Lu H, Soria C, et al. Endostatin exhibits a direct antitumor effect in addition to its antiangiogenic activity in colon cancer cells. *Hum Gene Ther.* 2003;14:997–1008.
- Kisker O, Becker CM, Prox D, et al. Continuous administration of endostatin by intraperitoneally implanted osmotic pump improves the efficacy and potency of therapy in a mouse xenograft tumor model. *Cancer Res.* 2001;61:7669–7674.
- Beecken WD, Fernandez A, Joussen AM, et al. Effect of antiangiogenic therapy on slowly growing, poorly vascularized tumors in mice. *J Natl Cancer Inst.* 2001;93:382–387.
- Bergers G, Javaherian K, Lo KM, Folkman J, Hanahan D. Effects of angiogenesis inhibitors on multistage carcinogenesis in mice. *Science.* 1999;284:808–812.
- Herlyn M, Clark WH, Rodeck U, Mancianti ML, Jambrosic J, Koprowski H. Biology of tumor progression in human melanocytes. *Lab Invest.* 1987;56:461–474.
- Straume O, Salvesen HB, Akslen LA. Angiogenesis is prognostically important in vertical growth phase melanomas. *Int J Oncol.* 1999;15:595–599.
- Rodeck U, Becker D, Herlyn M. Basic fibroblast growth factor in human melanoma. *Cancer Cells.* 1991;3:308–311.
- Potgens AJ, Lubsen NH, van Altena MC, Schoenmakers JG, Ruiter DJ, de Waal RM. Vascular permeability factor expression influences tumor angiogenesis in human melanoma lines xenografted to nude mice. *Am J Pathol.* 1995;146:197–209.
- Theys J, Landuyt W, Nuyts S, et al. Improvement of *Clostridium* tumour targeting vectors evaluated in rat rhabdomyosarcomas. *FEMS Immunol Med Microbiol.* 2001;30:37–41.
- Bleuel K, Popp S, Fusenig NE, Stanbridge EJ, Boukamp P. Tumor suppression in human skin carcinoma cells by chromosome 15 transfer or thrombospondin-1 overexpression through halted tumor vascularization. *Proc Natl Acad Sci USA.* 1999;96:2065–2070.

35. Streit M, Velasco P, Brown LF, et al. Overexpression of thrombospondin-1 decreases angiogenesis and inhibits the growth of human cutaneous squamous cell carcinomas. *Am J Pathol.* 1999;155:441–452.
36. Lawler J. The functions of thrombospondin-1 and 2. *Curr Opin Cell Biol.* 2000;12:634–640.
37. Bein K, Simons M. Thrombospondin type 1 repeats interact with matrix metalloproteinase 2. Regulation of metalloproteinase activity. *J Biol Chem.* 2000;275:32167–32173.
38. Rodriguez-Manzaneque JC, Lane TF, Ortega MA, Hynes RO, Lawler J, Iruela-Arispe ML. Thrombospondin-1 suppresses spontaneous tumor growth and inhibits activation of matrix metalloproteinase-9 and mobilization of vascular endothelial growth factor. *Proc Natl Acad Sci USA.* 2001;98:12485–12490.
39. Taraboletti G, Morbidelli L, Donnini S, et al. The heparin binding 25 kDa fragment of thrombospondin-1 promotes angiogenesis and modulates gelatinase and TIMP-2 production in endothelial cells. *FASEB J.* 2000;14:1674–1676.
40. Lawler J, Miao WM, Duquette M, Bouck N, Bronson RT, Hynes RO. Thrombospondin-1 gene expression affects survival and tumor spectrum of p53-deficient mice. *Am J Pathol.* 2001;159:1949–1956.
41. Guo Y, Kyprianou N. Restoration of transforming growth factor- β signaling pathway in human prostate cancer cells suppresses tumorigenicity via induction of caspase-1-mediated apoptosis. *Cancer Res.* 1999;59:1366–1371.
42. Twardzik DR, Ranchalis JE, McPherson JM, et al. Inhibition and promotion of differentiated-like phenotype of a human lung carcinoma in athymic mice by natural and recombinant forms of transforming growth factor- β . *J Natl Cancer Inst.* 1989;81:1182–1185.

Panning Phage Antibody Libraries on Cells: Isolation of Human Fab Fragments against Ovarian Carcinoma Using Guided Selection¹

Mariangela Figini, Laura Obici,² Delia Mezzanzanica, Andrew Griffiths, Maria I. Colnaghi, Greg Winter, and Silvana Canevari³

Istituto Nazionale per lo Studio e la Cura dei Tumori, Divisione di Oncologia Sperimentale E, Via Venezian 1, 20133 Milan, Italy [M. F., L. O., D. M., M. I. C., S. C.], and Medical Research Council Laboratory of Molecular Biology and Medical Research Council Centre for Protein Engineering, Hills Road, Cambridge CB2 2QH, United Kingdom [A. G. G. W.]

ABSTRACT

The display of repertoires of human antibody (Ab) fragments on filamentous phages and selection by binding of the phage to antigen (Ag) have provided a ready means of deriving human Ab against purified Ag. However, it has been more difficult to obtain phage Ab against an individual Ag of a complex mixture, such as cell surface Ag. Using the technique of "guided selection," we generated human Ab against the high-affinity folate-binding protein (FBP), a cell surface Ag that is overexpressed in many human ovarian carcinomas. The guiding Ab template was provided by the light chain of mouse monoclonal Ab Mov19 ($K_{\text{on}} 10^8 \text{ M}^{-1}$) directed against FBP; this was paired with repertoires of human heavy chains displayed on phages, and the hybrid Ab fragments were selected by binding to an ovarian carcinoma cell line (OVCAR3). The selected human heavy chains were then paired with repertoires of human light chains. Further panning led to the isolation of a human Fab fragment, C4, with a binding affinity of $0.2 \times 10^8 \text{ M}^{-1}$. This was highly specific for FBP, as demonstrated by ELISA and flow cytometry data and by immunoprecipitation of the relevant molecule from the cell surface of ovarian carcinoma cells. Moreover, C4 targeted the same or a closely related epitope of the Ag, as did the template rodent monoclonal Ab Mov19. These results suggest the usefulness of guided selection as a simple means to deriving human Ab against cell surface Ag for which a rodent Ab is available.

INTRODUCTION

The development of monoclonal Abs⁴ against tumor-associated Ags has generated considerable interest in the potential use of these reagents for cancer detection and immunotherapy (1, 2). However, clinical assessment of monoclonal Abs has generally yielded disappointing results, largely because of invariable induction of a human anti-mouse immune response that enhances the clearance of the murine monoclonal Abs from the circulation and blocks their therapeutic effects (3). Murine monoclonal Abs are also relatively ineffective as cytotoxic agents and in their ability to recruit effector cells or molecules of the complement system. Thus, recent efforts have focused on the construction of human Ab with reduced immunogenicity and improved effector functions using genetic engineering techniques.

The use of very small Ag-binding fragments, such as Fab or scFv fragments, would also be expected to provide reagents with improved tumor penetration and better pharmacokinetic properties (4-6).

Phage display technology has been used to generate human Ab from immune and nonimmune sources. In this approach, diverse repertoires of Ab fragments derived from the rearranged V genes of lymphocytes of human donors (7) or by assembly of human V-gene segments *in vitro* (8, 9) are cloned for display of Ab fragments on the surface of filamentous bacteriophage by fusion to the minor phage coat protein (pIII) (10). Phage-bearing Abs with specific binding activities are then isolated by binding to immobilized Ag.

Phage selection is very effective with purified Ag but more difficult with complex mixtures of Ags, such as cell surface Ags, which differ widely in type and expression levels. Very few phage Abs have been derived by selection on cells, and to date only hematopoietic (11, 12) and melanoma cells have been used successfully. In the latter case, an immune Ab repertoire was used (13).

One of the more specific tumor markers previously identified in our laboratory (14) is the α isoform of the FBP, a 38- to 40-kDa glycosylphosphatidyl-inositol-anchored molecule (15-18) that binds folic acid with high affinity. Detailed immunohistochemical analysis and evaluation of mRNA expression indicated that FBP is expressed at very low levels on the cell surface of normal epithelial tissues at medium levels on kidney, lung, and breast and at high levels on placental tissues (14, 19-22); overexpression of FBP has also been detected on approximately 90% of ovarian carcinomas (14, 22) in association with progression of the disease (18). We generated two mouse monoclonal Abs, Mov18 and Mov19, directed to nonoverlapping epitopes of FBP (14). Based on the encouraging clinical results obtained with murine anti-FBP monoclonal Abs (23-25), we sought to generate human phage Ab against FBP using the strategy of "guided selection" (26, 27). This technique is based on chain shuffling originally used to increase the affinity of Ab (28). In guided selection, the light or heavy chain of a rodent Ab serves as a template for pairing of human heavy or light chains, respectively, displayed on filamentous phage. Here, we used the light chain of the murine monoclonal Ab Mov19 as a guiding template and an ovarian cell line overexpressing FBP for selection.

MATERIALS AND METHODS

Cell Lines and Abs. The following human tumor cell lines were used: ovarian carcinomas IGROV1 (29), a gift from Dr. J. Bénard (Institut Gustave Roussy, Villejuif, France); OVCAR3, SKOV3, and SW626, provided by the American Type Culture Collection (ATCC); OVCA432, kindly provided by Dr. R. Knapp (Dana Farber Institute, Boston, MA); mammary carcinomas T47D, MCF7, MDA MB 35, MDA MB 361, MDA MB 231, Hs578T, and SKBR3 (ATCC); lung carcinomas CALU3 (ATCC) and N592 (kindly provided by Dr. J. D. Minna; Naval Hospital, Bethesda, MD); epidermoid carcinoma A431 (ATCC); and melanoma Mewo (kindly provided by the late Dr. J. Fogh; Memorial Sloan-Kettering Cancer Center, New York, NY). The murine hybridoma Mov19 (14) was used for mRNA extraction.

Monoclonal Abs MOV18 (IgG1) and MOV19 (IgG_{2a}) directed to FBP (14, 30) and monoclonal Ab 9E10 (IgG1) directed to a *myc* sequence (31) were

Received 8/11/97; accepted 1/5/98.

The costs of publication of this article were defrayed in part by the payment of page charges. This article must therefore be hereby marked advertisement in accordance with 18 U.S.C. Section 1734 solely to indicate this fact.

¹ This work was supported by the Associazione Italiana per la Ricerca sul Cancro/Fondazione Italiana per la Ricerca sul Cancro. Progetto Finalizzato RC. PF Applicazioni Cliniche della Ricerca Oncologica-Consiglio Nazionale delle Ricerche, Italian Health Ministry finalized program, and Italy-United States program "Therapy of Tumors."

² Present address: Policlinico San Matteo Medicina Interna ed Oncologia Medica, 27100 Pavia, Italy.

³ To whom requests for reprints should be addressed, at Division of Experimental Oncology E, Istituto Nazionale Tumori, Via Venezian 1, 20133 Milan, Italy. Phone: (39-2) 239-0567; Fax: (39-2) 236-2692.

⁴ The abbreviations used are: Ab, antibody; Ag, antigen; scFv, single-chain Fv antibody fragment; FBP, folate-binding protein; RAPAS, recombinant phage antibody system; 2 \times TY, 16 g of bacto-Trypton, 10 g of bacto-yeast, and 5 g of NaCl; AMP, ampicillin; GLU, glucose; tu, transforming unit; TEI, tetracycline; MPBS, nonfat dry milk-PBS; HRP, horseradish peroxidase; MFI, mean fluorescence intensity; HPLC, high-performance liquid chromatography; FACS, fluorescence-activated cell-sorting; ECL, enhanced chemiluminescence; CDR, complementarity determinant region.

affinity purified from mouse ascites or hybridoma supernatants on protein A-Sepharose CL-4B (Pharmacia/Biotech). MOV19 and MOV18 Fab were prepared using the Immun-Pure Fab preparation kit (Pierce, Rockford, IL).

Cloning Monoclonal Ab MOV19 Gene. The V genes of mouse monoclonal Ab MOV19 were reverse transcribed, amplified, and assembled to encode scFv fragments using PCR essentially as described (32) but using the RAPAS kit (Pharmacia/Biotech) according to the manufacturer's instructions. The assembled scFv was cloned into the phagemid pHEN1 (10). Functional scFv was selected on a monolayer of OVCAR3 cells as described below (see "Selection of FBP-binding Clones"). FBP-binding clones were sequenced (see below). The light chain (Vk-Ck) of the same monoclonal Ab was also amplified from the mRNA of the hybridoma MOV19 using the primers MoCK-FORNot (5'-CCA GCA TTC TGC GGC CGC CTC ATT CCT GTT GAA GCT CTT GAC-3') and VKBACKSfi (5'-CAT GAC CAC GCG GCC CAG CCG GCC ATG GCC GAC ATT GAG CTC ACC CAG TCT CCA-3') and cloned into pUC19SNmyc (26), and the sequence was checked against that of the MOV19 scFv. This plasmid was termed pUCMOV19K.

Phage Libraries. Construction of repertoires of human κ light (Vk-Ck) and λ light (V λ -C λ) and heavy (VH-CH1) chains has been described (26). The heavy chain repertoire (VH-CH1) was cloned in the phage vector fdDOG for display on the surface of phage fused with pIII (fdDOG-VH-Cyl); light chain libraries were cloned in the phagemid vector pHEN1 (pHENClib) (26).

Preparation of Phage Displaying Hybrid Mouse-Human Fab Fragments. *Escherichia coli* TG1 (33) cells bearing the plasmid pUCMOV19K were grown at 37°C with shaking in 10 ml of 2 \times TY-AMP-GLU broth (100 μ g/ml AMP and 1% GLU) (34). At A_{600} of 0.5, the culture was infected with 10^{12} tu of fd phage from the human VH-CH1 library. After 30 min at 37°C, the culture was centrifuged (2500 \times g, 10 min), and bacterial cells were resuspended in 1 ml of 2 \times TY broth and plated on a 243 \times 243-mm dish (Nunc) containing 2 \times TYE-AMP-TET (100 μ g/ml AMP and 12.5 μ g/ml TET) (34). After 18 h of incubation at 30°C, plates were scraped into 5 ml of 2 \times TY; 30 μ l of the mixture was inoculated in flasks containing 500 ml of 2 \times TY-AMP-TET and incubated 16 h for at 30°C with shaking. Phages were precipitated with polyethylene glycol from the culture supernatant as described (7) and resuspended in 5 ml of PBS (yield, $\sim 10^{12}$ tu of phage/ml).

Selection of FBP-binding Clones. The selection was performed on a monolayer of OVCAR3 cells in 100-mm Petri dishes. OVCAR3 cells were incubated in 20 ml of 2% MPBS for 2 h at 37°C, MPBS was removed, and $\sim 10^{12}$ tu of phage library displaying hybrid Fab fragments in 10 ml of 2% MPBS were added. After 1 h of incubation at room temperature with shaking, culture dishes were washed five times with 10 ml of PBS and 0.1% Tween 20 and 10 times with 10 ml of PBS. For infection, 10 ml of log phase *E. coli* TG1-bearing plasmid pUCMOV19K were added directly to the plates and incubated for 30 min at 37°C without shaking. Bacterial cells were plated in 243 \times 243-mm dishes containing TYE-AMP-TET, and after overnight incubation at 30°C, colonies were scraped from the plates, and phages were prepared as above.

Cloning of the selected human heavy chain into pHEN1-VLib was done as described (26). Positive clones were detected by phage ELISA after four rounds of selection.

ELISA. OVCAR3 cells were seeded and grown as monolayers in 96-well microtiter plates. Cells were fixed with 0.1% glutaraldehyde and saturated for 2 h with 2% MPBS at 37°C. Individual phage clones displaying heavy and light chains were assayed for binding by phage ELISA performed essentially as described (32), except using HRP-conjugated anti-M13 Ab (Pharmacia/Biotech). Phages displaying human Fab fragments or murine scFv were produced by superinfection of a single clone with helper phage. Phages displaying the hybrid murine-human Fab fragment (murine Vk-Ck-human VH-CH1) were produced as described above. All phages were polyethylene glycol precipitated.

For ELISA competition, the selected human Fab C4 (final concentration, 5 μ g/ml) was mixed with serial dilutions of purified murine MOV19 Fab or MOV18 Fab in 100 μ l of 2% MPBS and incubated for 1 h at room temperature. C4 binding was detected by rabbit anti-human λ (DAKO) plus peroxidase-conjugated anti-rabbit Ab (Amersham).

Subcloning, Expression, and Purification. To facilitate purification, the selected human Fab genes were subcloned into the expression vector pUC119SfiI-NorHismyc (35), which results in the addition of a hexahistidine tag at the COOH-terminal end of the Fab gene.

Bacteria containing human Fab fragments in pUC119SfiI-NorHismyc were inoculated into 2 \times TY-AMP-GLU, and the soluble products were induced with 1 mM isopropyl β -D-thiogalactoside as described (36). After induction, the culture was incubated for 12 h at 30°C with shaking, and Fab fragments were harvested from the periplasm and purified by immobilized metal affinity chromatography essentially as described (37). Purity of protein preparations was assessed by SDS-PAGE (PHAST System, Pharmacia) and Coomassie Blue staining and by HPLC (Sephadex 75, Pharmacia).

FACS Analysis. Approximately 5×10^9 phage particles bearing Ab were added to about 3×10^5 human tumor cells in 100 μ l of PBS and 1% BSA, and the mixture was incubated for 1 h at room temperature. Phage binding was detected by a 1:5000 dilution of anti-M13 Ab (Pharmacia/Biotech) for 30 min on ice, followed by a 1:1000 dilution of FITC-conjugated anti-sheep Ab (Sigma Chemical Co.) for another 30 min.

For each sample, 5000 cells were analyzed with a FACScan (Becton Dickinson) using Lysys II software. FACS analysis of soluble human Fab fragments was performed as above but incubated with 10 μ g/ml mouse monoclonal Ab 9E10 followed by FITC-conjugated anti-mouse Ab (Sigma).

Cell Surface Biotinylation. Plasma membrane proteins were surface labeled with *N*-hydroxysuccinimide-biotin ester using the ECL-protein biotinylation module, essentially as described by the manufacturer (Amersham, Little Chalfont, UK). After labeling, the biotinylation buffer was discarded, and cells were washed twice with ice-cold PBS and treated with lysis buffer (Tris-HCl, pH 7.4, 0.15 M NaCl, 5 mM EDTA, 1 mM phenylmethylsulfonyl fluoride, and 0.24 units/ml aprotinin) containing 1% octyl- β -glucoside (Boehringer Mannheim, Mannheim, Germany) for 1 h at 0°C. Detergent lysates were clarified by centrifugation (15,000 \times g, 15 min at 4°C). Protein concentration was determined by bicinchoninic acid protein assay (Pierce).

Immunoprecipitation and Western Blot. Immunoprecipitation was done using Mov19 immobilized on CNBr-activated Sepharose as described (14) and human C4 bound to Ni-NTA resin (Qiagen). Blots were saturated with Blotto (5% MPBS) containing 0.2% Tween 20, incubated with HRP-streptavidin, and developed for ECL assay (Amersham). Biotinylated protein molecular size markers for ECL (14.3–97.4 kDa) were from Amersham.

Radiolabeling and Affinity Measurement. Human selected Fab and murine MOV19 Fab were labeled with 125 I (Amersham) by lactoperoxidase-catalyzed iodination (38) to a mean specific activity of 6.9 and 3.6 mCi/mg, respectively. The K_{aff} was determined by Scatchard analysis of the binding data (39). OVCAR3 cells (3×10^4 /well in 50 μ l of RPMI 1640 plus 1% FCS) were incubated for 3 h on ice with serial dilutions of 125 I-labeled Ab. After three washes with cold buffer (PBS plus 0.03% w/v, BSA), cell-bound radioactivity was measured directly in a gamma counter. Background was determined in the presence of 100-fold excess of cold Fab.

DNA Sequencing. Nucleotide sequences of selected V regions were determined by the dideoxy chain termination method (40) using a Sequenase kit (United States Biochemical Corp.). Murine Ab V regions were sequenced with the sequencing primers for the RAPAS kit (S1, S3, S4, and S6; Pharmacia). For the human clones, V regions were sequenced with HUCHSEQ (5'-TAG TCC TTG ACC AGG CAG-3') for the VH and HULABDASEQ (5'-GTG TGG CCT TGT TGG CTT G-3') and HUKAPPASEQ (5'-CAC AAC AGA GGC AGT TCC-3') for the VL. Sequences were analyzed using MacVector 4.1.4 (IBI Kodak, New Haven, CT), and human VH genes were compared with a database of human germ line genes (41). V λ genes were compared with a directory of germ line V λ , as compiled by Williams and Winter (42).

Histochemistry. Five-micrometer cryostat sections were prepared and stained using a standard peroxidase method (43). Human Fab was tagged with anti-myc monoclonal Ab 9E10 followed by peroxidase-conjugated anti-mouse Ab, whereas murine MOV19 was tagged directly with peroxidase-conjugated anti-mouse Ab.

RESULTS

Cloning of Murine V Genes. The light chain of mouse monoclonal Ab Mov19 served as the "template." Both heavy and light chain V-genes of Mov19 were initially cloned for display as scFv in a filamentous phage vector and shown to bind to OVCAR3 target cells bearing the FBP. Table 1 lists the sequences of the polypeptide chains of each domain.

Table 1 Deduced protein sequences of murine and human V gene Ab recognizing FDP

Light chain	FR1	CDR1	FR2	CDR2	FR3	CDR3	FR4
MOV19 VK	DIETQSPASLAVSLQRAITSC	KASQSVSFAGTSLMIH	WYHQKPGQPKLLIY	RASNLEA	GVPTFSGSGSKTDFTLNIRHPVEEADAATYYC	QQSREYPTV	FGGGTKLEIK
Human VLC4	QSALTQSPASVSGSPGQSTITSC	TGTSSDVGSYNLVS	WYQHPGKAPKLMY	EGSKRPS	GVSNRFSGSKSGNAASLTISGLQAEDEADYYC	QSYDSSLSVY	FGGGTKLTVLG
GLDPL10	QSALTQSPASVSGSPGQSTITSC	TGTSSDVGSYNLVS	WYQHPGKAPKLMY	EGSKRPS	GVSNRFSGSKSGNTASLTISGLQAEDEADYYC	CSYAGSSTF	
GLDPL6	QSVVTPSPSVSGAPGQRTVITSC	TGSSNIGAGYDVH	WYQQLPCTAPKLLIY	GNSNRPS	GVPDFRSGSKSGASASLTISGLQAEDEADYYC	QSYDSSLSG	
Human VLD1	QSALTQSPASVSGSPGQSTITSC	TGTINDVGGYRFVS	WYQRRPGKAPKLIJ	DYIRRPS	GVPDFRSGSKSDNTAYLTISGLQAEDEADYYC	SSYTSSTLYV	FGTGTKVTVLG
GLDPL12	QSALTQSPASVSGSPGQSTITSC	TGTSSDVGGYNYVS	WYQHPGKAPKLMY	DYSKRPS	GVPDFRSGSKSGNTASLTISGLQAEDEADYYC	CSYAGSSTF	
Heavy chain	FR1	CDR1	FR2	CDR2	FR3	CDR3	FR4
MOV19 VH	QVQLQSGAEIVKPGASVKISCKASGYSTGYFMN	QVQLQSGAEIVKPGASVKISCKASGYSTGYFMN	WYQSHGKSLWIG	RHIPPYDGTFTYNNQFKD	KATLTVDKSSNTAHMELLSLTSEDAFAVYYCTR	YDGSRAMDY	WGQGTITVTV
Human VH8B	QVQLVESGGGLVQPGKSLRLSCTTSSTGFTG DYAMN	WARQAPGKGLWVS	SISSSSYIYVADSVKG	REFISRDNAKNSLYLQMNLSRAEDTAVYYCAR	ERYDFWSGMNDV	WGKGTITVTVSSA	
GLDP77	EVQLVESGGGLVQPGKSLRLSCTTSSTGFTG DYAMN	WYRQAPGKGLWVS	SISSSSYIYVADSVKG	REFISRDNAKNSLYLQMNLSRAEDTAVYYCAR			
GLDP31	EVQLVESGGGLVQPGKSLRLSCTTSSTGFTG DYAMN	WYRQAPGKGLWVS	SISSSSYIYVADSVKG	REFISRDNAKNSLYLQMNLSRAEDTAVYYCAR			

The nucleotide sequences of the V genes above have been assigned the following EMBL database accession numbers: MOV19 VL, X999994; VLC4, X999990; VLD1, X999991; MOV19 VH, X999993; and VH8B, X99992. FR, framework region; CDR, complementarity determinant region; GI, germ line.

Table 2 V-gene family and predicted CDR loop structure

Canonical structures were determined as described by Chothia *et al.* (45, 50, 51). References for all human germ line genes are from Tomlinson (41). CDR, complementarity-determinant region; GI, germ line

Family	Canonical loop		V gene
	CDR1	CDR2	
Light chain			
MOV19 VK	5	1	Mo VK3
Human VLC4	2	1	Hu V12
GI DPL10	2	1	Hu V12
GI DPL6	2	1	Hu V11
Human VLD1	2	1	Hu V12
GI DPL12	2	1	Hu V12
Heavy chain			
MOV19 VH	1	2	Mo VH2
Human VH 8B	1	3	Hu VH3
GI DP77	1	3	Hu VH3
GI DP31	1	3	Hu VH3

Selection of Human Heavy Chain. The light-chain V gene was recombined with the mouse Ck gene on a plasmid vector for secretion of the template light chain from the bacterial periplasm.

Bacteria containing the light chain were infected with fd phage encoding a repertoire (size, 10^7 clones) of human heavy chains (VH-CH1). Phages produced by these bacteria display hybrid Fab fragments (murine Vk-Ck-human VH-CH1); the heavy chains are fused at their COOH-termini to pIII, and their light chain partners associate spontaneously in the periplasmic space (10).

The hybrid murine-human Fab phage repertoire was selected by panning on a monolayer of OVCAR3 cells. Phages that bound to the cells were used to infect bacteria containing the light chain to produce phages bearing hybrid Fab fragments. This process was performed three times, with an enrichment in number colony of 4.7×10^4 – 2.4×10^6 from the first to the third round of panning. Individual clones from the third panning were grown in 96-well microtiter plates, and phages bearing the hybrid Fab fragments were screened for binding by ELISA to three different human ovarian carcinoma cell lines overexpressing FBP (OVCAR3, IGROV1, and SKOV3) and to two other tumor cell lines that do not overexpress FBP (Mewo and A431). Phages from 7 of 44 clones tested bound to each of the cell lines overexpressing FBP but not to the other two cell lines. All seven clones had the same human VH8B sequence (Table 1).

Selection of Human Light Chain. The VH-CH1 gene of the selected human heavy chain was inserted into the phagemid display vector pHEN1 containing repertoires of human κ and λ light chain genes (size, 10^5 clones for each chain). The resulting repertoire created (size, 10^6 clones) was rescued by infection with helper phage, and the phagemid particles were selected on OVCAR3 monolayers as above. The process was performed a total of four times with an enrichment of colony number from 3.27×10^6 in the first panning to 2.4×10^7 in the fourth panning. Phages from 20 of 80 of the phage clones tested by phage-ELISA bound specifically to the cell lines overexpressing FBP. Sequencing revealed two different λ light chains, human VLC4 (C4) and human VLD1 (D1) (Table 1).

V Gene Family and Predicted CDR Loop Structure. The human heavy chain sequence (human VH8B) appeared to derive from germ line segments DP31 and DP77, and the human C4 light chain sequence appeared to derive from germ line segments DPL10 and DPL6 (Table 1), presumably because of PCR crossover (44) in the construction of the V-gene library. The human D1 light chain sequence was derived from the DPL12 germ line only. The human light chains of C4 and D1 both derive from the human VL2 family, and the human heavy chain VH8B derives from the VH3 family (Table 2).

Comparison of the sequence of the murine Mov19 template and the related human Ab revealed little similarities; furthermore, there were

few similarities in loop structure. Ab loops can be classified into different lengths and structural classes or "canonical" loops (45). In the light chains, the CDR1 canonical loop of mouse Mov19 was 1 residue longer (Table 1) and had a different canonical fold (5 instead of 2) from that of the human light chains (Table 2). No differences in lengths or canonical loops (see Table 2) were observed for CDR2. The murine CDR3 was either 1 or 2 residues shorter than its human counterpart. In respect to the heavy chains, the CDR2 of Mov19 has a different canonical fold than the human heavy chain (2 instead of 3), and the murine CDR3 is 2 residues shorter than the human CDR3.

Binding Specificity of Human Fab Fragments. Phages displaying each of the two human Fab fragments, C4 and D1 (according to their light chains), the hybrid Fab fragment (with human heavy and mouse light chain), and the mouse MOV19 scFv fragment were analyzed by FACS on OVCAR3 cells to confirm their binding specificity for cells overexpressing FBP (Fig. 1). Phage expressing the human Ab fragments showed a pattern of reactivity superimposable on that of phage expressing the murine scFv of MOV19, with phage C4 reactivity slightly higher than that of phage D1 (MFI, 50 versus 35). MFI of hybrid phage was higher than either the human or murine phage value, consistent with previous observations during the selection of phage libraries against soluble Ags (26).

Soluble human Fab fragments were also expressed, harvested from

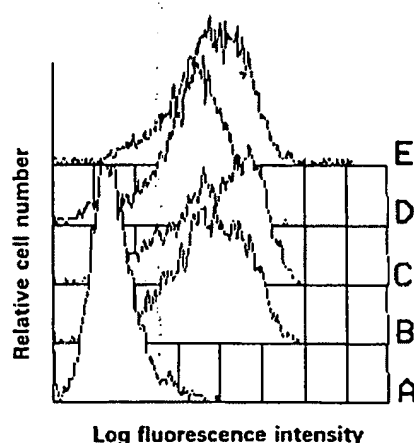


Fig. 1. FACS analysis of phage-binding activity on OVCAR3 cells. Cells were incubated for 1 h at room temperature with medium (A), murine scFv MOV19 (B), hybrid Fab (murine VK-CK-human VH-CH1; C), fully human Fab D1 (D), and fully human Fab C4 (E). Phage binding was detected by incubation with anti-M13 Ab followed by FITC-conjugated anti-sheep Ab.

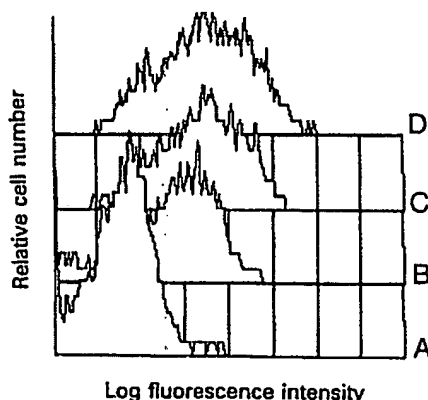


Fig. 2. Binding activity of bacterial periplasmic extracts on OVCAR3 cells. Cells were incubated for 1 h at room temperature with medium (A), soluble scFv MOV19 (B), soluble human Fab D1 (C), and soluble human Fab C4 (D). Binding of soluble fragments was detected with 9E10 monoclonal Ab followed by FITC-conjugated anti-mouse Ab.

the bacterial periplasm, and shown by FACS to bind specifically to OVCAR3 cells (Fig. 2). Clone C4 showed higher reactivity than D1, and C4 was selected for purification and specificity analysis on a wide panel of tumor cell lines. The C4 human fragment was purified as described in "Materials and Methods" with a yield of 2.5 mg/ml periplasm, and its purity was checked by HPLC and SDS-PAGE. The HPLC profile revealed a major peak with a retention time corresponding to a protein with an apparent molecular mass of 44,700 Da, similar to that of the murine Fab molecule (42,100 Da). A minor peak (~16% of the total) with an apparent molecular mass of 21,000 Da might represent the dissociated chains of the Fab. FACS analysis indicated identical binding specificity of C4 and MOV19, because only the cell lines recognized by MOV19 were also recognized by C4 (Table 3). The differences in MFI of the two Abs likely reflect the use of different detection reagents (see "Materials and Methods").

The fragment was also able to immunolocalize FBP in frozen sections of ovarian cancer surgical specimens by immunoperoxidase staining; specimens of other histotypes were negative for C4 reactivity (Fig. 3).

The molecular specificity of C4 was further analyzed on OVCAR3 cells in competition binding assay with mouse Fabs MOV19 and MOV18. Fab MOV19 efficiently competed with human C4 Fab, whereas Fab Mov18, even at the maximum concentration tested (100 μ g/ml) did not (Fig. 4). These results confirm that the Ab selection procedure targeted the same or a closely related epitope as the murine Ab used to guide the selection. However, the low concentration (IC_{50} , 0.25 μ g/ml) of murine Fab sufficient to compete with human Fab binding (5 μ g/ml) indicated a lower affinity of C4. Indeed, Scatchard analysis of the binding data for both the MOV19 Fab and human C4 Fab on OVCAR3 cells indicated a K_{aff} value for the human Fab ($0.2 \times 10^8 M^{-1}$) that was fivefold lower than for the murine Fab ($1 \times 10^8 M^{-1}$).

Immunoblot analysis of biotinylated FBP after immunoprecipitation with C4 revealed a single band at approximately 38,000 kDa migrating at the same position as the corresponding band immunoprecipitated with MOV19 (Fig. 5).

Table 3. Binding specificity of human C4 and murine MOV19 on different tumor cell lines^a

Cell type	MOV 19		C4	
	% positive ^b	MFI ^c	% positive	MFI
Ovarian carcinoma				
OVCAR3	90	263	70	290
IGROV1	87	135	74	131.4
OVCA432	88	105	85	91.3
SKOV3	14	7.5	6	27
SW626	7	38.9	16	38.5
Mammary carcinoma				
T47D	75	60	59	46
MCF7	- ^d	-	-	-
MDA-MB35	-	-	-	-
MDA-MB361	-	-	-	-
MDA-MB231	-	-	-	-
Hs578T	-	-	-	-
SKBR3	-	-	-	-
Lung carcinoma				
CALU3	-	-	-	-
N592	-	-	-	-
Epidermoid carcinoma				
A431	-	-	-	-
Melanoma				
MEWO	-	-	-	-

^a Evaluated by FACS analysis.

^b Percent positive cells was obtained after subtraction of negative control from Ab-treated cells.

^c Mean fluorescence intensity of positive cells.

^d - MFI <20 superimposable to negative controls.

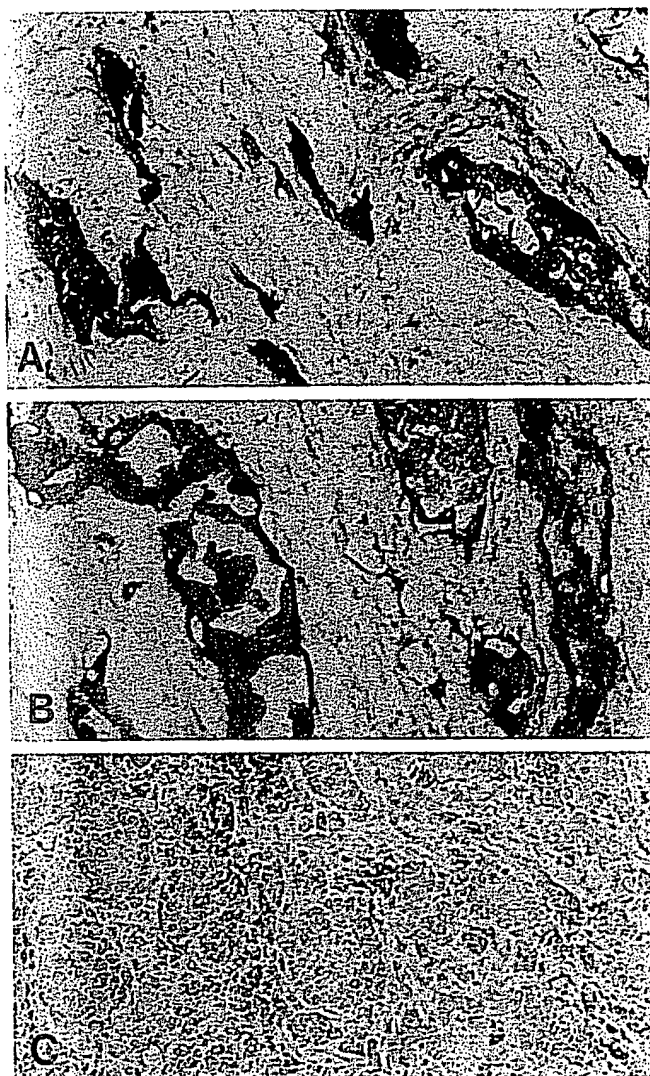


Fig 3. Immunohistochemical evaluation of the binding of human C4 Fab (A) and murine MOV19 (B) on cryostat sections from an FBP-positive ovarian carcinoma. All sections were counterstained with hematoxylin. C, negative staining of C4 on an FBP-negative breast carcinoma.

DISCUSSION

In the present study, we used the technique of guided selection to obtain a human Ab directed against a specific epitope of a tumor-associated Ag (FBP) that is overexpressed on ovarian carcinoma cells. This approach has the advantage that it obviates the need for purification of the cell surface Ag (such as the tumor marker or CD Ag on human lymphocytes) provided that a rodent monoclonal Ab is available.

The selected Ab fragment was highly specific for FBP, as demonstrated by ELISA and FACS binding data and by immunoprecipitation of FBP from the cell surface of ovarian carcinoma cells. The Ab was highly specific to FBP and targeted to the same epitope of the Ag as the template rodent Ab (MOV19).

The binding affinity of the human Fab fragment ($2 \times 10^7 \text{ M}^{-1}$) was approximately fivefold weaker than that of the murine Mov19. However, the observed affinity is adequate for *in vitro* studies and should be adequate for *in vivo* applications such as i.p. injection for metastatic localization of ovarian carcinoma (24). Moreover, it should be possible to improve the affinity by mutagenesis *in vitro* (46) or in bacterial mutator strains (47). Because of their small size, these Fab fragments are expected to have improved pharmacokinetic properties

in terms of biodistribution, penetrance of solid tissues, and clearance from the circulation, thus reducing accumulation in normal organs and enhancing target localization (48, 49).

The principle of guided selection, which involves the use of a (mouse) template chain to help fashion the Ag-binding site of a (human) Ab in combination with a complementary (human) chain from a repertoire, might be expected to select human chains that are structurally similar to the corresponding mouse chain and able to make similar contacts to the Ag. Indeed, earlier work with an anti-hapten Ab of known crystallographic structure showed that several of the critical Ag-binding contacts were retained (26). However, we found no clear structural similarities between the original mouse Ab and the selected Ag binding sites. The lack of structural similarities may reflect, in part, the lack of precise homologues in the human repertoire, as noted already (26).

Comparison with the human germ line sequences indicated that our selected anti-FBP Ab contained some mutations in framework regions and that both human C4 light and VH8B heavy chains appeared to derive from a combinations of two different germ line sequences. This presumably occurs by "PCR crossover" between two different germ line sequences during the assembling of the V gene library. Because crossover events are likely to constitute only a minor fraction of the V-gene library, this suggests that the extra combinatorial diversity of the sequences in the hypervariable loops is essential in this case and may also be important in other case of guided selection.

Our data indicate that completely human Ab can be obtained against a tumor target of interest for which clinical studies with murine monoclonal Ab have given promising results (23–25). Because C4 Ab is entirely of human origin, it is expected to be much less

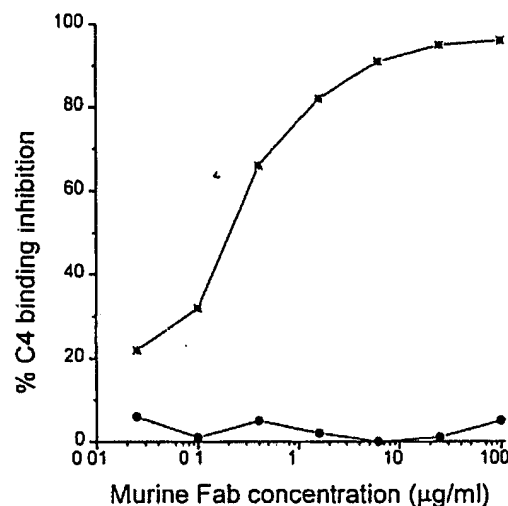


Fig 4. Inhibition of human Fab C4 binding on OVCAR3 cells. Cells were incubated for 1 h at room temperature with Fab C4 mixed with titrated doses of murine MOV19 (•) and MOV18 (●). Fab C4 binding was detected by ELISA using rabbit anti-human λ plus HRP-conjugated anti-rabbit Ab.

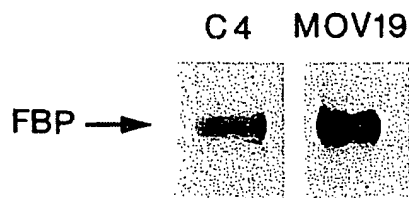


Fig 5. FBP precipitation by human C4 Fab (Lane 1) and MOV19 (Lane 2). Biotinylated cell surface proteins from IGROV1 ovarian carcinoma cells were immunoprecipitated by the relevant Ab, fractionated by 10% SDS-PAGE, Western blotted, and revealed by ECL.

immunogenic and therefore useful for sequential administration as a therapeutic reagent

ACKNOWLEDGMENTS

We are very grateful to Sylvie Ménard for helpful discussion. We also thank Renata Ferri and Elena Luisson for technical assistance, Laura Mameli and Daniela Labadini for manuscript preparation, and Mario Azzini for photographic reproduction

REFERENCES

- Maeda, M. and Firtel, R. A. Activation of the mitogen-activated protein kinase ERK2 by the chemottractant folic acid in dictyostelium *J Biol Chem.* 272: 23690-23695, 1997
- Reithmüller, G., Schneider-Gadick, E., and Johnson, J. P. Monoclonal antibodies in cancer therapy. *Curr Opin Immunol.* 5: 732-739, 1993
- Khazaeli, M. B., Conry, R. M., and LoBuglio, A. F. Human immune response to monoclonal antibodies. *J Immunother.* 15: 42-52, 1994
- De Kruijff, J., Van der Vuurst de Vries, L., Cilenti, L., Boel, E., Van Ewijk, W., and Logtenberg, T. New perspectives on recombinant human antibodies. *Immunol Today.* 17: 453-455, 1996
- Chester, K. A., and Hawkins, R. E. Clinical issues in antibody design. *Trends Biotechnol.* 13: 294-300, 1995
- Jain, R. K. Physiological barriers to delivery of monoclonal antibodies and other macromolecules in tumors. *Cancer Res.* 50 (Suppl 3): 814s-819s, 1990
- Marks, J. D., Hoogenboom, H. R., Bonnett, T. P., McCafferty, J., Griffiths, A. D., and Winter, G. By-passing immunization: human antibodies from V-gene libraries displayed on phage. *J Mol Biol.* 222: 581-597, 1991
- Hoogenboom, H. R., and Winter, G. Bypassing immunization: human antibodies from synthetic repertoires of germ line VH-gene segments rearranged *in vitro*. *J Mol Biol.* 227: 381-388, 1992
- Nissim, A., Hoogenboom, H. R., Tomlinson, I. M., Flynn, G., Midgley, C., Lane, D., and Winter, G. Antibody fragments from a "single pot" phage display library as immunochemical reagents. *EMBO J.* 13: 692-698, 1994
- Hoogenboom, H. R., Griffiths, A. D., Johnson, K. S., Chiswell, D. J., Hudson, P., and Winter, G. Multi-subunit proteins on the surface of filamentous phage: methodologies for displaying antibody (Fab) heavy and light chains. *Nucleic Acids Res.* 19: 4133-4137, 1991
- Marks, J. D., Ouwehand, W. H., Bye, J. M., Finnem, R., Gorick, B. D., Voak, D., Thorpe, S., Hughes-Jones, N. C., and Winter, G. Human antibody fragments specific for human blood group antigens from a phage display library. *BioTechnology.* 11: 1145-1149, 1993
- De Kruijff, J., Terstappen, L., Boel, E., and Logtenberg, T. Rapid selection of cell subpopulation-specific human monoclonal antibodies from a synthetic phage antibody library. *Proc Natl Acad Sci USA.* 92: 3938-3942, 1995
- Cai, X., and Garen, A. Anti-melanoma antibodies from melanoma patients immunized with genetically modified autologous tumor cells: selection of specific antibodies from single-chain Fv fusion phage libraries. *Proc Natl Acad Sci USA.* 92: 6537-6541, 1995
- Miotti, S., Canevari, S., Ménard, S., Mezzanzanica, D., Porro, G., Pupa, S. M., Regazzoni, M., Tagliabue, E., and Colnaghi, M. I. Characterization of human ovarian carcinoma-associated antigens defined by novel monoclonal antibodies with tumor-restricted specificity. *Int J Cancer.* 39: 297-303, 1987
- Luhers, C. A. A human membrane-associated folate binding protein is anchored by a glycosyl-phosphatidylinositol tail. *J Biol Chem.* 264: 21446-21449, 1989
- Lacey, S. W., Sanders, J. M., Rothberg, K. G., Anderson, R. G. W., and Kamen, B. A. Complementary DNA for the folate binding protein correctly predicts anchoring to the membrane by glycosyl-phosphatidylinositol. *J Clin Invest.* 84: 715-720, 1989
- Alberti, S., Miotti, S., Fornaro, M., Mantovani, L., Walter, S., Canevari, S., Ménard, S., and Colnaghi, M. I. The Ca-MOV18 molecule, a cell-surface marker of human ovarian carcinomas, is anchored to the cell membrane by phosphatidylinositol. *Biochem Biophys Res Commun.* 171: 1051-1055, 1990
- Toffoli, G., Cernigoi, C., Russo, A., Gallo, A., Bagnoli, M., and Boiocchi, M. Overexpression of folate binding protein in ovarian cancers. *Int J Cancer.* 74: 193-198, 1997
- Ross, J. F., Chaudhuri, P. K., and Ratnam, M. Differential regulation of folate receptor isoforms in normal and malignant tissues *in vivo* and in established cell lines: physiologic and clinical implications. *Cancer (Phila.)* 73: 2432-2443, 1994
- Veggian, R., Fasolato, S., Ménard, S., Minucci, D., Pizzetti, P., Regazzoni, M., Tagliabue, E., and Colnaghi, M. I. Immunohistochemical reactivity of a monoclonal antibody prepared against human ovarian carcinoma on normal and pathological female genital tissues. *Tumor.* 73: 510-513, 1989
- Boerman, O. C., Van Nierkerk, C. C., Makink, K., Hanselaar, T. G. J. M., Kenemans, P., and Poels, L. G. Comparative immunohistochemical study of four monoclonal antibodies directed against ovarian carcinoma-associated antigens. *Int J Gynecol Pathol.* 10: 15-25, 1991
- Mantovani, L. T., Miotti, S., Ménard, S., Canevari, S., Raspagliesi, F., Bottini, C., Bottero, F., and Colnaghi, M. I. Folate binding protein distribution in normal tissues and biological fluids from ovarian carcinoma patients as detected by the monoclonal antibodies MOV18 and MOV19. *Eur J Cancer.* 30A: 363-369, 1994
- Canevari, S., Stoter, G., Arienti, F., Bolis, G., Colnaghi, M. I., Di Re, E., Eggermont, A. M. M., Goey, S. H., Gratama, J. W., Lamers, C. H. J., Nooy, M. A., Parmiani, G., Raspagliesi, F., Ravagnani, F., Scarfone, G., Trimpos, J. B., Wamaar, S. O., and Bolhuis, R. L. H. Regression of advanced ovarian carcinoma by intraperitoneal treatment with autologous T-lymphocytes retargeted by a bispecific monoclonal antibody. *J Natl Cancer Inst.* 87: 1463-1469, 1995
- Crippa, F., Buraggi, G. L., Di Re, E., Gasparini, M., Seregni, E., Canevari, S., Gadin, M., Presi, M., Marini, A., and Seccamani, E. Radioimmunoscintigraphy of ovarian cancer with the MOV18 monoclonal antibody. *Eur J Cancer.* 27: 724-729, 1991
- Crippa, F., Bolis, G., Seregni, E., Gavoni, N., Bombardieri, E., Scarfone, G., Ferrari, C., and Buraggi, G. L. Single dose intraperitoneal radioimmunotherapy with the murine monoclonal antibody ¹³¹I-MOV18: clinical results in patients with minimal residual disease of ovarian cancer. *Eur J Cancer.* 31A: 686-690, 1995
- Figini, M., Marks, J. D., Winter, G., and Griffiths, A. D. *In vitro* assembly of repertoires of antibody chains on the surface of phage by renaturation. *J Mol Biol.* 239: 68-78, 1994
- Jespersen, L. S., Roberts, A., Mahler, S. M., Winter, G., and Hoogenboom, H. R. Guiding the selection of human antibodies from phage display repertoires to a single epitope of an antigen. *BioTechnology.* 12: 899-903, 1994
- Marks, J. D., Griffiths, A. D., Malmqvist, M., Clackson, T., Bye, J. M., and Winter, G. By-passing immunization: building high affinity human antibodies by chain shuffling. *BioTechnology.* 10: 779-783, 1992
- Bénard, J., De Silva, J., De Blois, M. C., Boyer, P., Duvilland, P., Chiric, E., and Riou, G. Characterization of a human ovarian adenocarcinoma line, IGROV1, in tissue culture and in nude mice. *Cancer Res.* 45: 4970-4979, 1985
- Coney, L. R., Tomassetti, A., Carayannopoulos, L., Frasca, V., Kamen, B. A., Colnaghi, M. I., and Zurawski, V. R. Cloning of a tumor-associated antigen: MOV18 and MOV19 antibodies recognize a folate-binding protein. *Cancer Res.* 51: 6125-6132, 1991
- Munro, S., and Pelham, H. R. B. An Hsp-like protein in the ER: identity with the 78kd glucose regulated protein and immunoglobulin heavy chain binding protein. *Cell.* 46: 291-300, 1986
- Clackson, T., Hoogenboom, H. R., Griffiths, A. D., and Winter, G. Making antibody fragments using phage display libraries. *Nature (Lond.)* 352: 624-628, 1991
- Gibson, T. J. Studies on the Epstein-Barr virus genome (Thesis). Cambridge UK: University of Cambridge, 1984
- Miller, J. H. Experiments in Molecular Genetics. Cold Spring Harbor, NY: Cold Springs Harbor Laboratory, 1972
- Griffiths, A. D., Williams, S. C., and Hartley, O. Isolation of high affinity human antibodies directly from large synthetic repertoires. *EMBO J.* 13: 3245-3260, 1994
- De Bellis, D., and Schwartz, I. Regulated expression of foreign genes fused to lac: control by glucose levels in growth medium. *Nucleic Acids Res.* 18: 1311, 1990
- Breitling, F., Dübel, S., Sechaus, T., Klewinghaus, I., and Little, M. A surface expression vector for antibody screening. *Gene (Amst.)* 104: 147-153, 1991
- Casali, P., Mezzanzanica, D., Valota, O., Adobati, E., Tomassetti, A., Colnaghi, M. I., and Canevari, S. Unidirectional potentiation of binding between two anti-FBP MAbs: evaluation of the involved mechanisms. *J Cell Biochem.* 58: 47-55, 1995
- Scatchard, G. The attractions of protein for small molecules and ions. *Ann NY Acad Sci.* 51: 660, 1949
- Sanger, F., Nicklen, S., and Coulson, A. R. DNA sequencing with chain-terminating inhibitors. *Proc Natl Acad Sci USA.* 74: 5463-5467, 1977
- Tomlinson, I. M. V. Base Sequence Directory. Cambridge, UK: Medical Research Council Centre for Protein Engineering
- Williams, S. C., and Winter, G. Cloning and sequencing of human immunoglobulin variable lambda gene segments. *Eur J Immunol.* 23: 1456-1461, 1993
- Mariani-Costantini, R., Colnaghi, M. I., Leoni, F., Ménard, S., Cerasoli, S., and Rilke, F. Immunohistochemical reactivities of a monoclonal antibody prepared against human breast carcinoma. *Virchows Arch. A Pathol Anat Hist.* 402: 389-404, 1984
- Griffiths, A. D., Malmqvist, M., Marks, J. D., Bye, J. M., Embleton, M. J., McCafferty, J., Baier, M., Holliger, K. P., Gorick, B. D., Hughes-Jones, N. C., Hoogenboom, H. R., and Winter, G. Human anti-self antibodies with high specificity from phage display libraries. *EMBO J.* 12: 725-734, 1993
- Chothia, C., and Lesk, A. M. Canonical structures for the hypervariable regions of immunoglobulins. *J Mol Biol.* 196: 901-917, 1987
- Hawkins, R. E., Russell, S. J., and Winter, G. Selection of phage antibodies by binding affinity: mimicking affinity maturation. *J Mol Biol.* 226: 889-896, 1992
- Low, N., Holliger, P., and Winter, G. Mimicking somatic hypermutation: affinity maturation of antibodies displayed on bacteriophage using a bacterial mutator strain. *J Mol Biol.* 260: 359-368, 1996
- Jain, R. K. Vascular and interstitial barriers to delivery of therapeutic agents in tumors. *Cancer Metastasis Rev.* 9: 253-266, 1990
- Milenic, D. E., Yokota, T., Filpula, D. R., Finkelman, M. A. J., Dodd, S. W., Wood, J. F., Whitlow, M., Snoy, P., and Schlom, J. Construction, binding properties, metabolism, and tumor targeting of a single-chain Fv derived from the pancreatic carcinoma monoclonal antibody CC49. *Cancer Res.* 51: 6363-6371, 1991
- Chothia, C., Lesk, A. M., Tramontano, A., Levitt, M., Smith-Gill, S. J., Air, G., Sheriff, S., Padlan, E. A., Davies, D., Tulip, W. R., Colman, P. M., Spinelli, S., Alzari, P. M., and Poljak, R. J. Conformations of immunoglobulin hypervariable regions. *Nature (Lond.)* 342: 877-883, 1989
- Chothia, C., Lesk, A. M., Gherardi, E., Tomlinson, I. M., Walter, G., Marks, J. D., Llewellyn, M. B., and Winter, G. Structural repertoire of the human VH segments. *J Mol Biol.* 227: 799-817, 1992

Gene transfer to mammalian cells using genetically targeted filamentous bacteriophage

DAVID LARocca,¹ PAUL D. KASSNER, ALISON WITTE, ROBERT CHARLES LADNER,*
GLENN F. PIERCE, AND ANDREW BAIRD

Selective Genetics Inc., San Diego, California 92121, USA; and *Dyax Corporation, Cambridge, Massachusetts 02115, USA

ABSTRACT We have genetically modified filamentous bacteriophage to deliver genes to mammalian cells. In previous studies we showed that noncovalently attached fibroblast growth factor (FGF2) can target bacteriophage to COS-1 cells, resulting in receptor-mediated transduction with a reporter gene. Thus, bacteriophage, which normally lack tropism for mammalian cells, can be adapted for mammalian cell gene transfer. To determine the potential of using phage-mediated gene transfer as a novel display phage screening strategy, we transfected COS-1 cells with phage that were engineered to display FGF2 on their surface coat as a fusion to the minor coat protein, pIII. Immunoblot and ELISA analysis confirmed the presence of FGF2 on the phage coat. Significant transduction was obtained in COS-1 cells with the targeted FGF2-phage compared with the nontargeted parent phage. Specificity was demonstrated by successful inhibition of transduction in the presence of excess free FGF2. Having demonstrated mammalian cell transduction by phage displaying a known gene targeting ligand, it is now feasible to apply phage-mediated transduction as a screen for discovering novel ligands.—Larocca, D., Kassner, P. D., Witte, A., Ladner, R. C., Pierce, G., Baird, A. Gene transfer to mammalian cells using genetically targeted filamentous bacteriophage. *FASEB J.* 13, 727–734 (1999)

Key Words: *phage display · transfection · receptor-mediated · ligand*

THE SELECTION OF affinity ligands from libraries of highly diverse peptides, cDNA encoded proteins, or antibodies displayed on the surface of phage has proved to be a successful strategy for ligand discovery because genes encoding binding peptides can be recovered from selected phage (1). Moreover, this method has been used to express various biologically active proteins, including growth factors, on phage (2–8), and therefore allows functional screening for mutations with improved properties. As originally described, phage libraries were screened by ‘biopanning’ against purified target protein bound to a solid

phase. More recent variations of phage display include selecting cell targeting ligands by screening phage libraries against whole cells (9) or even *in vivo* for identification of organ-specific ligands (10). The advantage of selection on cells is that cell-specific binding and internalizing ligands can be identified without previous knowledge or purification of the receptor. Our goal is to further adapt ligand display phage to both internalize and transduce the target cells, thus making it possible to directly select cell-specific ligands that are capable of binding and functional internalization. Since internalization is required but might not be sufficient for gene delivery, we anticipate that transduction screening will identify ligands that are particularly suitable for gene transfer.

Alternative ligands could greatly improve existing vectors for therapeutic gene delivery by targeting specific cells, thus reducing toxicity and allowing vectors to be administered systemically (11). In an effort to increase vector selectivity and potency, growth factors and other cell-specific ligands that bind cell surface receptors have been used for targeting both nonviral and viral vectors (12). For example, we used fibroblast growth factor (FGF2)² to target DNA condensates (13) and adenovirus (14, 15) to cells that overexpress FGF receptors, such as occurs in certain tumor cells and after injury. Targeting can even be applied to a single-stranded DNA bacterial virus, which normally has no tropism for mammalian cells. Recently, we showed that a modified filamentous bacteriophage can be specifically targeted to FGF receptor-bearing cells with nonco-

¹ Correspondence: Selective Genetics Inc., 11035 Roselle St., San Diego, CA 92121, USA. E-mail: laroccad@selectivegenetics.com

² Abbreviations: AEBF, 4-(2-aminoethyl)-benzene sulfonyl fluoride; BGH, bovine growth hormone; BSA, bovine serum albumin; DMEM, Dulbecco's modified Eagle's medium; ELISA, enzyme-linked immunoassay; FBS, fetal bovine serum; FGF2, fibroblast growth factor; GFP, green fluorescent protein; HRP, horseradish peroxidase; OD, optical density; PBST, phosphate-buffered saline with 0.05% Tween 20; PEG, polyethylene glycol; SDS, sodium dodecyl sulfate; SOE-PCR, splice overlap extension-polymerase chain reaction.

TABLE 1. Oligonucleotides used in phage vector construction:

#	Name	Sequence
1	NKAoriFor	PO ₄ -GGCGCCGGTACCGTATACGATGGCTGACTAATTTTT
2	SV40oriRev	ATGGGCTATGAACTAATGGCAAAAGCCTAGGCCTCC
3	PvuICMVf	CAATTACGATCGCATTAGTTCATAGCCCAT
4	CMVΔNcoIrev	CGCATCACCATGCTAATAGCGATGAC
5	CMVΔNcoIfor	CTATTAGCATGGTGATGCGGTTTTG
6	CMVMCSrev	TCTAGATATCGCGCGCGATCTGACGGTTCAC
7	MCSBGH _p Af	TCGCGCGCGATATCTAGAGATCAGCCTCGACTGTGC
8	BGH _p Arev3	PO ₄ -GGCGCCGAAGCCATAGAGCCCACC
9	EGFPfor	PO ₄ -TTGGCGCCGACAATGGTGAGCAAGGGCCAG
10	EGFPrev	PO ₄ -CGTCTAGATTACTTCTACAGCTCGTC
11	FGF2/3for	PO ₄ -GACCATGGCAGCAGGATCAATAACA
12	FGF2C78r	CAGGTAACGGTTAGCAGACACTCCTTTGATAGA
13	FGF2C78f	TCTATCAAAGCAGTGTCTGCTAACCGTTACCTG
14	FGF2/3rev2	PO ₄ -CTGCAGAGCCTCCTCCACCGCTCTTAGCAGACATTGG

valently attached FGF2, resulting in successful foreign transgene expression (16). Based on these observations, we reasoned that if targeted phage transduction could also be accomplished by genetically displaying a targeting ligand on the phage surface, it would then be feasible to identify novel ligands by direct selection of those that mediate gene transfer.

In the present study, we transduced COS-1 cells with filamentous phage displaying a known gene targeting ligand, FGF2. We constructed FGF2 display phage by fusing the FGF2 gene to the pIII gene encoding the minor coat protein. The phage were modified for transduction of mammalian cells by inserting a green fluorescent protein (GFP) reporter gene transcriptionally driven by the cytomegalovirus immediate early promoter (CMV) into the phage genome. Specificity of the FGF2-phage-mediated transduction was demonstrated by inhibition of transduction in the presence of excess free FGF2. These data support our hypothesis that phage transduction can be used to screen display libraries for novel ligands capable of gene transfer.

MATERIALS AND METHODS

Materials

The FGF2 used in the competition experiments described here and for preparing the biotinylated FGF2 (16) was mutagenized so that the cysteine at position 96 in wild-type FGF2 had been changed to serine. It was produced and purified as described previously (17). This single mutant contains one free cysteine, which simplified the chemical derivitization with biotin. Homogeneity was established by amino acid analysis, amino-terminal sequence analyses, and using mass spectroscopy to determine the molecular mass. All other materials and reagents described in this study were purchased where indicated.

Modification of phage for mammalian cell reporter gene expression

A mammalian cell expression cassette consisting of the SV40 origin of replication (SVori), the CMV immediate early promoter, a multiple cloning site, and the bovine growth hormone (BGH) polyadenylation and transcriptional termination signals was inserted into an ampicillin-resistant M13 phage vector, MANP, to create the MCMV vector. These elements were assembled using splice overlap extension-polymerase chain reaction (SOE-PCR) (18). Briefly, the primer pairs [1, 2], [3, 4], and [5, 6] (Table 1) were used to amplify SVori and CMV DNA fragments from pEGFP-N1 (Clontech, Palo Alto, Calif.), and the primer pair [7, 8] (Table 1) was used to amplify the BGH DNA terminator fragment from pcDNA3.1 (Invitrogen, Carlsbad, Calif.). DNA fragments were gel purified, combined, and used as template for amplification using flanking primers 1 and 8. The resulting 1 kb product was subcloned into the unique *PvuII* site of the MANP vector. The EGFP gene is human codon optimized and has a mutation, described by Cormack et al. (19), that results in a 35-fold increase in fluorescence intensity over wild-type GFP. The EGFP gene was amplified from pEGFP-N1 (Clontech) by PCR with primers 9 and 10 (Table 1), subcloned into *SmaI* digested pBS+ (Stratagene, San Diego, Calif.). After sequencing, the EGFP gene was removed with *BssHII* and *XbaI* and inserted into the multiple cloning site of the *BssHII*/*XbaI* digested MCMV phage vector to create MG3. This vector encodes a short peptide extension on the amino terminus of pIII (CGSPPPVRWC).

Construction of FGF2 display phage

To avoid potential folding and aggregation problems that might occur as a result of expressing the FGF2 (C96S) mutant with an unpaired cysteine (C78), we created DNA encoding a 155 amino acid double mutant of mature FGF2 (C78S,C96S) and inserted it in frame with the pIII gene of M13, using the *NcoI* and *PstI* sites in the MG3 vector (Fig. 1) such that the insert is downstream from the pIII signal peptide encoding sequence. The DNA sequence between the *NcoI* and *PstI* sites encoding the peptide (CGSPPPVRWC) was replaced with the FGF2 gene. The double mutant was created by site-directed mutagenesis of a FGF2 C96S mutant (17). SOE-PCR was used to amplify DNA from the FGF2 template using primer pairs [11, 12], and [13, 14] (Table 1). Amplified DNA fragments were purified by gel electrophoresis and used as template for amplification with primers 11 and 14 (Table 1). With this

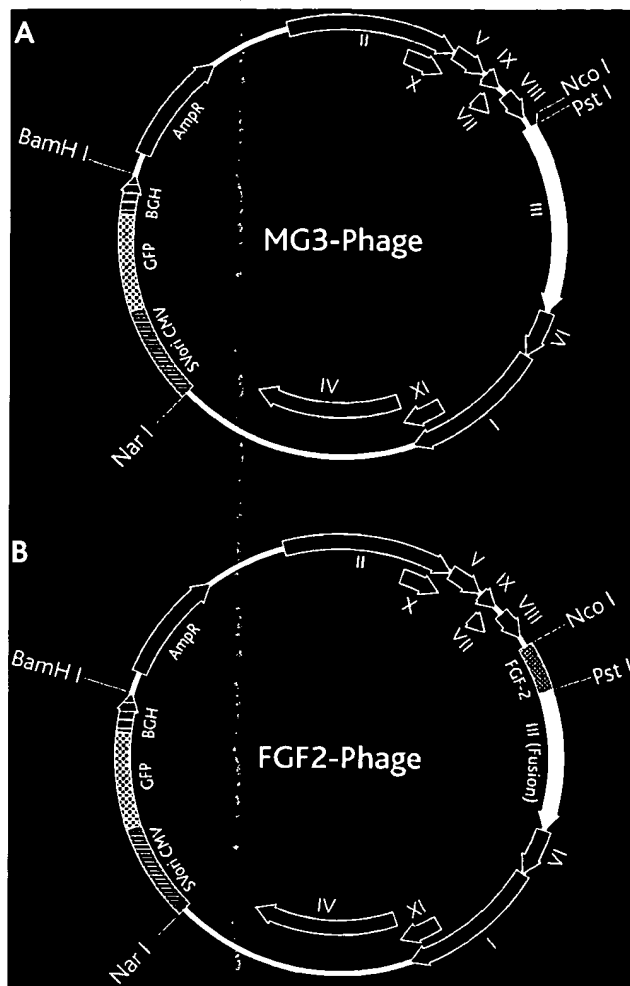


Figure 1. Phage vectors for mammalian cell transduction. A) Parent phage with native pIII coat protein. B) FGF2-pIII fusion display phage. Base vector is M13 genome with ampicillin resistance (Amp^R) gene and GFP expression cassette inserted into the intergenic region between pIV and pII. ori-CMV, SV40 replication origin and CMV promoter; GFP, green fluorescent protein gene; BGH, bovine growth hormone polyadenylation sequence.

strategy, a cysteine to serine mutation was made at amino acid 78 of FGF2, the termination codon was removed, a gly-gly-gly-ser linker was added, and *NcoI* and *PstI* sites were introduced for subcloning. Sequencing of the FGF2-phage vector indicated that a single base pair error was introduced during assembly, which resulted, however, in a silent mutation.

Purification of phage particles and determination of titer

Phage were purified by standard polyethylene glycol (PEG) precipitation (1). Briefly, ~20 ampicillin-resistant colonies of phage infected Top10F' host bacteria (Invitrogen) were seeded into one liter of LB media containing 100 μ g/ml ampicillin and grown for 16 h at 37°C with shaking. Bacteria were removed by centrifugation (20 min at 11,800 *g*) and supernatant was transferred to fresh bottles. AEBSF (4-(2-aminoethyl)-benzene sulfonyl fluoride) was added to a final concentration of 0.2 mM. Phage particles were precipitated by addition of 1/6th volume of 30% PEG 8000 in 1.5M NaCl, incubation at 4°C for 2 h, and centrifugation (30 min at

11,800 *g*). The pellet was resuspended in 30 ml of PBS containing 0.2 mM AEBSF at 4°C for 30 min with occasional vortexing. Residual bacteria were removed by centrifugation (20 min at 26,000 *g*) and supernatant transferred to fresh tubes. Phage particles were again precipitated by addition of 1/6th volume of 30% PEG 8000 in 1.5M NaCl, incubation at 4°C for 30 min, and centrifugation (30 min at 26,000 *g*). The final phage pellet was resuspended in 10 ml PBS containing 0.2 mM AEBSF, titered, and stored at 4°C.

For CsCl purified phage, 4 g of CsCl were added to 2 ml of phage in PBS and 6 ml TE (10 mM Tris pH 8.0, 1 mM EDTA). After 16 h of centrifugation at 211,000 *g* at 15°C, the upper translucent band was removed from the top with a 18 g needle and 1 ml syringe. Phage were dialyzed against PBS overnight at 4°C and titered in XL-1Blue MRF' host cells (Stratagene) using standard protocols (1). The smaller plaques generated by the FGF2 display phage were counted to determine titer for mammalian cell transduction assays. Some preparations contained large revertant plaques that resulted from phage containing deletions of all or part of the FGF2 gene. Only preparations containing >95% small plaques were used.

Analysis of FGF2 expression on display phage

CsCl purified phage were boiled in 1× Tris-glycine-sodium dodecyl sulfate (SDS) sample buffer (Novex, San Diego, Calif.) containing 5% 2-mercaptoethanol for 3 min prior to loading on 8% polyacrylamide Tris-glycine gels (Novex) for immunoblot analysis. After separation, proteins were transferred to pure nitrocellulose filters (0.2 μ m pore) (Bio-Rad, Richmond, Calif.) in 96 mM glycine, 12 mM Tris Base, 0.01% SDS and 20% methanol. The filter was blocked in 1% bovine serum albumin (BSA) in PBST (phosphate-buffered saline with 0.05% Tween 20) for 1 h at RT and probed with mouse anti-FGF2 antibody (Transduction Laboratories, Lexington, Ky.) at a 1:500 dilution, or mouse anti-pIII antibody (Mo-BiTec, Göttingen, Germany) at a 1:1000 dilution, in 1% BSA in PBST for 1 h at room temperature. After five 5 min washes with PBST, filters were incubated with biotinylated donkey anti-mouse antibody (Jackson ImmunoResearch, West Grove, Pa.) at a 1:5000 dilution in 1% BSA in PBST for 1 h. After five 5 min washes with PBST, filters were incubated with a horseradish peroxidase (HRP) streptavidin conjugate (Amersham Life Sciences, Arlington Heights, Ill.) at a 1:20,000 dilution in 1% BSA in PBST for 15 min. Filters were washed five times for 5 min with PBST and developed with chemiluminescent substrates, SuperSignal or SuperSignal ULTRA (Pierce Chemical, Rockford, Ill.), for 1 min, then exposed to film.

A sandwich enzyme-linked immunoassay (ELISA) was used to detect immunologically reactive FGF2 on recombinant phage. Rabbit anti-phage antiserum and mouse anti-FGF2 antibody (#B1786 and #F3393, respectively; Sigma, St. Louis, Mo.) in 0.1 M carbonate/bicarbonate buffer (pH 9.6) were adsorbed onto 96-well plates overnight. Wells were washed three times with PBST, blocked with Superblock (Pierce Chemical) for 3 h, and washed three times with PBST prior to addition of phage dilutions (50 μ l/well). Phage were incubated overnight at 4°C, washed eight times with PBST, and incubated with HRP-conjugated anti-M13 antibody (Pharmacia Biotech, Piscataway, N.J.) at a 1:5000 dilution for 1 h. After five washings with PBST, signal was developed with 50 μ l/well *o*-phenylenediamine dihydrochloride substrate (Sigma) for ~5 min. All incubations were done at room temperature. Reactions were stopped with 20 μ l 3M HCl, optical density (OD) was read at 490 nm, and data were analyzed with SoftMax Pro software (Molecular Devices, Sunnyvale, Calif.).

Phage transfection and detection of reporter gene

The ability of FGF2 displaying phage particles to transduce cells was evaluated using the COS-1 cell line (ATCC, Rockville, Md.) that was grown in Dulbecco's modified Eagle's medium (DMEM) containing 10% FCS, 2 mM L-glutamine, pyruvate, and nonessential amino acids. The COS-1 cell line is a derivative of CV-1 monkey kidney cells and carries a single copy of the SV40 T-antigen, which permits high copy replication of DNAs that contain an SV40 origin of replication. Cells were transferred into six-well plates at densities of 40,000 cells 24 h prior to phage particle addition. The phage were added at 10^{11} pfu/ml and incubated with the cells ($\sim 75,000$ /well) for 4 h at 37°C in DMEM containing 2% BSA (bovine serum albumin) as a blocking agent. In some instances, free FGF2 was added to a final concentration of 2 μ g/ml or blocking phage were added at a 100-fold excess at the time of phage addition. The blocking phage particles (β -gal phage) do not display FGF2 or contain a GFP gene. They were prepared from pRC-CMV β phagemid-transformed host bacteria by rescue with M13 helper phage as described previously (16). After washing to remove unbound phage, the cells were returned to the incubator for an additional 72 h.

Nongenetic phage targeting was performed by assembling a phage-FGF2 receptor complex at the cell surface as described previously (16). Briefly, the cells were washed twice with ice-cold PBS/FBS (PBS with 2% fetal bovine serum), followed by the sequential addition of biotinylated FGF2, neutravidin (Pierce Chemical), and biotinylated anti-M13 antibody on ice for 15 min each, with a cell wash in between each step. Fifteen minutes after adding biotinylated anti-M13 antibody, the cells were washed and phage was added in PBS/FBS to form a complex at the cell surface. After 1 h on ice, the cells were washed, put into fresh culture media and returned to the incubator at 37°C to permit internalization. GFP expression was measured 72 h later.

Transduction was measured by counting all of the GFP-positive autofluorescent cells in each well. Transfections were done in triplicate and performed at least twice. The cells were washed twice in PBS/FBS and 1 ml of Dulbecco's PBS was added to each well. Fluorescent cells were detected directly in the culture plates using an epifluorescent inverted microscope (Nikon Diaphot) equipped with a fluorescein isothiocyanate filter set.

RESULTS

Construction of MG3-phage

We modified the M13 phage vector for transduction of COS-1 cells by inserting a CMV-driven GFP reporter gene into the intergenic region of the phage genome to construct the MG3 vector (Fig. 1A). This GFP expression cassette included an origin of replication from SV40 to ensure high copy number replication in SV40 T-antigen-containing cells. COS-1 cells were transfected with double-stranded phage DNA by CaPO₄ coprecipitation to confirm that the GFP expression cassette was functional (not shown).

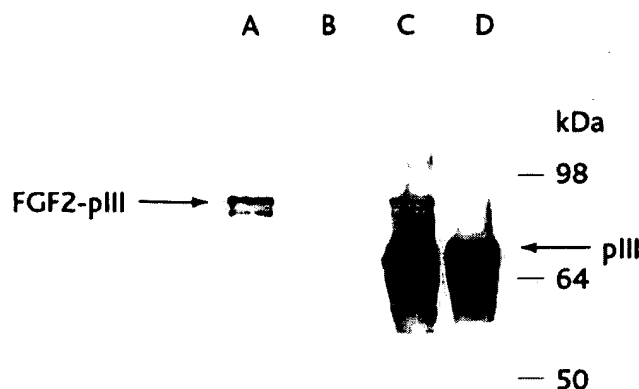


Figure 2. Detection of FGF2-pIII fusion protein in protein extracts from purified FGF2-phage by immunoblotting. Extracts from equivalent phage titers of purified FGF2 phage (lanes a and c) and MG3 control phage (lanes b and d) were separated by polyacrylamide gel electrophoresis and blotted onto nitrocellulose. Phage immunoblots were probed with anti-FGF2 antibody (lanes a and b), or anti-pIII antibody (lanes c and d).

Display of FGF2 on MG3-phage

Although our strategy for expressing FGF2 on the surface of filamentous phage was similar to one used to display IL-3 (5), it was unclear how the inclusion of the CMV-GFP expression cassette would affect display. DNA encoding FGF2 was fused 5' to DNA encoding the full-length minor coat protein pIII, so that three to five copies of targeting ligand fused at the amino terminus of the coat protein were expected to be displayed per phage (Fig. 1B). Because earlier attempts to display FGF2 (C96S) were less successful, we used an FGF2 gene derivative that contained two mutations, resulting in the conversion of the two free surface cysteines to serines to reduce the probability of misfolding and aggregation. The (C96S,C78S) mutant of FGF2 has previously been produced in bacteria and shown to have equivalent biological activity as recombinant wild-type FGF2 (20). Recombinant phage were identified by the smaller plaque size, probably caused by the foreign pIII extension reducing phage productivity.

The FGF2-pIII fusion was detected on phage particles by immunoblot analysis of FGF2-phage. An immunoblotted fusion protein of ~ 85 kDa was detected in the lane loaded with an extract of 10^{10} FGF2-phage but not in the lane containing an equivalent amount of parent phage (lanes a and b, Fig. 2). This immunoreactive protein migrates at the predicted combined molecular mass of FGF2 (~ 18 kDa) and pIII (migrates anomalously at 65–70 kDa). When an identical blot was prepared in parallel and probed with an anti-pIII antibody, a protein band corresponding to native pIII was seen in both FGF2-phage and in the parent MG3-phage extracts (lanes c and d, Fig. 2). An additional higher molecular mass but less abundant protein migrating at the expected

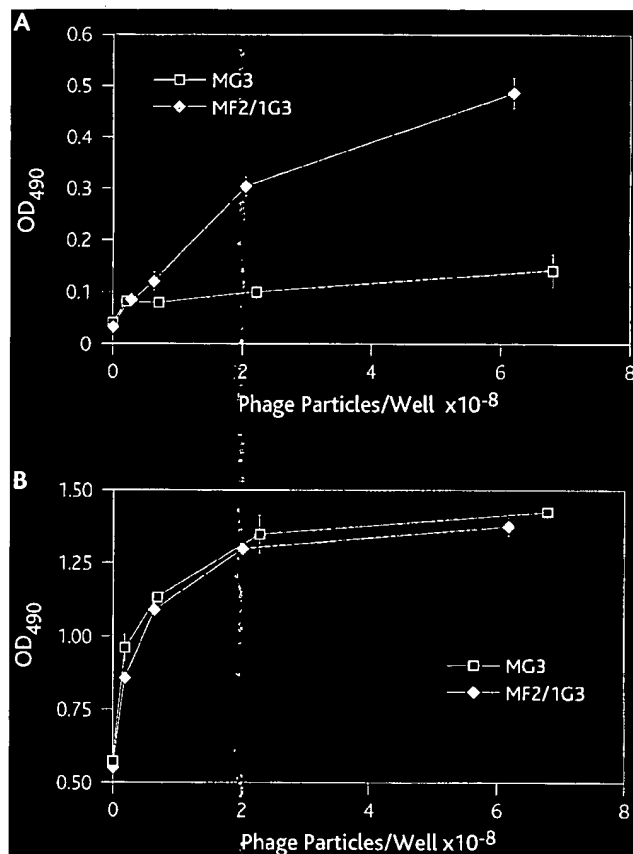


Figure 3. Detection of FGF2 on FGF2-phage by ELISA. Phage were captured with anti-FGF2 antiserum (A) or anti-phage antiserum (B) bound to the plate well. An HRP-conjugated anti-M13 antibody was used to detect the bound phage. An increased OD indicated the presence of FGF2 on FGF2-phage when phage were captured with anti-FGF2 antiserum. When anti-phage antibody was used to capture the phage, an equivalent OD was observed for both control MG3 phage and FGF2-phage, indicating that equivalent phage particles are applied to the plate.

molecular mass of the FGF2-pIII fusion protein was detected only in the extracts from FGF2-phage (lane c). The smaller immunoreactive pIII protein in the FGF2-phage lane was not detected by anti-FGF2 antibody and migrated slightly faster than the MG3-phage encoded pIII, indicating that it was probably the result of cleavage within the amino terminus of pIII. These data suggest that both truncated pIII and FGF2-pIII fusion protein were present on the FGF2-phage particles. We estimated from a dilution series on additional immunoblots (not shown) that the abundance of the fusion coat protein was $\sim 1/50$ th of the free pIII protein. If 3–5 pIII molecules are present on each phage, then 6–10% of phage would display FGF2.

We also assessed the presence of FGF2 on the phage coat by sandwich ELISA. There was a significant increase in FGF2-phage retained on the ELISA plate by FGF2 antibody compared with the MG3 parent phage (Fig. 3A). There was little difference in

the amount of either phage retained on the ELISA plate by anti-M13 antibody (Fig. 3B).

Transduction of COS-1 cells with FGF2-phage

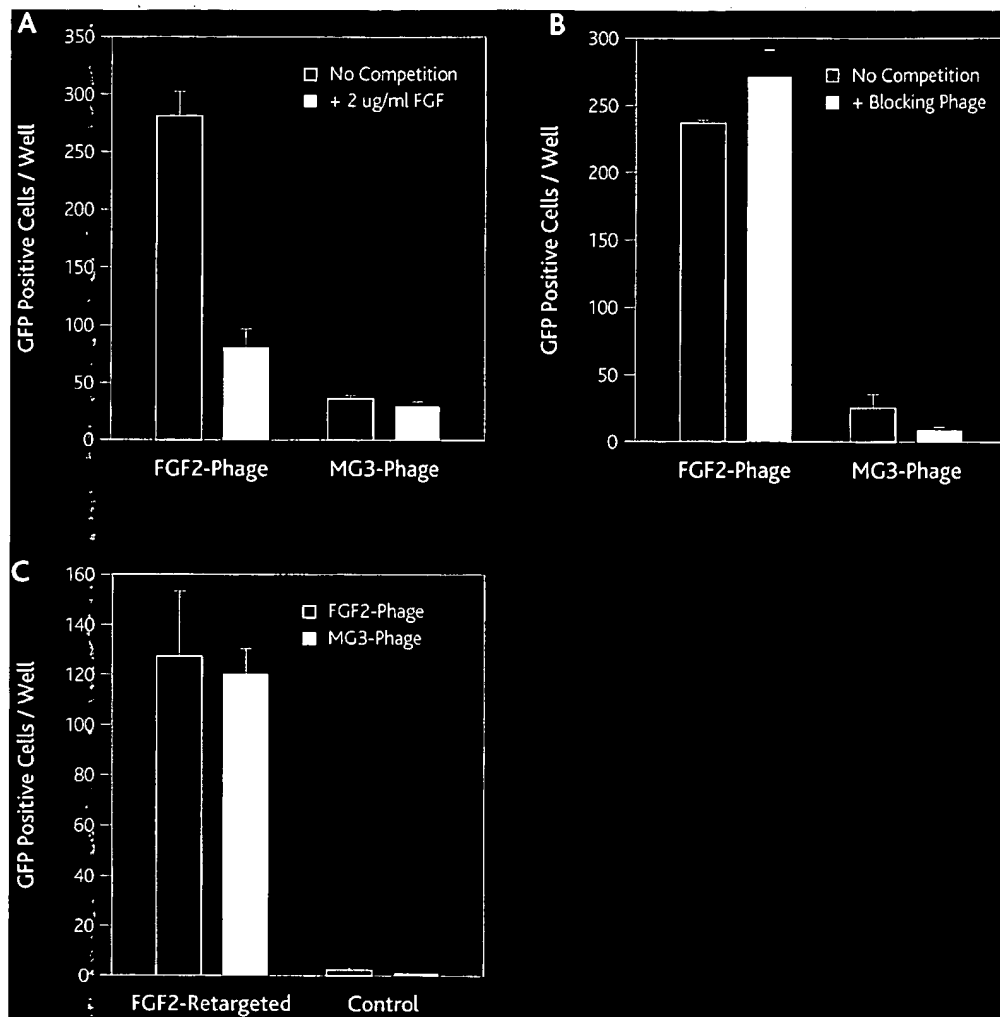
FGF2 display phage and MG3 control phage were compared for their ability to transduce COS-1 cells. Transfection with the FGF2-phage resulted in about a 10-fold greater transduction efficiency than the control phage (Fig. 4A). These findings indicate that the FGF2 ligand on the surface of the phage particles results in FGF2-dependent binding and internalization of phage because expression of the phage DNA encoded GFP requires nuclear transport, transcription, and translation in the target cell. The specificity of the FGF2-phage-mediated transduction for the FGF receptor complex was demonstrated by successful inhibition of transduction by these phage in the presence of an excess of free FGF2 (Fig. 4A). Competition with FGF2 had no effect on nonspecific transduction by MG3 control phage.

We further demonstrated the specificity of the targeting pathway of FGF2-phage by adding an excess of phage particles with no GFP gene and no targeting ligand to the incubation media. These 'blocking phage' were expected to interfere with any nonspecific uptake of GFP containing phage, thus reducing the transduction efficiency of untargeted phage. As anticipated, transduction of cells by MG3 control phage was significantly inhibited by a 100-fold excess of blocking phage. Moreover, the presence of excess blocking phage did not inhibit FGF2 targeting and, if anything, slightly increased FGF2-phage transduction (Fig. 4B).

It was also important to rule out the possibility that the increased transduction efficiency of FGF2-phage was due to structural differences in the phage particles themselves or, alternatively, to differences in the amount of transduction competent particles in the phage preparation. To investigate this possibility, we compared the transduction ability of FGF2-phage and MG3 control phage by nongenetically targeting both phages. Equivalent titers of each phage were used to transfect COS-1 cells using avidin-biotin FGF2 targeting (16), and there was no significant difference in transduction between FGF2-phage and control phage (Fig. 4C). Thus, both FGF2-phage and MG3 control phage preparations have the same capacity to transduce COS-1 cells, once appropriately targeted.

DISCUSSION

Because of their inherent simplicity, the use of bacteriophage for gene delivery to mammalian cells is an attractive concept. Indeed, attempts to trans-



duce mammalian cells with bacteriophage particles began as early as 25 years ago, but with little success (21). Later studies successfully used chemical methods to transduce mammalian cells with both single-stranded filamentous phage (22, 23) and double-stranded λ phage (24, 25), but there was no attempt to target the phage particles in these experiments. Recently, filamentous phage have been targeted to the cell surface and shown to be internalized with RGD peptides (26) or selected random peptides (9). Mammalian cell transfection has been reported with an RGD tail tube modified λ phage (27), however, this was achieved by growing cells directly on RGD-phage that had been adsorbed to the culture dish. We show here that filamentous phage containing a CMV-driven GFP gene and genetically displaying the growth factor ligand, FGF2, can transduce COS-1 cells in an FGF2-specific manner. To our knowledge, this is the first report to demonstrate mammalian cell gene transfer by genetically targeted filamentous phage. These data are consistent with and extend our previous results demonstrating that filamentous phage that normally have no tropism for mammalian

cells can be adapted for cell-specific mammalian cell transduction when appropriately targeted.

Consistent with previous reports describing the functional display of various small peptide cytokines and growth factors as pIII fusion proteins on the surface of M13 phage (2–8), we found that FGF2 can be displayed on the phage surface as a pIII fusion. Early attempts to express FGF2 fused to the pIII or pVIII coat protein in other vector systems designed to include expression of both fusion protein and native pIII coat protein (1) resulted in only native pIII and no detectable FGF2 fusion protein by immunoblot analysis (data not shown). We therefore attempted expression of an FGF2-pIII fusion onto the phage coat by expressing it in the phage vector described here, which contains only the FGF2-fused copy of the pIII gene. Even in this system, the FGF2-pIII fusion represented only ~2–3% of the total pIII protein present on phage particles, indicating low but detectable expression of FGF2-pIII. Together, these data suggest that there is strong selective pressure against bacterial expression of the FGF2 fusion in the periplasm where phage assembly oc-


curs, thus resulting in more of the free pIII protein on the phage particle. The free pIII presumably is the result of proteolytic cleavage of the FGF2 fusion protein.

The significant albeit low transduction efficiency obtained with FGF2-phage could be explained by the expression of a single FGF2 on 6–10% of phage particles, which is similar to what is obtained for other ligands with vectors designed for monovalent phage display (1). Since heparin-induced FGF2 dimerization is thought to activate FGF2 (28), this process, and therefore biological activity, might be increased by multivalent display. Sequences in the phage vector itself could also contribute to the lower transduction efficiency. Noncovalent FGF2 targeting in the present study resulted in about a 12-fold lower transduction efficiency than expected from our previous results with a smaller phagemid vector system (16). Therefore, we expect that more efficient ligand expression on the phage surface and further modifications of the vector will improve transduction efficiency. This increased efficiency could potentially exceed that which we have previously reported for nongenetic targeting [~1%, (16)].

Our ELISA data showed binding of a neutralizing anti-FGF2 antibody to the displayed FGF2, suggesting that the FGF2 on the phage surface is properly folded and therefore active. This notion is further supported by the observation that significant transduction of COS-1 cells with FGF2-phage was obtained relative to the parent phage, MG3. Moreover, the FGF2-phage-mediated transduction was specific for FGF receptors, as shown by the substantial inhibition of transduction in the presence of excess free FGF2. The low level of nonspecific transduction by the control MG3 phage was not affected by the presence of excess FGF2, suggesting that simple adhesion to the cell surface and subsequent internalization were not mediated by FGF receptors. However, the presence of a 100-fold excess of nontransducing phage particles significantly inhibited this nonspecific transduction but not the specific FGF2-phage transduction, providing further evidence of specificity. These data indicate that FGF2 display phage can transduce mammalian cells, that the transduction is specifically mediated by the displayed ligand, and that FGF2-phage were internalized by a distinct pathway from the untargeted phage.

Our results extend the proposal that peptide display phage might themselves be used as gene delivery vehicles (9, 16). Indeed, in many ways, bacteriophage fit the description of the ideal gene therapy vector (11). Though immunogenic, like animal viral vectors, phage might be safer because they are much less likely to generate a replication-competent virus in animal cells. Phage would also be less likely to infect nontargeted tissues because of their natural

lack of tropism for eukaryotic cells. Thus, the targeted phage particles resemble synthetic DNA conjugates that can be biologically produced. The results described here suggest that development of an improved gene delivery vehicle could be achieved by further modification and selection of genetically altered phage, resulting in safe and efficient gene transfer into mammalian target cells.

Having demonstrated transduction by phage genetically displaying a known gene targeting ligand, it should be possible to apply selective phage transduction and the power of combinatorial phage libraries to the discovery of new gene targeting ligands. Current phage display methods for identifying cell- or organ-specific targeting ligands select only for phage binding and/or internalization (9, 10) and require recovery of infective phage. Noninfective phage that are, for example, uncoated and trafficked to the nucleus for expression, would be missed by existing screening methods. Therefore, selection of ligand targeted phage using phage internalization and subsequent expression of a selectable reporter gene could directly identify novel ligands capable of both cell-specific internalization and trafficking required for gene delivery. We anticipate that the discovery of such ligands will greatly improve the efficacy of existing gene therapy vectors. 

The authors thank Ana Maria Gonzalez, Wendy Johnson, Bob Shopes, and Barbara Sosnowski for their input and insightful discussions regarding this work, and Anne Larocca for critical review of the manuscript. We also thank Ed Cohen for technical assistance.

REFERENCES

1. Kay, B. K., Winter, J., and McCafferty, J. (1998) *Phage Display of Peptides and Proteins: A Laboratory Manual*, pp. 55–65, Academic Press, San Diego
2. Bass, S., Greene, R., and Wells, J. A. (1990) Hormone phage: an enrichment method for variant proteins with altered binding properties. *Proteins* 8, 309–314
3. Saggio, I., Gloaguen, I., and Laufer, R. (1995) Functional phage display of ciliary neurotrophic factor. *Gene* 152, 35–39
4. Buchli, P. J., Wu, Z., and Ciardelli, T. L. (1997) The functional display of interleukin-2 on filamentous phage. *Arch. Biochem. Biophys.* 339, 79–84
5. Gram, H., Strittmayer, U., Lorenz, M., Glück, D., and Zenke, G. (1993) Phage display as a rapid gene expression system: production of bioactive cytokine-phage and generation of neutralizing monoclonal antibodies. *J. Immunol. Methods* 161, 169–176
6. Souriau, C., Fort, P., Roux, P., Hartley, O., Lefranc, M. P., and Weill, M. (1997) A simple luciferase assay for signal transduction activity detection of epidermal growth factor displayed on phage. *Nucleic Acids Res.* 25, 1585–1590
7. Vispo, N. S., Callejo, M., Ojalvo, A. G., Santos A., Chinea, G., Cabilondo, J. V., and Arana, M. J. (1997) Displaying human interleukin-2 on the surface of bacteriophage. *Immunotechnology* 3, 185–193
8. Merlin, S., Rowold, E., Abegg, A., Berglund, C., Klover, J., Staten, N., McKearn, J. P., and Lee, S. C. (1997) Phage presentation and affinity selection of a deletion mutant of human interleukin-3. *Appl. Biochem. Biotechnol.* 67, 199–214
9. Barry, M. A., Dower, W. J., and Johnston, S. A. (1996) Toward cell-targeting gene therapy vectors: Selection of cell-binding

- peptides from random peptide-presenting phage libraries. *Nat. Med.* **2**, 299–305
10. Pasqualini, R., and Rouslahti, E. (1996) Organ targeting in vivo using phage display peptide libraries. *Nat. Biotechnol.* **12**, 771–771
 11. Hodgson, C. P. (1995) The vector void in gene therapy. *Bio/Technology* **13**, 222–225
 12. Michael, S. I., and Curiel, D. T. (1994) Strategies to achieve targeted gene delivery via the receptor-mediated endocytosis pathway. *Gene Ther.* **1**, 223–232
 13. Sosnowski, B. A., Gonzalez, A. M., Chandler, L. A., Buechler, Y. J., Pierce, G. F., and Baird, A. (1996) Targeting DNA to cells with basic fibroblast growth factor (FGF2). *J. Biol. Chem.* **271**, 33647–33653
 14. Goldman, C. K., Rogers, B. E., Douglas, J. T., Sosnowski, B. A., Ying, W., Siegal, G. P., Baird, A., Campain, J. A., and Curiel, D. T. (1997) Targeted gene delivery to Kaposi's sarcoma cells via the fibroblast growth factor receptor. *Cancer Res.* **57**, 1447–1451
 15. Rogers, B. E., Douglas, J. T., Sosnowski, B. A., Ying, W., Pierce, G. F., Buchsbaum, D. J., Manna, D. D., Baird, A., and Curiel, D. T. (1998) Enhanced *in vivo* gene delivery to human ovarian cancer xenografts utilizing a tropism-modified adenovirus vector. *Tumor Targeting* **3**, 25–31
 16. Larocca, D., Witte, A., Johnson, W., Pierce, G. F., and Baird, A. (1998) Targeting bacteriophage to mammalian cell surface receptors for gene delivery. *Hum. Gene Ther.* **9**, 2393–2399
 17. Lappi, D. A., Matsunami, R., Martineau, D., and Baird, A. (1993) Reducing the heterogeneity of chemically conjugated targeted toxins: homogeneous basic FGF-saporin. *Anal. Biochem.* **212**, 446–451
 18. Vallejo, A. N., Pogulis, R. J., and Pease, L. R. (1995) Mutagenesis and synthesis of novel recombinant genes using PCR. In *PCR Primer. A Laboratory Manual* (Diffenbach, C. W., and Dveksler, G. S., eds) pp. 603–612, Cold Spring Harbor Laboratory Press, Cold Spring Harbor, N.Y.
 19. Cormack, B. P., Valdivia, R. H., and Falkow, S. (1996) FACS-optimized mutants of the green fluorescent protein (GFP). *Gene* **173**, 33–38
 20. Fox, G. M., Schiffer, S. G., Rohde, M. F., Tsai, L. B., Banks, A. R., and Arakawa, T. (1988) Production, biological activity, and structure of recombinant basic fibroblast growth factor and an analog with cysteine replaced by serine. *J. Biol. Chem.* **263**, 18452–18458
 21. Horst, J., Kluge, F., Beyreuther, K., and Gerok, W. (1975) Gene transfer to human cells: Transducing phage λ plac gene expression in GM₁-gangliosidosis fibroblasts. *Proc. Natl. Acad. Sci. U. S. A.* **72**, 3531–3535
 22. Yokoyama-Kobayashi, M., and Kato, S. (1993) Recombinant f1 phage particles can transfect monkey COS-7 cells by DEAE dextran method. *Biochem. Biophys. Res. Commun.* **192**, 935–939
 23. Yokoyama-Kobayashi, M., and Kato, S. (1994) Recombinant f1 phage-mediated transfection of mammalian cells using lipopolyamine technique. *Anal. Biochem.* **223**, 130–134
 24. Ishiura, M., Hirose, S., Uchida, T., Hamada, Y., Suzuki, Y., and Okada, Y. (1982) Phage particle-mediated gene transfer to cultured mammalian cells. *Mol. Cell. Biol.* **2**, 607–616
 25. Okayama, H., and Berg, P. (1985) Bacteriophage lambda vector for transducing a cDNA clone library into mammalian cells. *Mol. Cell. Biol.* **5**, 1136–1142
 26. Hart, S. L., Knight, A. M., Harbottle, R. P., Mistry, A., Hunger, H. D., Cutler, D. F., Williamson, R., and Coutelle, C. (1994) Cell binding and internalization by filamentous phage displaying a cyclic Arg-Gly-Asp-containing peptide. *J. Biol. Chem.* **269**, 12468–12474
 27. Dunn, I. S. (1996) Mammalian cell binding and transfection mediated by surface-modified bacteriophage lambda. *Biochimie (Paris)* **78**, 856–861
 28. Herr, A. B., Ornitz, D. M., Sasisekharan, R., Venkataraman, G., and Waksman, G. (1997) Heparin-induced self-association of fibroblast growth factor-2. *J. Biol. Chem.* **272**, 16382–16389

Received for publication November 9, 1998.

Revised for publication February 5, 1999.

Targeted Gene Delivery to Mammalian Cells by Filamentous Bacteriophage

Marie-Alix Poul and James D. Marks*

Departments of Anesthesia and
Pharmaceutical Chemistry
University of California
San Francisco, Rm. 3C-38
San Francisco General Hospital
1001 Potrero Avenue
San Francisco, CA 94110, USA

We report that prokaryotic viruses can be re-engineered to infect eukaryotic cells resulting in expression of a reporter gene inserted into the bacteriophage genome. Phage capable of binding mammalian cells expressing the growth factor receptor ErbB2 and undergoing receptor-mediated endocytosis were isolated by selection of a phage antibody library on breast tumor cells and recovery of infectious phage from within the cell. As determined by immunofluorescence, F5 phage were efficiently endocytosed into 100% of ErbB2 expressing SKBR3 cells. To achieve reporter gene expression, F5 phage were engineered to package the green fluorescent protein (GFP) reporter gene driven by the CMV promoter. These phage when applied to cells underwent ErbB2-mediated endocytosis leading to GFP expression. GFP expression occurred only in cells overexpressing ErbB2, was dose-dependent reaching, 4% of cells after 60 hours and was detected with phage titers as low as 2.0×10^7 cfu/ml (500 phage/cell). The results demonstrate that bacterial viruses displaying the appropriate antibody can bind to mammalian receptors and utilize the endocytic pathway to infect eukaryotic cells, resulting in expression of a reporter gene inserted into the viral genome. This represents a novel method to discover targeting molecules capable of delivering a gene intracellularly into the correct trafficking pathway for gene expression by directly screening phage antibodies. This should significantly facilitate the identification of appropriate targets and targeting molecules for gene therapy or other applications where delivery into the cytosol is required. This approach can be adapted to directly select, rather than screen, phage antibodies for targeted gene expression. The results also demonstrate the potential of phage antibodies as an *in vitro* or *in vivo* targeted gene delivery vehicle.

© 1999 Academic Press

Keywords: endocytosis; ErbB2; gene therapy; phage display; single chain Fv antibodies

*Corresponding author

Introduction

Widespread application of gene therapy requires the ability to target a therapeutic gene to the appropriate cell or tissue type with high efficiency (Michael & Curiel, 1994). Targeting of retroviral vectors has been reported by inserting receptor ligands or single chain Fv (scFv) antibody fragments into the viral envelope protein (Kasahara *et al.*, 1994; Somia *et al.*, 1995). Targeting of adeno-

viral vectors has been achieved by use of "adapter" fusion molecules consisting of an antibody fragment that binds the adenoviral knob and a cell targeting molecule such as a receptor ligand or antibody (Douglas *et al.*, 1996; Watkins *et al.*, 1997). Targeting of non-viral vectors using cell surface receptor ligands or antibodies has also been reported (Fominaya & Wels, 1996; Michael & Curiel, 1994). All of these approaches depend on the use of targeting molecules that bind a cell-surface receptor, resulting in internalization of the gene delivery vehicle with subsequent delivery of the DNA to the nucleus. Identification of appropriate targeting molecules has largely been performed by individually screening receptor ligands or antibodies. In the case of scFv antibody fragments, this typically requires construction of the scFv from the

Abbreviations used: ECD, extracellular domain; CMV, cytomegalovirus; FGF, fibroblast growth factor; GFP, green fluorescent protein; MFI, mean fluorescent intensity; cfu, colony-forming units.

E-mail address of the corresponding author:
jim_marks@quickmail.ucsf.edu

V-genes of a hybridoma, construction of the targeted gene delivery vehicle, and *in vitro* evaluation of targeting ability.

More recently, it has proven possible to directly select peptides and antibody fragments binding cell-surface receptors from filamentous phage libraries (Andersen *et al.*, 1996; Barry *et al.*, 1996; Cai & Garen, 1995; de Kruif *et al.*, 1995; Marks *et al.*, 1993). This has led to a marked increase in the number of potential targeting molecules. The ability of bacteriophage to undergo receptor-mediated endocytosis (Hart *et al.*, 1994; Barry *et al.*, 1996; Becerril *et al.*, 1999) indicates that phage libraries can be selected not only for cell binding but also for internalization into mammalian cells. If the phage single-stranded phage genome can be transcribed and translated, then it should prove possible to screen or select for phage that bind receptors in a manner that leads to endocytosis and delivery of the phage genome into the correct trafficking pathway leading to expression. It has been shown that phage can enter mammalian cells after chemical alteration of the cell membrane leading to reporter gene expression (Okayama & Berg, 1985; Yokoyama-Kobayashi & Kato, 1993). More recently, Larocca *et al.* (1998) showed that indirect bacteriophage-mediated gene delivery could occur by targeting biotinylated phage *via* streptavidin and biotinylated fibroblast growth factor (FGF) to mammalian cells expressing FGF receptor.

Here, we show that filamentous phage displaying the anti-ErbB2 scFv F5 as a genetic fusion with the phage minor coat protein pIII can directly infect mammalian cells expressing ErbB2 leading to expression of a reporter gene contained in the phage genome. This offers a new way to discover targeting molecules for intracellular drug delivery or gene therapy by directly screening phage antibodies to identify those capable of undergoing endocytosis and delivering a gene intracellularly into the correct trafficking pathway for gene expression. This should significantly facilitate the identification of appropriate targets and targeting molecules for gene therapy or other applications where delivery into the cytosol is required. We also discuss how this approach might be used to directly select phage antibodies for targeted gene expression. Finally, we discuss the potential for use of phage antibodies themselves for *in vitro* or *in vivo* targeted gene delivery vectors.

Results

Internalization of ErbB2 binding monovalent and multivalent F5 phage particles by ErbB2 expressing cells

We isolated the anti-ErbB2 scFv-F5 from a library of scFv displayed on the surface of bacteriophage as fusions to pIII (Sheets *et al.*, 1998) by selection on ErbB2 expressing SKBR3 breast tumor

cells and recovery of infectious phage from within the cell (M.-A. *et al.*, unpublished results). This selection strategy (Hart *et al.*, 1994; Barry *et al.*, 1996; Becerril *et al.*, 1999) was employed to select scFv capable of undergoing endocytosis upon receptor binding. When the pHEN-F5 phagemid vector is rescued with VCS-M13 helper phage, the resulting virus particles (F5-phagemid) display an average of one copy of scFv-pIII fusion protein and three to four copies of the wild-type pIII minor coat protein from the helper phage (Marks *et al.*, 1992). As a result, the phagemid bind monovalently. To improve the binding of the virus particles to ErbB2 expressing cells, multivalent phage antibodies were created by subcloning the F5 scFv DNA into the phage vector fd-Sfi/Not for fusion with the pIII protein. Virus particles, referred to as fd-F5 phage, display four to five copies of scFv-pIII fusion protein (Marks *et al.*, 1992).

To determine whether F5 phage antibodies could be internalized by mammalian cells, SKBR3 cells overexpressing ErbB2 were incubated for 16 hours with fd-F5 phage (10^9 cfu/ml), F5 phagemid (10^{11} cfu/ml), or with phagemids displaying an irrelevant anti-botulinum scFv-pIII fusion protein (10^{12} cfu/ml; Amersdorfer *et al.*, 1997) as a negative control. The cell surface was stripped of phage antibodies using low-pH glycine buffer, the cells permeabilized and fixed, and intracellular phage detected with anti-M13 antibody. Remarkably, all cells showed strong intracellular staining when incubated with fd-F5 phage or with F5 phagemid but not when incubated with the anti-botulinum phagemid (Figure 1). This demonstrates the dependence of phage entry on the specificity of the scFv fused to pIII.

Preparation of ErbB2-binding phages and phagemids packaging a reporter gene for expression in eukaryotic cells

Two strategies were used to investigate whether F5 phage could deliver a reporter gene to mammalian cells leading to expression. To make monovalent phage containing a reporter gene, we cloned the gene for green fluorescent protein (GFP) driven by the CMV promoter into the phagemid vector pHEN-F5 generating the vector pHEN-F5-GFP (Figure 2, upper panel). *Escherichia coli* TG1 containing pHEN-F5-GFP (ampicillin resistant) were infected with helper phage (kanamycin resistant) and high titers of monovalent F5-GFP phagemids were obtained (5.0×10^{10} ampicillin-resistant cfu/ml of culture supernatant). The ratio of packaged phagemid DNA *versus* helper phage DNA (ampicillin *versus* kanamycin resistant cfu) was determined to be 100:1. To make multivalent phage containing a reporter gene, fd-F5-GFP phage were generated by infecting *E. coli* TG1 carrying the pcDNA3-GFP phagemid (ampicillin-resistant) with fd-F5 phage (tetracycline-resistant), thus using fd-F5 phage as a helper phage. The fd-F5-GFP phage

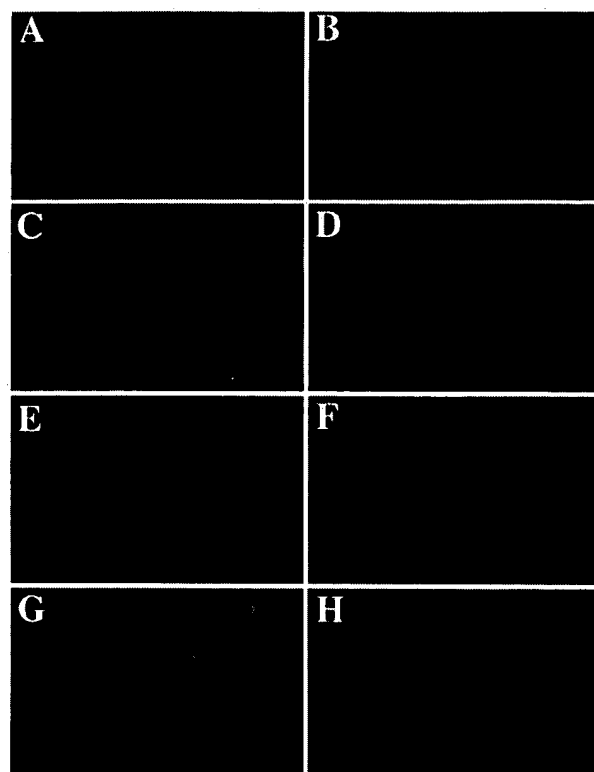


Figure 1. Internalization of anti-ErbB2 phagemids (monovalent) and phages (multivalent). SKBR3 cells (4.0×10^5) were incubated at 37°C with (a) and (b) no phage, (c) and (d) 10^{12} cfu/ml of anti-Botulinum phagemid (non specific phagemid), (e) and (f) 10^9 cfu/ml of anti-ErbB2 fd-F5-phage or (g) and (h) 10^{11} cfu/ml of anti-ErbB2 F5-phagemid. After 16 hours, the cell surface was stripped to remove the extracellular phages. Cells were fixed, permeabilized and stained with Hoechst dye (left column) to detect the cell nucleus and biotinylated anti-M13 antibody and streptavidin Texas-Red (right column) to detect intracellular phage particles.

titer was approximately 5.0×10^8 ampicillin resistant cfu/ml of culture supernatant. Lower phage titers result when fd is used as a helper phage because it lacks a plasmid origin of replication leading to interference from the phagemid fl origin (Cleary & Ray, 1980). The ratio of packaged reporter gene DNA *versus* phage DNA (ampicillin *versus* tetracycline-resistant cfu) was 1:1. The lower ratio of reporter gene/helper genome when using fd as a helper phage is due to the presence of a fully functional packaging signal on the fd genome compared to the mutated packaging signal in VCS-M13 (Vieira & Messing, 1987). Both phage and phagemid preparations were assessed for SKBR3 cell binding (Figure 3). While both preparations bound SKBR3 cells, binding could be detected with as little as 10^8 cfu/ml of fd-F5-GFP phage cfu/ml (160 fM) compared to 10^{10} cfu/ml of F5-GFP phagemids (15 pM). Thus multivalent binding leads to an increase in the apparent binding constant of virus particles.

Targeted phagemid and phage-mediated gene transfer into ErbB2 expressing breast cancer cells

To determine if ErbB2 binding phagemids were capable of targeted gene delivery, 2.0×10^5 SKBR3 cells (a breast tumor cell line expressing high levels of ErbB2) or 2.0×10^5 MCF7 cells (a low ErbB2 expressing breast tumor cell line) were incubated with 5.0×10^{11} cfu/ml F5-GFP phagemids at 37°C . SKBR3 cells express at least 27 to 170 times more ErbB2 than MCF7 cells (Lewis *et al.*, 1993). Cells were analyzed for GFP expression by FACS after 48 hours (Figure 4(a)). Of the SKBR3 cells, 1.37 % expressed GFP after incubation with F5-GFP phagemids (Figure 4(a6)). GFP expression was identical regardless of the orientation of the fl packaging signal (data not shown), indicating that transcription/translation was proceeding *via* synthesis of the complementary DNA strand. GFP expression was not detected in SKBR3 cells incubated with no phage or with helper phage packaging the reporter gene (Figure 4(a4) and 4(a5)). Expression was also not seen in MCF7 cells incubated with no phage, helper phage or pHEN-F5-GFP, indicating the requirement of ErbB2 expression for targeted gene delivery (Figure 4(a1), 4(a2) and 4(a3)). Since gene transfer applications are likely to involve targeting of specific cells in a heterogeneous cell population, we performed the same experiment on a co-culture of SKBR3 and MCF7 cells (Figure 4(b)). Cells were stained for ErbB2 expression to discriminate MCF7 from SKBR3 cells and the GFP expression of each subpopulation was analyzed by FACS. Only SKBR3 cells (1.91 %) expressed GFP. Similar results were found using F5-GFP phages instead of F5-GFP phagemids (data not shown). These data confirm that fd-F5-GFP phage and F5-GFP phagemid-mediated gene delivery is restricted to ErbB2-over-expressing cells and can be targeted to such cells in the presence of non-expressing cells.

Characterization of phage-mediated gene transfer

To determine the dose-response characteristics of phage-mediated gene transfer, SKBR3 cells were incubated for 60 hours with increasing amounts of fd-F5-GFP phage or F5-GFP phagemids and the percentage of GFP-positive cells determined (Figure 5(a) and 5(b)). The minimal phage concentration required for detection of a significant number of GFP positive cells (Figure 5(a)) was approximately 4.0×10^7 cfu/ml for fd-F5-GFP phage (0.13 %) and 1.0×10^{10} cfu/ml for F5-GFP phagemid (0.12 %). The values correlate closely with the binding curves (Figure 3) and indicate that multivalent phage are 100 to 1000 time more efficient than phagemids in terms of gene expression. No significant number of positive cells were observed with up to 4.0×10^{13} cfu/ml of helper phage packaging the reporter gene. For both phage and phagemid, the percentage of GFP-

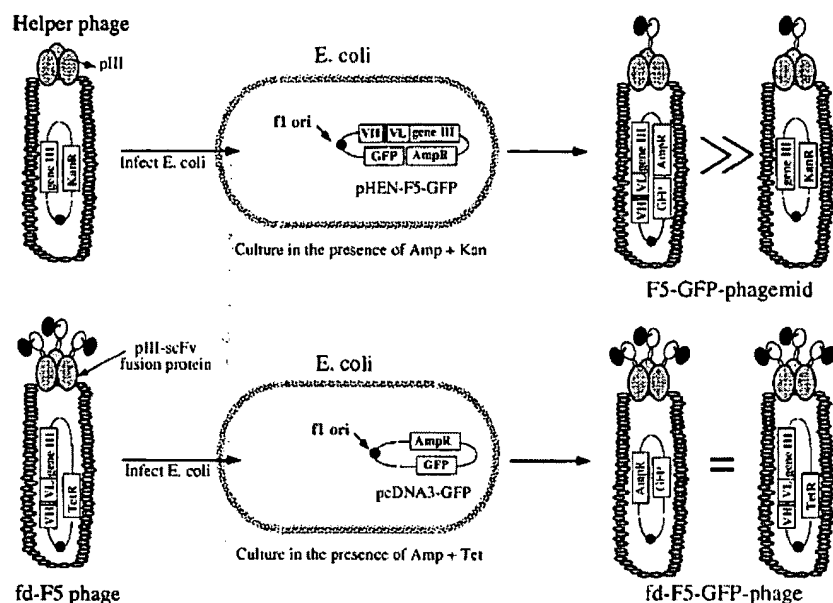


Figure 2. Strategies for producing anti-ErbB2 phagemids and phages packaging an eukaryotic reporter gene. Upper panel: helper phage are used to infect TG1 containing pHEN-F5-GFP, a phagemid composed of an f1 origin of replication (f1 ori), the anti-ErbB2 F5 scFv gene fused to gene III and a eukaryotic GFP reporter gene driven by the CMV promoter. Phages recovered from the culture supernatant display an average of 1 scFv-pIII fusion protein and 99% of them package the GFP reporter gene. Lower panel: the anti-ErbB2 F5 scFv gene is cloned into the fd phage genome for expression as a scFv-pIII fusion. fd-F5 phages are used to infect TG1 containing a GFP reporter phagemid vector (pcDNA3-GFP). Phages purified from the culture supernatant display multiple scFv-pIII fusion protein and approximately 50% package the GFP reporter gene.

positive cells increased with phage concentration with no evidence of a plateau. The maximum values achieved were 2% of cells for fd-F5-GFP phage and 4% for F5-GFP phagemids and appear to be limited by the phage titer applied (1.5×10^9 cfu/ml and 4.0×10^{12} cfu/ml, respectively). The amount of GFP expressed per cell (estimated by the mean fluorescent intensity (MFI), Figure 5(b))

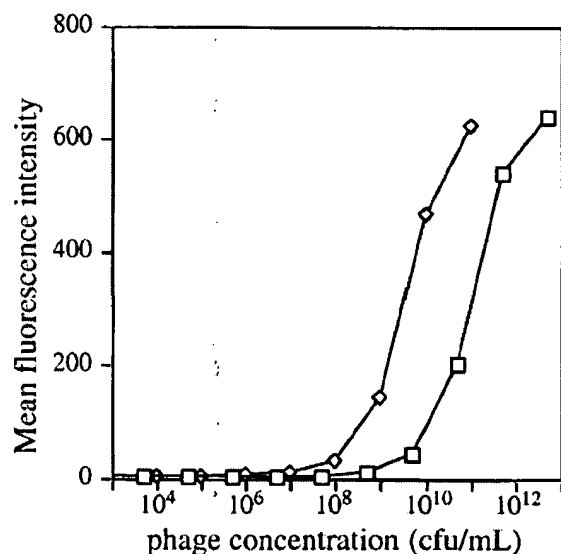


Figure 3. Comparison of anti-ErbB2 phagemid and phage binding on cells: 10^5 ErbB2 expressing SKBR3 cells were incubated with increasing concentrations of F5-phagemids (\square) or fd-F5-phage (\diamond) at 4°C for one hour. Cell surface-bound phages were detected with biotinylated anti-M13 and streptavidin-PE. Binding was detected by FACS and the results are expressed as mean fluorescent intensity (MFI).

also increased with phage concentration, with a small number of cells showing expression with phage titers as low as 2.0×10^7 cfu/ml (fd-F5-GFP phage) to 1.0×10^{10} cfu/ml (F5-GFP phagemid).

To compare the yield of gene expression obtained with phage to traditional transfection methods, single-stranded (ssDNA) or double-stranded DNA (dsDNA) was transfected into SKBR3 using lipofectamine. Per microgram of ssDNA, efficiency of phagemid-mediated gene delivery (approximately 1%) was comparable to lipofectamine transfection of ssDNA (0.98%) and dsDNA (1.27%; Table 1). Efficiency was approximately 500-fold higher for phage-mediated transfection, with 2.25 ng of ssDNA resulting in transfection of 0.87% of cells.

To determine the time-course of gene expression, 5.0×10^{11} cfu/ml of F5-GFP phagemid was incubated with SKBR3 cells. After 48 hours, the culture medium was replaced by fresh medium. GFP-expressing cells can be detected within 24 hours after phage are applied and the percentage of positive cells increases linearly with increasing time to a maximum of 4.5% by 120 hours (Figure 5(c)). The GFP content of the positive cells, as estimated by the MFI, increases up to 96 hours (Figure 5(d)). After 96 hours, the number of GFP-positive cells continues to increase but the MFI decreases, probably due to the repartition of GFP molecules to daughter cells during cell division.

Discussion

We demonstrate that filamentous phage displaying an anti-ErbB2 scFv antibody fragment as a genetic fusion with the minor coat protein pIII can be directly targeted to mammalian cells expressing

the specificity of the scFv. Such phage undergo receptor-mediated endocytosis and enter an intracellular trafficking pathway that ultimately leads

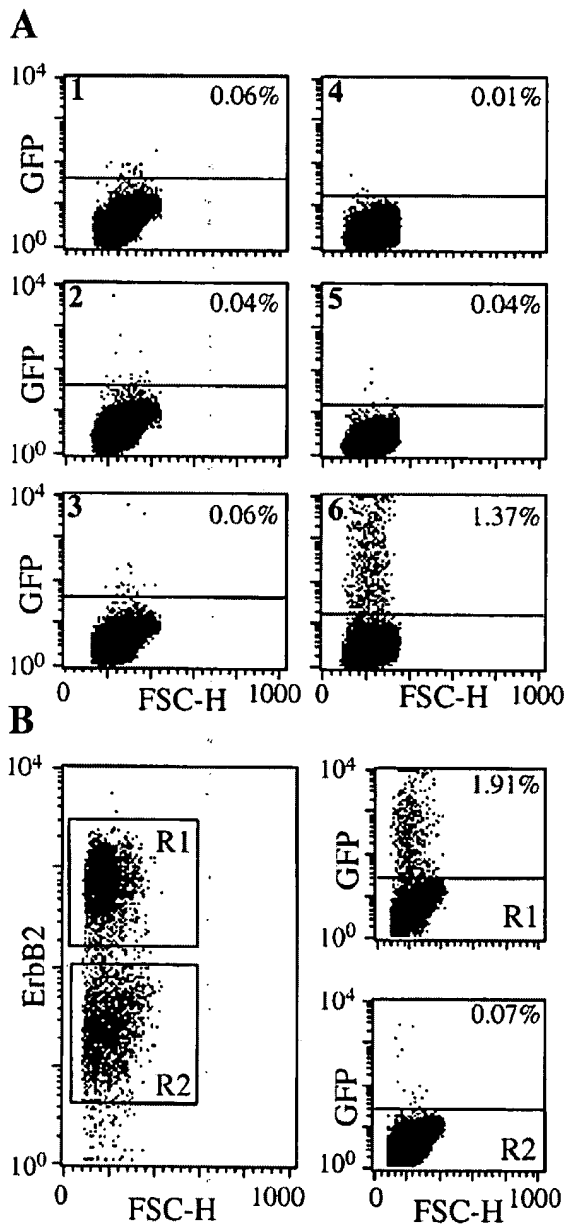


Figure 4. Phagemid-mediated gene transfer in breast cancer cell lines. (a) (1-3) 2.0×10^5 MCF7 (low ErbB2 expression) or (4-6) 2.0×10^5 SKBR3 (high ErbB2 expression) cells grown in six-well plates were incubated with (1 and 4) no phage, (2 and 5) 5.0×10^{12} cfu/ml of helper phage packaging GFP, or (3 and 6) 5.0×10^{11} cfu/ml of F5-GFP-phagemids for 48 hours. Cells were trypsinized and GFP detected by FACS. (b) An equal number of MCF7 and SKBR3 cells (1.0×10^5) were grown together and incubated with 5.0×10^{11} cfu/ml of F5-GFP-phagemids for 48 hours. Cells were trypsinized and stained for ErbB2 expression using 4D5 antibody and rhodamine-conjugated sheep anti-mouse Ig to discriminate SKBR3 (region R1) and MCF7 (region R2) cells. The GFP content of each subpopulation was determined by FACS.

to reporter gene expression. This is a remarkable finding, demonstrating that prokaryotic viruses can be re-engineered to infect eukaryotic cells, resulting in expression of a reporter gene inserted into the bacteriophage genome. Gene expression was detected with as few as 2.0×10^7 cfu of phage and increased with increasing phage titer up to 4% of cells. Multivalent display decreased the threshold for detectable gene expression approximately 500-fold compared to monovalent display, most likely due to an increase in the functional affinity and an increased rate of receptor-mediated endocytosis from receptor crosslinking. The maximum percentage of cells transfected, however, was higher for monovalent display (phagemid) due to the significantly higher phage titer generated. The lower titer of multivalent phage is due to interference of the f1 origin of replication on the reporter phagemid with the fd phage antibody origin of replication (Cleary & Ray, 1980).

Targeted infection of mammalian cells using phage that bind endocytosable receptors is likely to be a general phenomenon. For example, fusing an anti-transferrin receptor scFv to gene III of pHEN-GFP results in GFP expression in 10% of MCF7 cells, 4% of SKBR3 cells, 1% of LNCaP cells and 1% of primary melanoma cells (M. Huie & J.D.M., unpublished results). Similarly, targeted GFP gene delivery to FGF receptor-expressing cells using biotinylated phage and a streptavidin-FGF fusion molecule was recently reported (Larocca *et al.*, 1998). However, direct genetic fusion of the targeting molecule *via* gene III may be more efficient than using adapter molecules. Thus, while the maximum percentage of cells transfected using the FGF-adapter molecule was not reported, we estimate it to be only 0.03% of FGF expressing L6 rat myoblasts based on the number of cells infected, the time after infection to the measurement of gene expression and the number of cells expressing GFP. While a greater frequency of expression (0.5%) was seen in COS-1 cells, this results from the presence of large T antigen and SV40-mediated DNA replication and thus is not generalizable to most cells.

The approach we describe represents a novel method to discover ligands for targeted intracellular drug or gene delivery. Phage antibody or peptide libraries are first selected for endocytosis by mammalian cells (Barry *et al.*, 1996; Becerril *et al.*, 1999, M.-A.P. *et al.*, unpublished results) or for binding to purified antigen, cells, tissues or organs. After subcloning the selected scFv genes into the pHEN-GFP vector, phage produced from individual colonies can be directly screened for gene expression. This is possible, since expression can be detected with as little as 1.0×10^{10} cfu of phagemids. This permits direct identification of endocytosed scFv and the subset of receptor antibodies that undergo proper trafficking for gene expression. If multivalent display is necessary for efficient endocytosis, the scFv genes can be subcloned into fd-Sfi-Not, which is then used to rescue

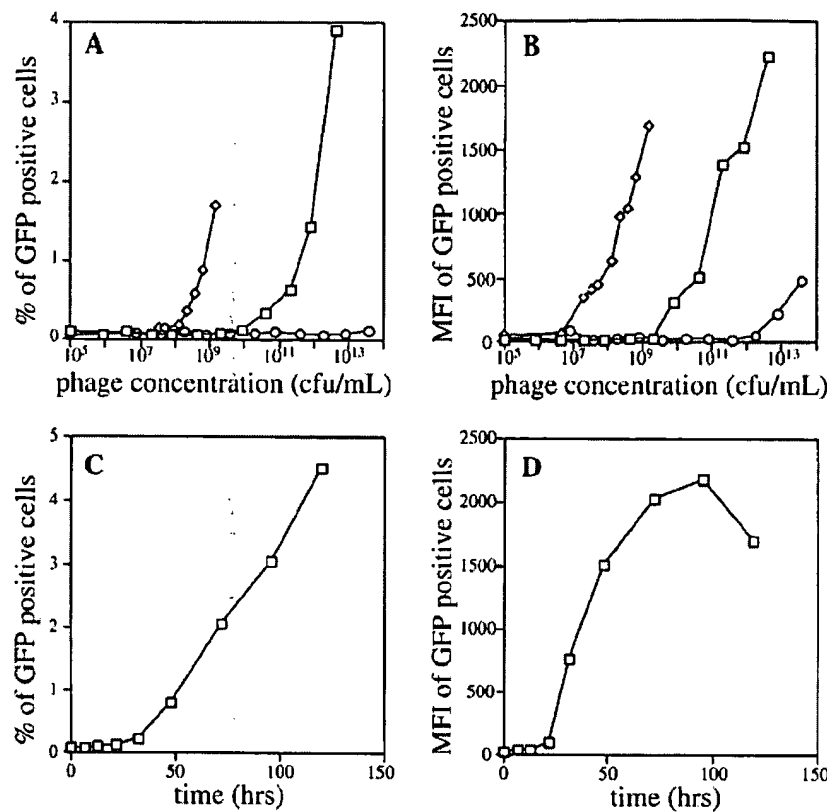


Figure 5. (a) and (b) Concentration-dependence of phagemid and phage-mediated GFP expression in SKBR3 cells. 5.0×10^4 cells were grown in 24-well plates and incubated with increasing concentrations of F5-GFP-phagemids (\square), fd-F5-GFP-phage (\diamond) or GFP-helper phage (\circ). After 60 hours, the cells were trypsinized and analyzed by FACS for GFP expression. (c) and (d) Time-dependence of phagemid-mediated GFP expression in SKBR3 cells. The 5.0×10^4 cells were incubated with 5×10^{11} cfu/mL of F5-GFP-phagemid and analyzed for GFP expression by FACS. For incubation times longer than 48 hours, the phage were added to 2.5×10^4 cells and the culture medium was replaced by fresh medium after 48 hours of incubation. The results are expressed as (a) and (c) percentage of GFP-positive cells, and (b) and (d) MFI of the GFP-positive cells.

the reporter phagemid. Use of scFv-fd phage also allows the targeting of a large number of different reporter genes in various expression vectors, since many commercially available mammalian vectors contain f1 origins of replication. As such, antibody-targeted phage might prove to be useful transfection reagents, especially for cells that are difficult to transfect by standard techniques.

It may also prove possible to use this approach to directly select, rather than screen, antibodies for targeted gene delivery. For example, mammalian cells are incubated with a phage antibody library containing the GFP gene, and then sorted based on GFP expression using FACS. Phage antibody DNA would be recovered from the mammalian cyto-

plasm by cell lysis and used to transfect *E. coli* and prepare more phage for another round of selection. If the quantities of recoverable phage DNA are inadequate, inclusion of the neomycin gene in the pHEN-GFP vector would permit selection of GFP-expressing mammalian cells using G418 (Larocca *et al.*, 1998).

Finally, this system has promise as a targetable *in vitro* or *in vivo* gene therapy vehicle. The main limitations are infection efficiency, pharmacokinetics and immunogenicity. With respect to infection efficiency, values achieved by targeted phage in this study (8.0×10^4 /ml of phage preparation) are not dissimilar to values reported for targeted retrovirus ($10^3 - 10^5$ /ml of virus; Kasahara *et al.*,

Table 1. Transfection efficiencies in SKBR3 cells

Transfection method	Reporter plasmid	Amount of reporter plasmid DNA	% of GFP positive cells
F5-phagemid-mediated	pHEN-F5-GFP	15 μ g	3.84
		3.1 μ g	1.44
		0.78 μ g	0.64
fd-F5-phage-mediated	pcDNA3-GFP	5 ng	1.69
		2.25 ng	0.87
		1.25 ng	0.57
Helper phage-mediated	pN ₂ GFP	100 μ g	0.12
		20 μ g	0.07
		5 μ g	0.06
Lipofectamine	pN ₂ GFP	1 μ g	1.27
		ssDNA	0.98

* Cells were analysed 48 hours after transfection for GFP expression using FACS. Results are expressed in % of GFP positive cells. For phage, the amount of reporter plasmid was calculated from the plasmid size and the number of ampicillin (pHEN-F5-GFP or pcDNA3-GFP) or kanamycin (pN₂GFP) resistant colonies. Mock transfected cells contained an average of 0.05 % GFP-positive cells.

1994; Somia *et al.*, 1995) but less than reported for adenovirus targeting strategies (up to 100 % of cells; Douglas *et al.*, 1996; Watkins *et al.*, 1997). The factors limiting higher infection efficiencies, however, are likely to differ between the systems. Thus while the percentage of cells infected by retrovirus is significantly higher than observed for bacteriophage, infection is limited by the problems encountered in producing large numbers of virus that can enter the cell. Since all cells take up the targeted phage (Figure 1), gene expression is limited by one or several post-uptake events (e.g. degradation of phage to release DNA, endosomal escape, nuclear targeting or transcription). More detailed study of the fate of the phage and its DNA is likely to suggest where the block lies, permitting engineering of phage to increase infection efficiency. For example, endosomal escape could be enhanced by co-administering replication-defective adenovirus (Curiel *et al.*, 1991) or incorporating endosomal escape peptides (Wagner *et al.*, 1992) or proteins (Fominaya & Wels, 1996) into the phage major coat protein pVIII. Alternatively, infection efficiency could be increased combinatorially by creating scFv-targeted libraries of pVIII mutants and selecting for increased gene expression. With respect to pharmacokinetics, though not extensively studied, concentrations of phage are much higher in the intravascular space than in tissue (Rajotte *et al.*, 1998). This would not affect *in vitro* phage gene therapy, but might limit *in vivo* uses to those targeting the vasculature. This still leaves numerous applications, including those where neovascularization plays a role, such as cancer. With respect to immunogenicity, it is likely that phage will be immunogenic, thus limiting the number of times that phage could be administered *in vivo*. Alternatively, it might prove possible to evolve the major coat protein pVIII to reduce or eliminate immunogenicity, for example by negatively selecting a pVIII library on immune serum (Jenne *et al.*, 1998).

Experimental protocol

Anti-ErbB2 F5 scFv

An anti-ErbB2 scFv (F5) in the vector pHEN-1 (Hoogenboom *et al.*, 1991; pHEN-F5) was obtained by selecting a non-immune phage antibody library (Sheets *et al.*, 1998) on ErbB2-expressing SKBR3 cells followed by screening for binding on recombinant ErbB2 extracellular domain (ECD) (M.-A.P. *et al.*, unpublished results). The native F5 scFv binds ErbB2 ECD with $K_d = 1.6 \times 10^{-7}$ M as determined by surface plasmon resonance in a BIA-core (Schier *et al.*, 1996).

Phage and phagemid vectors

pcDNA3-GFP (6.1 kbp) was obtained by subcloning the *HindIII*/*NotI* fragment of pN₂EGFP (4.7 kbp; Clontech) into the pcDNA3-HisB/LacZ (Invitrogen) *HindIII*/*NotI* backbone. An fd-F5-phage vector was constructed by subcloning the *Sfi* I/*Not* I scFv-F5 insert from pHEN-1 into the *Sfi* I/*Not* I sites of fd-*Sfi*/*Not* (constructed from

fd-tet-DOG (Clackson *et al.*, 1991) by changing the *Apal* I cloning site in the gene III leader to *Sfi* I; a gift from Dr Andrew Griffiths, MRC, Cambridge). The pHEN-F5-GFP phagemid vector (6.8 kbp) was obtained by subcloning the 1.6 kbp pN₂EGFP-blunted *AseI*/*Afl* III fragment into the blunted *EcoRI* site of pHEN-F5. The orientation of the insert was analyzed by *NotI* restriction digest.

Cell line culture and transfection

SKBR3 and MCF7 were grown in RPMI complemented with 10 % fetal bovine serum (FBS) (Hyclone). The 50 % confluent SKBR3 cells grown in six-well plates were transfected with 1 µg of DNA per well using lipofectamine (GIBCO BRL) as recommended by the manufacturer. pN₂EGFP dsDNA was prepared by alkaline lysis using the Maxiprep Qiagen Kit (Qiagen Inc.). ssDNA was extracted from 500 µl of phagemid preparation (see below) by two extractions with phenol followed by precipitation in ethanol. DNA was quantified by spectrophotometry with 1.0 A_{260} equal to 40 µg/ml for ssDNA or 50 µg/ml for dsDNA. For GFP detection, cells were detached using a trypsin-EDTA mix (GIBCO BRL) and analyzed on a FACScan (Becton Dickinson).

Phagemid and phage preparation

pHEN-F5, pHEN-F5-GFP, pcDNA3-GFP or pN₂EGFP phagemids were prepared from *E. coli* TG1 by superinfection with VCS-M13 helper phage (Stratagene) as described (Marks *et al.*, 1991). Fd-F5-phage were prepared from *E. coli* TG1 as described (McCafferty *et al.*, 1990). F5-GFP-phage and F5-LacZ-phage were prepared by superinfection of *E. coli* TG1 containing pcDNA3-GFP with fd-F5-phage. Virus particles were purified from the culture supernatant by two precipitations in polyethylene glycol (Sambrook *et al.*, 1990) resuspended in phosphate-buffered saline, pH 7.4 (PBS), filtered through a 0.45 µm filter and stored at 4 °C. Alternatively, the preparations were submitted to an additional CsCl ultracentrifugation step (Smith & Scott, 1993). The ratio of packaged helper phage DNA versus phagemid DNA was determined by titring (Sambrook *et al.*, 1990) the phage for ampicillin and kanamycin-resistance (for helper phage-rescued pHEN-F5) or ampicillin and tetracycline-resistance (for fd-F5 phage-rescued pcDNA3-GFP).

Phage FACS

Cells were trypsinized, washed with FACS buffer (PBS containing 1 % FBS) and resuspended at 10^6 cells/ml in the same buffer. The staining procedure was performed on ice with reagents diluted in FACS buffer. Aliquots (100 µl) of cells were distributed in conical 96-well plates (Nunc), centrifuged at 300 g and the cell pellets resuspended in 100 µl of serial dilutions of phage or phagemid preparation and incubated for one hour. Cells were centrifuged and washed twice, the cell pellets resuspended in 100 µl of biotinylated anti-M13 antibody (5 Prime, 3 Prime Inc.: diluted 1/400) and incubated for 45 minutes. Cells were washed as above, resuspended in 100 µl of streptavidin-Phycoerythrin (Jackson Inc.; diluted 1/400) and incubated for 20 minutes. After a final wash, the cells were analyzed by FACS.

Immunofluorescence

Cells were grown on coverslips to 50% confluency in six-well plates. Phage preparation (less than 10% of the culture medium) was added and the cells were incubated for 16 hours. The coverslips were washed six times with PBS, three times for ten minutes with glycine buffer (50 mM glycine (pH 2.8), 500 mM NaCl), neutralized with PBS and fixed with PBS-4% paraformaldehyde for five minutes at room temperature. Cells were permeabilized with cold acetone for 30 seconds, saturated with PBS-1% BSA and incubated with anti-M13 antibody (diluted 1/300 in the saturation solution) followed by streptavidin-Texas Red (Amersham; diluted 1/300 in the saturation solution). Coverslips were analyzed with a Zeiss Axioskop fluorescent microscope (Zeiss).

Bacteriophage mediated cell infection

CsCl phage preparations were diluted at least tenfold in cell culture medium, filtered through a 0.45 µm filter and added to 30% to 80% confluent cells. After incubation, the cells were trypsinized, washed with FACS buffer and analyzed for GFP expression by FACS. In the experiments where MCF7 and SKBR3 were co-cultured, ErbB2 expression was quantified by FACS using the anti-ErbB2 mouse mAb 4D5 which binds ErbB2 ECD (a gift from Paul Carter, Genentech, Inc.; 10 µg/ml for one hour), biotinylated sheep anti-mouse immunoglobulins (Amersham) and streptavidin-Phycoerythrin.

Acknowledgments

M.-A.P. was supported by a fellowship from the Association pour la Recherche contre le Cancer, France. This work was supported, in part, by the U.S. Army Medical Research, Development, Acquisition, and Logistics Command (Prov.) under grant no. DAMD17-94-J-4433 and DAMD-17-96-1-6244.

References

- Amersdorfer, P., Wong, C., Chen, S., Smith, T., Desphande, S., Sheridan, R., Finnern, R. & Marks, J. D. (1997). Molecular characterization of the murine humoral immune response to Botulinum neurotoxin type A binding domain as assessed by using phage antibody libraries. *Infect. Immun.* 65, 3743-3752.
- Andersen, P. S., Stryhn, A., Hansen, B. E., Fugger, L., Engberg, J. & Buus, S. (1996). A recombinant antibody with the antigen-specific, major histocompatibility complex-restricted specificity of T cells. *Proc. Natl Acad. Sci. USA*, 93, 1820-1824.
- Barry, M. A., Dower, W. J. & Johnston, S. A. (1996). Toward cell-targeting gene therapy vectors: selection of cell-binding peptides from random peptide-presenting phage libraries. *Nature Med.* 2, 299-305.
- Becerril, B., Poul, M.-A. & Marks, J. D. (1999). Towards selection of internalizing antibodies from phage libraries. *Biochem. Biophys. Res. Commun.* 255, 386-393.
- Cai, X. & Garen, A. (1995). Anti-melanoma antibodies from melanoma patients immunized with genetically modified autologous tumor cells: selection of specific antibodies from single-chain Fv fusion phage libraries. *Proc. Natl Acad. Sci. USA*, 92, 6537-6541.
- Clackson, T., Hoogenboom, H. R., Griffiths, A. D. & Winter, G. (1991). Making antibody fragments using phage display libraries. *Nature*, 352, 624-628.
- Cleary, J. M. & Ray, D. (1980). Replication of the plasmid pBR322 under the control of a cloned replication origin from the single-stranded DNA phage M13. *Proc. Natl Acad. Sci. USA*, 77, 4638-4642.
- Curiel, D. T., Agarwal, S., Wagner, E. & Cotten, M. (1991). Adenovirus enhancement of transferrin-polylysine-mediated gene delivery. *Proc. Natl Acad. Sci. USA*, 88, 8850-8854.
- de Kruif, J., Terstappen, L., Boel, E. & Logtenberg, T. (1995). Rapid selection of cell subpopulation-specific human monoclonal antibodies from a synthetic phage antibody library. *Proc. Natl Acad. Sci. USA*, 92, 3938-3942.
- Douglas, J. T., Rogers, B. E., Rosenfeld, M. E., Michael, S. L., Feng, M. & Curiel, D. T. (1996). Targeted gene delivery by tropism-modified adenoviral vectors. *Nature Biotechnol.* 14, 1574-1578.
- Fominaya, J. & Wels, W. (1996). Target cell-specific DNA transfer mediated by a chimeric multidomain protein. Novel non-viral gene delivery system. *J. Biol. Chem.* 271, 10560-10568.
- Hart, S. L., Knight, A. M., Harbottle, R. P., Mistry, A., Hunger, H. D., Cutler, D. F., Williamson, R. & Coutelle, C. (1994). Cell binding and internalization by filamentous phage displaying a cyclic Arg-Gly-Asp-containing peptide. *J. Biol. Chem.* 269, 12468-12474.
- Hoogenboom, H. R., Griffiths, A. D., Johnson, K. S., Chiswell, D. J., Hudson, P. & Winter, G. (1991). Multi-subunit proteins on the surface of filamentous phage: methodologies for displaying antibody (Fab) heavy and light chains. *Nucl. Acids Res.* 19, 4133-4137.
- Jenne, S., Brepoels, K., Collen, D. & Jespers, L. (1998). High resolution mapping of the B cell epitopes of staphylokinase in humans using negative selection of a phage-displayed antigen library. *J. Immunol.* 161, 3161-3168.
- Kasahara, N., Dozy, A. M. & Kan, Y. W. (1994). Tissue specific targeting of retroviral vectors through ligand-receptor interactions. *Science*, 266, 1373-1376.
- Larocca, D., Witte, A., Johnson, W., Pierce, F. G. & Baird, A. (1998). Targeting bacteriophage to mammalian cell surface receptor for gene delivery. *Hum. Gene Ther.* 9, 2393-2399.
- Lewis, G. D., Figari, I., Fendly, B., Wong, W. L., Carter, P., Gorman, C. & Shepard, M. (1993). Differential responses of human tumor cell lines to anti-p155^{HER2} monoclonal antibodies. *Cancer Immunol. Immunother.* 37, 255-263.
- Marks, J. D., Hoogenboom, H. R., Bonnert, T. P., McCafferty, J., Griffiths, A. D. & Winter, G. (1991). By-passing immunization: human antibodies from V-gene libraries displayed on phage. *J. Mol. Biol.* 222, 581-597.
- Marks, J. D., Hoogenboom, H. R., Griffiths, A. D. & Winter, G. (1992). Molecular evolution of proteins on filamentous phage: mimicking the strategy of the immune system. *J. Biol. Chem.* 267, 16007-16010.
- Marks, J. D., Ouwehand, W. H., Bye, J. M., Finnern, R., Gorick, B. D., Voak, D., Thorpe, S., Hughes-Jones, N. C. & Winter, G. (1993). Human antibody fragments specific for blood group antigens from a phage display library. *BioTechnol.* 11, 1145-1149.

- McCafferty, J., Griffiths, A. D., Winter, G. & Chiswell, D. J. (1990). Phage antibodies: filamentous phage displaying antibody variable domains. *Nature*, **348**, 552-554.
- Michael, S. I. & Curiel, D. T. (1994). Strategies to achieve targeted gene delivery via the receptor-mediated endocytosis pathway. *Gene Ther.* **1**, 223-232.
- Okayama, H. & Berg, P. (1985). Bacteriophage lambda vector for transducing a cDNA clone library into mammalian cells. *Mol. Cell. Biol.* **5**, 1136-1142.
- Rajotte, D., Arap, W., Hagedorn, M., Koivunen, E., Pasqualini, R. & Ruoslahti, E. (1998). Molecular heterogeneity of the vascular endothelium revealed by in vivo phage display. *J. Clin. Invest.* **102**, 430-437.
- Sambrook, J., Fritsch, E. F. & Maniatis, T. (1990). *Molecular Cloning: A Laboratory Manual*, Cold Spring Harbor Laboratory Press, Cold Spring Harbor, NY.
- Schier, R., Bye, J. M., Apell, G., McCall, A., Adams, G. P., Mahlnqvist, M., Weiner, L. M. & Marks, J. D. (1996). Isolation of high affinity monomeric human anti-c-erbB-2 single chain Fv using affinity driven selection. *J. Mol. Biol.* **255**, 28-43.
- Sheets, M. D., Amersdorfer, P., Finnern, R., Sargent, P., Lindqvist, E., Schier, R., Hemingsen, G., Wong, C., Gerhart, J. C. & Marks, J. D. (1998). Efficient construction of a large nonimmune phage antibody library: the production of high-affinity human single-chain antibodies to protein antigens. *Proc. Natl Acad. Sci. USA*, **95**, 6157-6162.
- Smith, G. P. & Scott, J. K. (1993). Libraries of peptides and proteins displayed on filamentous phage. *Methods Enzymol.* **217**, 228-257.
- Somia, N. V., Zoppe, M. & Verma, I. M. (1995). Generation of targeted retroviral vectors by using single-chain variable fragment: an approach to *in vivo* gene therapy. *Proc. Natl Acad. Sci. USA*, **92**, 7570-7574.
- Vieira, J. & Messing, J. (1987). Production of single-stranded plasmid DNA. *Methods Enzymol.* **153**, 3-11.
- Wagner, E., Flank, C., Zatloukal, K., Cotten, M. & Bimstiel, M. L. (1992). Influenza virus hemagglutinin HA-2 N-terminal fusogenic peptides augment gene transfer by transferrin-polylysine-DNA complexes: toward a synthetic virus-like gene-transfer vehicle. *Proc. Natl Acad. Sci. USA*, **89**, 7934-7938.
- Watkins, S. J., Mesyanzhinov, V. V., Kurochkina, L. P. & Hawkins, R. E. (1997). The 'adenobody' approach to viral targeting: specific and enhanced adenoviral gene delivery. *Gene Ther.* **4**, 1004-1012.
- Yokoyama-Kobayashi, M. & Kato, S. (1993). Recombinant f1 phage particles can transfect monkey COS-7 cells by DEAE dextran method. *Biochem. Biophys. Res. Commun.* **193**, 935-939.

Edited by J. Karn

(Received 18 January 1999; received in revised form 8 March 1999; accepted 8 March 1999)

**This Page is Inserted by IFW Indexing and Scanning
Operations and is not part of the Official Record**

BEST AVAILABLE IMAGES

Defective images within this document are accurate representations of the original documents submitted by the applicant.

Defects in the images include but are not limited to the items checked:

- ☐ BLACK BORDERS
- ☒ IMAGE CUT OFF AT TOP, BOTTOM OR SIDES
- ☐ FADED TEXT OR DRAWING
- ☐ BLURRED OR ILLEGIBLE TEXT OR DRAWING
- ☐ SKEWED/SLANTED IMAGES
- ☒ COLOR OR BLACK AND WHITE PHOTOGRAPHS
- ☐ GRAY SCALE DOCUMENTS
- ☒ LINES OR MARKS ON ORIGINAL DOCUMENT
- ☐ REFERENCE(S) OR EXHIBIT(S) SUBMITTED ARE POOR QUALITY
- ☐ OTHER: _____

IMAGES ARE BEST AVAILABLE COPY.

As rescanning these documents will not correct the image problems checked, please do not report these problems to the IFW Image Problem Mailbox.